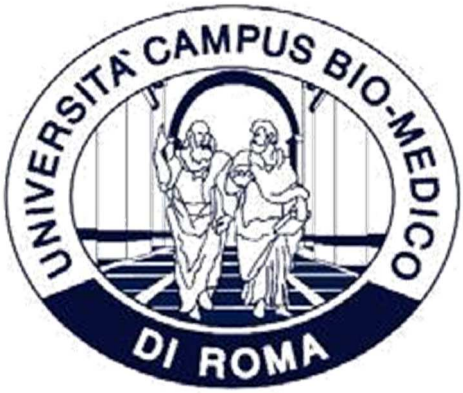

Università Campus Bio-Medico di Roma

Corso di dottorato di ricerca in Scienze Biomediche Integrate e Bioetica

Università Campus Bio-Medico

XXXIV ciclo a.a. 2018-2019

SOMATIC AND GERMLINE MOLECULAR ANALYSIS AND MORPHOLOGICAL ASPECTS OF UNUSUAL VARIANTS OF MALIGNANT MELANOMA AND UNCOMMON MELANOCYTIC NEOPLASMS

Michele Donati, MD

PhD Coordinator

Prof. Raffaele Antonelli Incalzi

Supervisor for Campus Bio-Medico University

Prof. Paolo Persichetti

Supervisor for Charles University

Prof. MUDr. Dmitry Kazakov, PhD (1.10.2020-28.2.2022)
Prof. MUDr. Alena Skálová, CSc (1.3.2022-25.5.2022)

Roma, 15 January 2022

SOMATIC AND GERMLINE MOLECULAR ANALYSIS AND MORPHOLOGICAL ASPECTS OF UNUSUAL VARIANTS OF MALIGNANT MELANOMA AND UNCOMMON MELANOCYTIC NEOPLASMS

Michele Donati, MD

Thesis leading to the degree of

PhD in Integrated Biomedical Science and Bioethics

Curriculum: Scienze dell'invecchiamento e della rigenerazione tissutale

January 2022

Supervisor for Campus Bio-Medico University: Prof. Paolo Persichetti

Supervisor for Charles University: Prof. Dmitry V. Kazakov

University Campus Bio-Medico, Rome, Italy
Co-tutelle agreement with
Charles University, Prague, Czech Republic

TABLE OF CONTENTS

DECLARATION

I declare hereby that I made this dissertation thesis by myself and that I mentioned and cited properly all the sources and literature. At the same time, I declare that this thesis was not used to obtain another or the same title.
I agree with permanent deposition of an electronic version of my thesis in the system database of interuniversity project Thesis.cz for a permanent control of similarities of theses.

In Pilsen,

Michele Donati, April 2022

STATEMENT OF ORIGINALITY AND CO-TUTELLE STATEMENT

Unless otherwise stated, the work described in this thesis was carried out with a co-tutelle agreement at Biopticka laboratory, Sikl Department of Pathology, Charles University Medical Faculty, Pilsen, Czech Republic and Campus Bio-Medico University, Rome, Italy.

The author designed the studies that are reported in this thesis and/or analyses and described the results.

I hereby declare that this that this thesis entitled "**Somatic and germline molecular analysis and morphological aspects of unusual variants of malignant melanomas and uncommon melanocytic neoplasms**" is my own work and that, to the best of my knowledge and belief, it contains no material previously published or written by another person nor material which to a substantial extent has been accepted for the award of any other degree or diploma of the university or other institute of higher learning, except where due acknowledgment has been made.

Michele Donati, January 2022

1. RESEARCH QUESTION

Can molecular analysis represent a useful tool to detect uncommon melanocytic neoplasms and unusual variants of malignant melanoma?

1.1 ABSTRACT

Introduction: Spitz neoplasms represent a heterogeneous group of melanocytic lesions histologically characterized by large epithelioid and/or spindled melanocytes with ample cytoplasm associated with specific epidermal and stromal changes, exhibiting a range of cytological and architectural variability that results in variable morphologic presentations. Thanks to the new data on the molecular alterations, our understanding of these neoplasms and their classification is undergoing a revision. We report a case of a polypoid atypical Spitz tumor a with prominent fibrosclerotic stromal component.
Methods: Molecular analysis was performed by TruSight Tumor 170 panel (Illumina, San Diego, CA) targeting the following genes *AKT1, AKT2, AKT3, ALK, APC, AR, ARID1A, ATM, ATR, BAP1, BARD1, BCL2, BCL6, BRAF, BRCA1, BRCA2, BRIP1, BTK, CARD11, CCND1, CCND2, CCND3, CCNE1, CD79A, CD79B, CDH1, CDK12, CDK4, CDK6, CDKN2A, CEBPA, CREBBP, CSF1R, CTNNB1, DDR2, DNMT3A, EGFR, EP300, ERBB2, ERBB3, ERBB4, ERCC1, ERCC2, ERG, ESR1, EZH2, FAM175A, FANCI, FANCL, FBXW7, FGF1, FGF10, FGF14, FGF19, FGF2, FGF23, FGF3, FGF4, FGF5, FGF6, FGF7, FGF8, FGF9, FGFR1, FGFR2, FGFR3, FGFR4, FLT1, FLT3, FOXL, GEN1, GNA11, GNAQ, GNAS, HNF1A, HRAS, CHEK1, CHEK2, IDH1, IDH2, INPP4B, JAK2, JAK3, KDR, KIT, KRAS, LAMP1, MAP2K1, MAP2K2, MCL1, MDM2, MDM4, MET, MLH1, MLL, MLLT3, MPL, MRE11A, MSH2, MSH3, MSH6, MTOR, MUTYH, MYC, MYCL1, MYCN, MYD88, NBN, NF1, NOTCH1, NOTCH2, NOTCH3, NPM1, NRAS, NRG1, PALB2, PDGFRA, PDGFRB, PIK3CA, PIK3CB, PIK3CD, PIK3CG, PIK3R1, PMS2, PPP2R2A, PTEN, PTCH1, PTPN11, RAD51, RAD51B, RAD51C, RAD51D, RAD54L, RAF1, RB1, RET, RICTOR, ROS1, RPS6KB1, SLX4, SMAD4, SMARCB1, SMO, SRC, STK11, TERT, TET2, TFRC, TP53, TSC1, TSC2, VHL,* and *XRCC2*.

FusionPlex Solid Tumor Kit (ArcherDX) containing 288 targets in 53 genes, and all steps were performed according to the Archer's FusionPlex protocol for Illumina (ArcherDX, Inc, Boulder, CO). The targeted genes included *ABL1, AKT1, ALK, APC, ATM, AURKA, BRAF, CCNE1, CDH1, CDK4, CDKN2A, CSF1R, CTNNB1, DDR2, EGFR, ERBB2, ERBB3, ERBB4, ESR1, EZH2, FBXW7, FGFR1, FGFR2, FGFR3, FLT3, FOXL2, GNA11, GNAQ, GNAS, H3F3A, HNF1A, HRAS, IDH1, IDH2, JAK2, JAK3, KDR, KIT, KRAS, MAP2K1, MET, MLH1, MPL, NOTCH1, NPM1, NRAS, PDGFRA, PIK3CA, PIK3R1, PTEN, PTPN11, RB1, RET, RHOA, ROS1, SMAD4, SMARCB1, SMO, SRC, STK11, TERT, TP53,* and *VHL.*

Results: Molecular analysis detected *CLIP2-BRAF* fusion, which has hitherto been not reported in melanocytic lesions. The neoplasm occurred in a 78-year-old male patient and appeared microscopically as a predominantly dermal, barely symmetrical, polypoid lesion composed mainly of epithelioid cells showing moderate degree of nuclear pleomorphism with ample amphophilic cytoplasm arranged in nests, fascicles, or single units. The mitotic rate was 2/mm2, and mitoses were confined to the upper portion of the lesion. The Breslow thickness was 2.3 mm. The stroma contained conspicuous plumped fibroblasts and thickened collagen bundles associated with dilated medium-sized vessels. Focally, sclerotic areas were found. A moderately dense, lymphocyte-predominant inflammatory infiltrate scattered through the whole lesion was seen. Despite strong nuclear and cytoplasmic positivity of p16 was, FISH revealed homozygous loss in locus 9p21. A *CLIP2-BRAF* fusion was found by next-generation sequencing. No other genetic alterations including *TERT-promoter* mutation was found. The patient is disease-free without recurrence or evidence of metastatic disease after 5 years and 2 months of follow-up.

Conclusions: We report a case of a polypoid atypical Spitz tumor a with prominent fibrosclerotic stromal component, harboring a *CLIP2-BRAF* fusion, which has hitherto been not reported in melanocytic lesions.

1.2 ABSTRACT

Introduction: Primary cutaneous desmoplastic melanoma (DM) is a group of rare melanocytic tumors arising on severely sun-damaged skin, histologically characterized by the proliferation of spindled melanocytes in a prominent desmoplastic stroma, with a range of morphological presentations.

Methods: Molecular analysis was performed by TruSight Tumor 170 panel (Illumina, San Diego, CA) and FusionPlex Solid Tumor Kit (ArcherDX) containing 288 targets in 53 genes, and all steps were performed according to the Archer's FusionPlex protocol for Illumina (ArcherDX, Inc, Boulder, CO).

Results: Molecular analysis detected a mutation in the *NF1* gene [c.4084C > T, p.(Arg1362Ter)], 2 different pathogenic mutations in *TP53* [c.742C > T, p.(Arg248Trp), AF:12%, COSM1640831 and c.528C > G, p.(Cys176Trp), AF:12%, COSM11114], and a mutation in *GNAS* [c.601C > T, p.(Arg201Cys), AF: 9%, COSM123397].

Conclusions: In this article, we report a unique case of primary cutaneous DM composed of a nodular proliferation of highly pleomorphic spindled and epithelioid cells, pseudoglandular structures, clear cell change, and unusual collagen rosettes. To the best of our knowledge, this is the first case reporting collagen rosettes and pseudoglandular features in primary cutaneous DM.

2. RESEARCH QUESTION

Can morphological-molecular correlation detect new subgroups of melanocytic neoplasms?

2. ABSTRACT

Introduction: Specific alterations involving MAPK genes (*MAP3K8* fusions, *MAP3K3* fusions) have been recently detected in a subgroup of spitzoid neoplasms that seem to constitute a distinctive clinicopathologic group, occur mostly in younger patients (median age 18 years) and present with atypical histologic features associated with frequent homozygous deletion of CDKN2A, qualifying a high proportion of them as Spitz melanoma (malignant Spitz tumor). Apart from lesions with spitzoid morphology harboring *MAP3K8* or *MAP3K3* fusion, a single case with *MAP2K1* deletion has been identified.

Methods: The 4 cases constituting the subject of this report were encountered in routine or referral practice of the authors and were identified among 346 melanocytic lesions studied by DNA and RNA Next Generation Sequencing (NGS), using 2 panels (VariantPlex and FusionPlex Solid tumor; ArcherDX, Boulder, CO). The Archer VariantPlex Solid Tumor Kit (VST) includes hotspot regions of the following genes: *ABL1, AKT1, ALK, APC, ATM, AURKA, BRAF, CCND1, CCNE1, CDH1, CDK4, CDKN2A, CSF1R, CTNNB1, DDR2, EGFR, ERBB2, ERBB3, ERBB4, ESR1, EZH2, FBXW7, FGFR1, FGFR2, FGFR3, FLT3, FOXL2, GNA11, GNAQ, GNAS, H3F3A, HNF1A, HRAS, IDH1, IDH2, JAK2, JAK3, KDR, KIT, KRAS, MAP2K1, MDM2, MET, MYC, MYCN, MLH1, MPL, NOTCH1, NPM1, NRAS, PDGFRA, PIK3CA, PIK3R1, PTEN, PTPN11, RB1, RET, RHOA, ROS1, SMAD4, SMARCB1, SMO, SRC, STK11, TERT, TP53, VHL.*

Results: The authors report herein 4 melanocytic lesions with a *MAP2K1* mutation, all showing similar microscopic appearances, including spitzoid cytology and dysplastic architectural features, resembling so-called SPARK nevus.

Conclusions: *MAP2K1*-mutated melanocytic neoplasms with a SPARK-Like morphology may represent another distinctive group of melanocytic tumors.

3. RESEARCH QUESTION

Can DNA and RNA molecular analysis on morphologically selected uncommon melanocytic neoplasm detect new mitogenic driver mutations?

3.1 ABSTRACT

Introduction: BRCA1-associated protein (*BAP1*)-inactivated melanocytic tumor (BIMT) is a group of epithelioid melanocytic neoplasms characterized by the loss of function of BAP1, a tumor suppressor gene located on chromosome 3p21. They occur sporadically or in the setting of an autosomal-dominant cancer susceptibility syndrome that predisposes to the development of different internal malignancies. Most of these cutaneous lesions are associated with a *BRAF*-mutated melanocytic nevus and therefore are included in the group of combined nevi in the last WHO classification of skin tumors. Apart from a *BRAF* mutation, an *NRAS* mutation has been reported in rare cases, whereas in some lesions no driver mutation has been detected.

Methods: Cases were tested by Sanger sequencing for *BAP1* gene mutation, using Polymerase Chain Reaction (PCR) amplification of the whole coding sequence with in-house designed primers, with the annealing temperature of was 608C and by DNA and RNA next generation sequencing (NGS), using 2 panels (VariantPlex and FusionPlex Solid tumor, ArcherDX, Boulder, CO).

Results: Sanger sequencing revealed a *BAP1* mutation (c.1832_1842del, p. Glu611GlyfsTer3). TruSight Tumor 170 panel identified a BAP1 gene mutation (c.14 G.A, p. Trp5Ter) with an allele frequency of 6% (verified by repeating the NGS from independent DNA sample), whereas the RNA panel showed a and the FusionPlex Solid Tumor panel identified a *GIT2-RAF1* fusion and *TRAK1-RAF1* fusion respectively. Both neoplasms were *BRAF* and *NRAS* tested wild type.

Conclusions: Here we report 2 cases of BIMTs with a *BAP1* mutation and a *RAF1* fusion. We suggest that *RAF1* fusions can represent an underlying driver genetic event in these cases. Our study extends the morphological and molecular spectrum in BIMTs.

3.2 ABSTRACT

Introduction: Pigmented epithelioid melanocytoma is a highly pigmented, predominantly dermal melanocytic neoplasm composed by epithelioid and spindled melanocytes. It is characterized by a limited number of specific genomic alterations principally involving protein kinase A regulatory subunit alpha (PRKAR1A) and fusion of protein kinase C alpha isoform (PRKCA). However, in some of these neoplasms, no genetic aberrations have been detected.

Methods: We performed genomic analysis of a nodular heavily pigmented intradermal proliferation composed of monomorphic epithelioid melanocytes with slight cytologic atypia consisting with pigmented epithelioid melanocytoma occurring on the vulva of a 24-year-old woman.

Results: A novel fusion transcript HTT-PKN1 and an ATM (Val410Ala) missense mutation were found. No other mutations including TERT promoter hotspot mutation analysis was detected.

Conclusions: The data expand the spectrum of molecular alterations in sporadic case of pigmented epithelioid melanocytoma.

4. RESEARCH QUESTION

Can germline and somatic mutational analysis of uncommon melanocytic neoplasm detected familial cases associate with tumor predisposition syndrome?

4. ABSTRACT

Introduction: BAP1-inactivated melanocytic tumor (BIMT) is a group of melanocytic neoplasms with epithelioid cell morphology molecularly characterized by the loss of function of *BAP1*, a tumor suppressor gene located on chromosome 3p21, and a mutually exclusive mitogenic driver mutation, more commonly *BRAF*. BIMTs can occur as a sporadic lesion or, less commonly, in the setting of an autosomal dominant cancer susceptibility syndrome caused by a *BAP1* germline inactivating mutation. Owing to the frequent
identification of remnants of a conventional nevus, BIMTs are currently classified within the group of combined melanocytic nevi. "Pure" lesions can also be observed.

Methods: We studied 50 BIMTs from 36 patients. Inclusion criteria were the typical microscopic features with the loss of BAP1 nuclear staining on epithelioid melanocytes detected immunohistochemically. The lesions were molecularly and histologically assessed to detect novel morphologic and genomic findings. All these data were correlated with the follow up of the patients.

Results: Most lesions were composed of epithelioid melanocytes of varying size and shapes, resulting extreme cytomorphological heterogeneity. Several distinctive morphological variants of multinucleated/giant cells were identified. Some hitherto underrecognized microscopic features, especially regarding nuclear characteristics included nuclear blebbing, nuclear budding, micronuclei, shadow nuclei, peculiar cytoplasmic projections (ant-bear cells) often containing micronuclei and cell-in-cell structures (entosis). In addition, there were mixed nests of conventional and BAP1-inactivated melanocytes and squeezed remnants of the original nevus. Of the 26 lesions studied, 24 yielded a *BRAF* mutation, while in the remaining two cases there was a *RAF1* fusion. *BAP1* biallelic and singe allele mutations were found in 4/22 and 16/24

neoplasms, respectively. In five patients, there was a *BAP1* germline mutation. Six novel, previously unreported *BAP1* mutations have been identified. *BAP1* heterozygous loss was detected in 11/22 lesions. Fluorescence in situ hybridization for copy number changes revealed a related amplification of both RREB1 and MYC genes in one tumor, whereas the remaining 20 lesions studied were negative; no *TERT-p* mutation was found in 14 studied neoplasms. Tetraploidy was identified in 5/21 BIMTs. Of the 21 patients with available follow-up, only one child had a locoregional lymph node metastasis.

Conclusions: Our results support a progression of BIMTs from a conventional BRAF mutated in which the original nevus is gradually replaced by epithelioid BAP1-inactivated melanocytes. Some features suggest more complex underlying pathophysiological events that need to be elucidated.

STATEMENT OF ATTRIBUTION

1.1 Author's contributions for the following study: **"*Polypoid Atypical Spitz Tumor With a Fibrosclerotic Stroma, CLIP2-BRAF Fusion, and Homozygous Loss of 9p21*"**.

Conceived and designed the study: Michele Donati, Dmitry V. Kazakov. *Performed the study*: Michele Donati. *Analyzed and interpretated the data*: Michele Donati, Dmitry V. Kazakov. *Wrote the manuscript:* Michele Donati, Dmitry V. Kazakov.

1.2 Author's contributions for the following study: **"*Primary Cutaneous Desmoplastic Melanoma With Collagen Rosettes and Pseudoglandular Features*"**.

Conceived and designed the study: Michele Donati, Dmitry V. Kazakov. *Performed the study*: Michele Donati. *Analyzed and interpretated the data*: Michele Donati, Dmitry V. Kazakov. *Wrote the manuscript:* Michele Donati, Dmitry V. Kazakov.

2 Author's contributions for the following study: **"*MAP2K1-Mutated Melanocytic Neoplasms With a SPARK-Like Morphology*"**.

Conceived and designed the study: Michele Donati, Dmitry V. Kazakov. *Performed the study*: Michele Donati. *Analyzed and interpretated the data*: Michele Donati, Dmitry V. Kazakov. *Wrote the manuscript:* Michele Donati, Dmitry V. Kazakov.

3.1 Author's contributions for the following study: **"*RAF1 Gene Fusions as a Possible Driver Mechanism in Rare BAP1-Inactivated Melanocytic Tumors: A Report of 2 Cases*"**.

Conceived and designed the study: Michele Donati, Dmitry V. Kazakov. *Performed the study*: Michele Donati. *Analyzed and interpretated the data*: Michele Donati, Dmitry V. Kazakov. *Wrote the manuscript:* Michele Donati, Dmitry V. Kazakov.

3.2 Author's contributions for the following study: **"*Vulvar Pigmented Epithelioid Melanocytoma with a Novel HTT-PKN1 Fusion: A Case Report*".**

Conceived and designed the study: Michele Donati, Dmitry V. Kazakov. *Performed the study*: Michele Donati. *Analyzed and interpretated the data*: Michele Donati, Dmitry V. Kazakov. *Wrote the manuscript:* Michele Donati, Dmitry V. Kazakov.

4 Author's contributions for the following study: **"*Novel insights into the BAP1-inactivated melanocytic tumor*".**

Conceived and designed the study: Michele Donati, Dmitry V. Kazakov. *Performed the study*: Michele Donati. *Analyzed and interpretated the data*: Michele Donati, Dmitry V. Kazakov. *Wrote the manuscript:* Michele Donati, Dmitry V. Kazakov.

ABBREVIATIONS

aCGH: Array comparative genomic hybridization
BAP1: BRCA1-associated protein
CGH: Comparative genomic hybridization
CNV: Copy number variation
CSN: Chronic sun-damaged skin
DM: Desmoplastic melanoma
DNA: Deoxyribonucleic acid
FISH: Fluorescence in situ hybridization
IAMPUS: Intraepidermal atypical melanocytic proliferation of uncertain significance
MAPK: Mitogen-activated protein kinase
MELTUMP: Melanocytic tumor of uncertain malignant potential
LOH: Loss of heterozygosis
NGS: Next generation sequencing
PCR: Polymerase chain reaction
PEM: Pigmented epithelioid melanocytoma
RNA: Ribonucleic acid
SAMPUS: Superficial atypical melanocytic proliferation of uncertain significance
SNP: Single nucleotide polymorphism
ST: Spitz tumor
DPN: Deep penetrating nevus
TERT-p: Telomerase reverse transcriptase gene promoter
UV: Ultraviolet
WT: Wild type

GENERAL BACKGROUND

I. Epidemiology of melanoma and melanocytic neoplasms

Melanoma is a malignant melanocytic tumor arising from melanocytes of the skin, melanin producing cells located in the basal layer of the epidermis, but it can develop also form melanocytes of internal organ, with gastro-intestinal tract and central nervous system the most common site of presentation after the skin. The incidence of melanoma is estimated between 3 - 7% in Europe and 2.6% in the United State. Melanoma represent around the 1% of skin cancer but is incidence has risen rapidly over the last 50 years. It is slightly more common in man than in women (ratio 1.5:1) and it accounts for majority of mortality due to skin cancer [1].

The main risk factors for developing melanoma are fair skinned populations (Fitzpatrick scale I - II), a positive family and personal history of melanoma, intense intermittent sun exposure (or artificial UV radiation sources), increased mole count (> 50), and a dysplastic nevus phenotype. Recently, several genetic predisposing factors have been detected named germline mutation in *CDKN2A, CDK4, MITF, TERT, ACD, TERF2IP, POT1, MC1R* or *BAP1* genes [2].

I.I Classification of melanoma and melanocytic tumor

Histological examination remains today the gold standard in the diagnosis of this aggressive neoplasm and Breslow depth (vertical measure taken from the granular layer of epidermis since the deepest tumor cell) is the most important prognostic factor. On the bases of the morphological analysis, it was suggested that melanoma evolve through 2 major stages of progression; the first termed the radial growth phase (RGP) is considered to be the early stage of the lesions in which neoplastic melanocytes growth horizontally in the dermo-epidermal junction. The second stage of progression,

called vertical growth phase (VGP) tumor cells infiltrate into the dermis growing vertically trough the dermis and the subcutaneous tissue [3], [4].

These phases have important clinical implications given that patients with RGP melanomas have an excellent prognosis compared to those with VGP melanomas that frequently develop a metastatic and potentially lethal disease. Several other histological factors have been linked to an unfavorable outcome including ulceration, presence of microsatellites and in-transit metastases, a higher mitotic rate, perineural and lympho-vascular invasion, and a minimal or absent intratumoral lymphocytic infiltrate [5].

Four major histological categories of melanoma have been recognized, three with an identifiable RGP named superficial spreading melanoma (SSM), lentigo maligna melanoma (LMM) and acral lentiginous melanoma (ALM) and nodular melanoma (NM) in which a radial growth phase is lacking by definition [6] [7].

In the last years, the concept of melanoma as a single entity have been questioned [8]. Considering clinicopathological and genetic data some authors have suggested a stepwise model of evolution of melanocytic neoplasm to melanoma from a conventional nevus [9]. Thus, nine pathways to melanoma have been identified in the last WHO classification of melanocytic tumors [10], based on a multidimensional pathogenetic factors the role of ultraviolet (UV) radiation, the tissue of origin and recurrent genomic drivers. With this approach, two main categories have been identified: 1) Cumulative sun damage (CSD) (pathways I - III), fourthly subdivided in Low-CSD (superficial spreading melanoma / L CSD nodular melanoma) High-CSD (lentigo maligna melanoma / H-CSD nodular melanoma / desmoplastic melanoma) and 2) not consistently associated with cumulative sun damage (pathways IV - IX) Spitz melanoma, acral melanoma, mucosal melanoma, melanoma arising in congenital nevus, melanoma arising in blue nevus and uveal melanoma [9].

Moreover, although the tumor genesis and tumor progression involve an interaction of genomic, environmental and host factors, a multistep, non-consequential model of melanoma progression have been proposed. The first step is represented by a mitogenic activating mutation (i.e. *BRAF V600E* mutation) [11]; the second step is the escaping

from primary senescence (i.e. *CDKN2A* loss); the third step is the overcoming of apoptosis (i.e. *TP53* mutation); the fourth step is the immortalization (i.e. *TERT-p* mutation).

Several molecular pathways are involved in melanoma pathogenesis with mitogen activated protein kinase (MAPK) pathway (RAS / RAF / MEK / ERK) is by far the most common. Other involved pathways are PI3K / AKT / mTOR and WNT / beta catenin signaling pathway [12].

Since today, the histopathological diagnosis of melanocytic tumors represented one of the greatest challenges of pathology. Several subgroups of melanocytic neoplasms have been recognized on the bases of their clinical and histological presentation. The microscopic assessment of these lesions is based upon the detection of a constellation of morphological features, some of which lack interobserver reproducibility [13], [14], [15]. Moreover, some subgroups of melanocytic tumors are characterized by ambiguous histological aspect and unpredictable biological [16], [14].

These neoplasms had one or more atypical characteristics, and some of them are morphologically indistinguishable from a melanoma.

A multitude of descriptive term have been proposed during the years to report this margin of diagnostic uncertainty such as “intraepidermal atypical melanocytic proliferation of uncertain significance (IAMPUS)” or “superficial atypical melanocytic proliferation of uncertain significance (SAMPUS)” for superficial melanocytic tumor rising morphological concern to an early melanoma without fulfilling diagnostic criteria of melanoma and, eventually, “melanocytic tumor of uncertain malignant potential (MELTUMP)” for those tumor with a variably deep dermal extension. This margin of uncertainty in the morphological diagnosis carried into clinical practice has important consequences in the management of the patient.

The clinicopathological shadow area between benign and malignant melanocytic tumors have been partially enlighten by the concept of melanocytic neoplasms of low malignant potential and the term “melanocytoma” have been proposed to embrace morphological and molecularly different melanocytic neoplasms that share a similar intermediate biological behavior.

Eventually, thanks to the advance of molecular biology, we are witnessing to a revolution to melanoma classification and treatment [17]. *BRAF* mutation testing is recommended for patients with stage III - IV melanoma while in patients with *BRAF* wild-type melanomas immunotherapy is the first line of treatment [18]. However, we are still far from understanding all the aspects of melanocytic neoplasm biology and the genomic analysis of these neoplasms represent a new frontier land. The detection of the genomic alterations that underlie the melanoma pathogenesis seems to be the key to develop a tailored management of the patients.

I.II Uncommon variant of melanocytic neoplasms

I.II.I Spitz Tumor (ST)

Spitz tumor is a subgroup of melanocytic neoplasms characterized by large epithelioid and/or spindled melanocytes arranged in fascicles or nests sometimes accompanied by characteristic epidermal and stromal changes. They include Spitz nevi, with well-defined bland histological aspects and benign behavior, and frankly malignant lesions called malignant Spitz tumors that can have an aggressive clinical course [19]. The term atypical Spitz tumor (AST) is often applied to lesions that manifest atypical histological features that however do not suffice for the diagnosis of an overt malignancy. ASTs mostly affect young patients and may involve regional lymph nodes [20]. Several studies have demonstrated that the classification of Spitz tumors along the spectrum of benign to malignant shows a poor interobserver reproducibility and a poor correlation with the clinical outcomes.

Spitz tumors harbor different molecular driver than most conventional nevi and melanomas. In 2015, a brilliant work by Thomas Wiesner has shown that a large subgroup of these neoplasms possesses structural genomic alterations named chromosomal translocations in receptor tyrosine kinases and serine threonine kinases [21]. After his work, thorough the morphological and molecular correlation several variants of Spitz tumor have been proposed to be associated with specific morphological features that can allow the pathologist to predict the underling

molecular alteration [22], [23], [24], [25], [26], [27], [28]. Moreover, a study on a large series of Spitz tumors demonstrated the impact of genomic analysis in predicting the biological behavior of these morphologically challenge melanocytic neoplasms [29].

I.II.II Pigmented epithelioid melanocytoma (PEM)

Pigmented epithelioid melanocytoma (PEM) is a melanocytic neoplasm histologically characterized by a dermal proliferation of epithelioid and spindled/dendritic melanocytes with copious intracytoplasmic melanin admixed with melanophages [30]. This tumors are microscopically indistinguishable from other melanocytic lesions formerly named as "animal-type" or pigment-synthesizing melanoma and epithelioid blue nevus occurring in the setting of Carney complex or sporadically [31], [32]. Clinically, PEM
typically presents with a darkly pigmented nodule located on the face, trunk, extremities, or genitalia of young patients [30].
Although PEM may present with alarming histological features it is considered a low-grade melanocytic tumor. Recently, specific genomic aberrations in the regulatory subunit alpha (PRKAR1A) mutations have been detected in both syndromic and sporadic forms of PEM while protein kinase C alpha isoform (PRKCA) fusion has been frequently observed in the sporadic cases [33], [34]. Moreover, it has been reported that hot spot mutation in *TERT-p* is predictive of aggressive clinical course in this group of melanocytic neoplasms [35].

I.II.III BAP1-inactivated melanocytic tumor (BIMT)

BAP1-inactivated melanocytic tumor (BIMT) is a group of rare melanocytic tumors characterized by two demonstrable genetic alteration, namely a *BRAF* V600E mutation and the biallelic inactivation of *BAP1* gene [36].

BIMTs may occur at any age, with equal sex distribution and clinically present as a flesh-colored papule or nodule favoring the head and neck region, trunk and upper extremities [37].

They occur sporadically or, less common, in the setting of an autosomal dominant cancer susceptibility syndrome caused by a BAP1 germline inactivating mutation that predisposes to uveal and cutaneous melanoma, mesothelioma, renal cell carcinoma, lung cancer and several other neoplasms [38].

Nowadays, cases of *BAP1*-inactivated melanoma have been reported and their molecular characterization it is largely unknown [39].

I.II.IV Deep penetrating nevus (DPN)

Deep penetrating nevus/melanocytoma is a subgroup of symmetric, roughly wedge-shaped proliferation of pigmented oval to spindle-shaped melanocytes organized in short fascicles or nests with a plexiform arrangement growing deeply through the dermis or subcutis [40]. They are molecularly characterized by two genetic alterations, a *BRAF* or *MAP2K1* mitogenic driver mutation and a *beta-catenin* or *APC* mutation. They are also considered to be low-grade melanoma or indeterminate risk melanocytic neoplasm [41]. A more detailed description of this tumors is beyond the topics treated in this thesis.

I.II.V Novel uncommon variant of melanocytic neoplasms

Recently, thanks to the wide used of molecular analysis novel uncommon variant of melanocytic neoplasms have been recognized. In the group of Spitz tumors a novel translocations involving *MAP3K8* have been detected in a spitzoid melanocytic tumor microscopically characterized by a prominent number of multinucleated giant cells. Moreover, *MAP3K8*-translocated tumor seems to present a more aggressive biological behavior compared to the receptor tyrosine kinases fusioned Spitz tumors [42]. A new

variant of combined melanocytic tumor harboring *NRAS* and *IDH1* mutation have been proposed to be in the spectrum of DPN [43].

A *CYSLTR2*-mutant cutaneous melanocytic neoplasms that simulate PEM have been also recently described [44]. Eventually, a primary intradermal nodular unpigmented tumor with a melanocytic immunophenotype associated with a novel CRTC1-TRIM11 fusion represent a new differential diagnosis with clear cell sarcoma [45].

Thus, thorough the morphological and molecular correlation the landscape of melanocytic neoplasm is evolving continuously, and classification of these new entities will be a challenge for the next WHO classification of melanocytic tumors of the skin.

1.1 Ancillary methods in the diagnosis of melanocytic tumors

Several ancillary techniques have been developed over the years to aid the pathologist in interpreting these difficult lesions. The diagnostic algorithm that is emerging considers the ease of execution, the time and costs necessary for these methods. Immunohistochemistry is an easy to perform method, requires short times and low costs. It allows to obtain additional information such as the presence or absence of melanocyte marker expression, the tumor proliferation index and the loss of nuclear p16 protein in the melanocyte population. In fact, it has been observed that the expression of melanocytic markers such as HMB45 gradually decreases towards the deep portion of the lesion [46].

The proliferation index evaluated by Ki 67 showed a trend of progressive increase of expression in the borderline groups of melanocytic tumors (2%, between 2 and 10%, 10%). Furthermore, the presence of a greater proliferative index at the level of the base of the lesion is a further parameter that points towards the diagnosis of melanoma [47].

Loss of p16 nuclear expression in melanomas and its preservation in benign nevi, with a characteristic “checkerboard” pattern in Spitz tumors, represent a surrogate test to investigate the homozygous deletion of the *CDKN2A* gene located in chromosomal region 9p21 [48].

In recent years, thanks to the development of molecular biology, a significant step forward has been made in the diagnosis of melanocytic neoplasms. The first molecular studies on these neoplasms investigating of loss of homozygosity (LOH) have shown that melanomas, unlike benign nevi, are characterized by considerable genomic instability, showing multiple chromosomal aberrations [49]. Subsequently, thanks to the studies carried out through Comparative Genomic Hybridization (CGH), then with the more refined array CGH (aCGH), specific areas of gain or loss of chromosomal portions were identified. Compared to melanocytic nevi, melanomas frequently show the loss of the 6q, 8p, 9p, 17p and 20q regions and a gain of gene copies in the chromosomal areas 1q, 6p, 8q, 17q, 20q [50].

On this basis, several kits have been developed for fluorescent in situ hybridization (FISH) applicable to paraffin tissue sections. A first kit involved the use of four probes, targeting three regions located on chromosome 6 (6p25, 6q23 and centromere 6) and one on chromosome 11 (11q13), showing discriminatory power between nevi and melanomas with a sensitivity of 86.7% and a specificity of 95.4% [51, 52].

This method was subsequently optimized, with the creation of a second kit which includes two other probes, one directed towards the chromosomal region 9p21, home of the CDKN2A gene and the other towards the 8q24 region (MYC). The application of both sets allowed a significant increase in sensitivity (94%) and specificity (98%), especially in the subgroup of morphologically ambiguous melanocytic neoplasms [53].

However, both aCGH and FISH have limitations. aCGH requires a high content of neoplastic DNA and required a minimum of chromosomal alterations (30-50%) present in the sample under examination. On the other hand, FISH is an operator dependent method, in which it is crucial to evaluate the emission of nuclear signals in malignant melanocytes, a task that may represent a challenge especially for melanomas arising in a benign nevus. Furthermore, both methods do not allow to identify balanced translocations and mutations.

These limitations have been overcome thanks to new next generation genomic sequencing (NGS) techniques. These methods allow the simultaneous analysis of multiple genomic regions, trough analyze both DNA and RNA molecules, allowing the

identification of chromosomal alterations, including balanced translocations and point mutations that could underlie the neoplastic process. Moreover, NGS methods require minimal amounts of tumor tissue and relatively short execution times. Currently, the main limitations of this method are related to costs and to the interpretation of the pathogenetic value of the detected alterations given the large amount of data provided from each tumor tissue analysis. There are currently different NGS machines available that use different processes essentially based on the same principles. Several genomic panels have been developed that investigate the main molecular pathways involved in human cancers. Simultaneous and targeted sequencing with the use of specific software allows detection of single nucleotide variations (SNVs), gene copy number variations (CNVs), insertions and deletions. In our study, three different NGS panels were employed. In each of our studies we reported the used ones.

CHAPTER 1: RESEARCH PROJECT N°1

1.1 Polypoid Atypical Spitz Tumor with a Fibrosclerotic Stroma, *CLIP2-BRAF* Fusion, and Homozygous Loss of 9p21*

* *This article has been published in American Journal of Dermatopathology in 2020 (Am J Dermatopathol. 2020 Mar;42(3):204-207).*

1.1.1 Introduction

Spitz neoplasms represent a heterogeneous group of melanocytic lesions histologically characterized by large epithelioid and/or spindled melanocytes with ample cytoplasm associated with specific epidermal and stromal changes, exhibiting a range of cytological and architectural variability that results in variable morphologic presentations. Thanks to the new data on the molecular alterations, our understanding of these neoplasms and their classification is undergoing a revision [10]. Specifically, mutually exclusive genomic rearrangements involving the tyrosine kinase receptors *ALK, NTRK1, NTRK2, NTRK3, MET, RET,* and *ROS1* and the serine-threonine kinase *BRAF* are frequently involved in Spitz lesions and some of them seem to be associated with specific histological features [21], [26], [22], [23], [24]. Since the study by Wiesner et al in 2010,3 few detailed morphological descriptions of Spitz neoplasms with *BRAF* fusions have been reported. A *BRAF* fusion is estimated to be present in around 5% of Spitz tumors; a correlation with specific morphological changes has not yet been clearly defined, although some studies consistently revealed a combination epithelioid cell morphology and conspicuous sclerotic stroma [54]. Recently, 2 cases of unclassified sclerosing malignant melanomas with an *AKAP9-BRAF* gene fusion have been described [55]. The illustrations of that article suggest a Spitzoid phenotype. We hereby report a case of an ambiguous polypoid Spitz tumor with a prominent fibrosclerotic stromal component, harboring a *CLIP2-BRAF* fusion that has not been reported to date in melanocytic lesions.

1.1.2 Case Report

A 78-year-old man with no personal or family history of melanoma presented with a 0.6-cm nodule on his left/right thigh that has been present for 3 years, slowly increasing in size over time. The lesion was surgically excised, and the histological

examination showed a predominantly dermal, barely symmetrical, polypoid melanocytic neoplasm composed mainly of epithelioid cells, with copious amphophilic cytoplasm showing moderate degree of nuclear pleomorphism. Melanocytes with prominent eosinophilic nucleoli were also observed. The cells were arranged in nests and fascicles, with no or minimal confluence. Singular cells surrounded by stroma were focally seen. The mitotic rate was 2/mm2. The mitoses were confined to the upper dermal portion of the lesion. No atypical mitotic figures were seen. Breslow thickness was 2.3 mm. The lesion was amelanotic and displayed an uneven flat base, not reaching the subcutaneous tissue. Maturation was preserved. The stroma contained conspicuous plumped fibroblasts and thickened collagen bundles associated with dilated medium-sized vessels. Focally, sclerotic areas were found. A moderately dense, lymphocyte predominant inflammatory infiltrate scattered through the whole lesion was seen. The epidermis overlying the lesion was slightly hyperplastic, with an increased number of medium-sized epithelioid melanocytes at the dermoepidermal junction not extending beyond the dermal component. No junctional nests, Kamino bodies, or pagetoid spread was seen. No perineural or intravascular involvement was observed (Figs. 1 and 2).

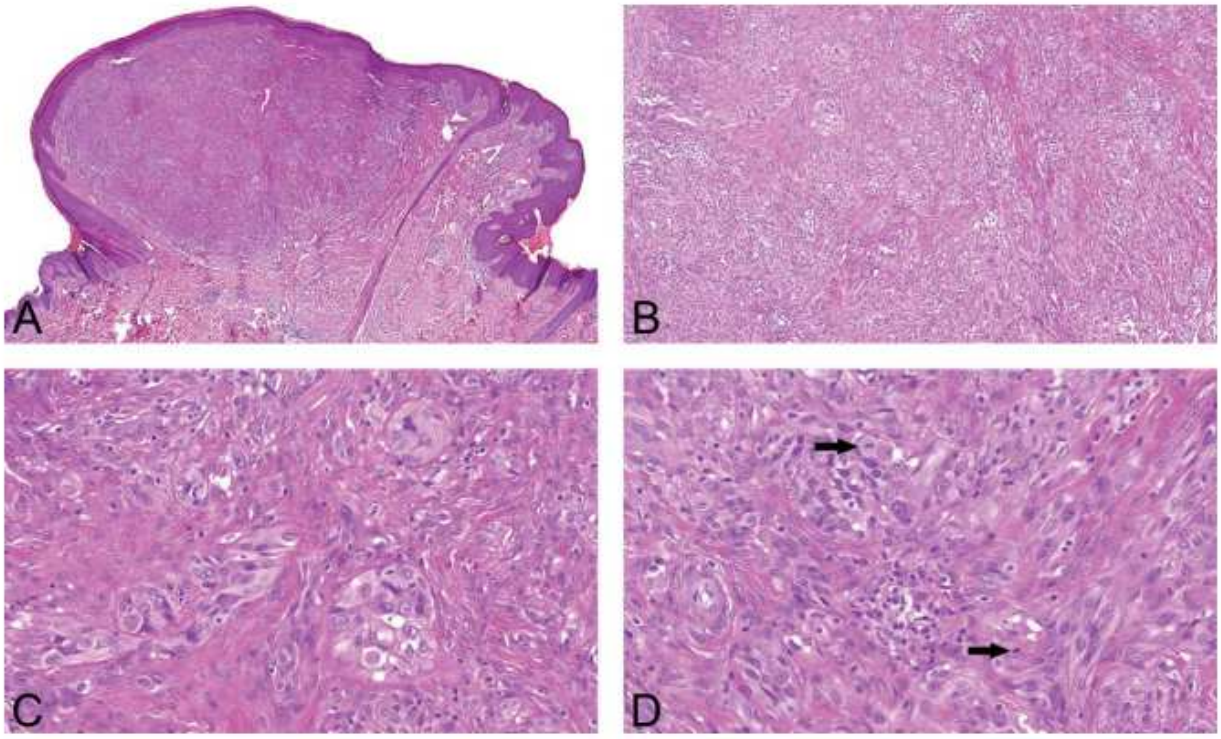

Fig.1 A barely symmetrical, polypoid neoplasm showing a predominantly dermal growth without subcutaneous tissue involvement, with fibrosclerotic stroma containing dilated medium-sized vessels (A). Small- to medium-sized nests and short fascicles of melanocytes surrounded by fibrosclerotic stroma and moderate lymphocytic infiltrate can be seen. B, A close-up view of the lesion: epithelioid melanocytes with copious amphophilic cytoplasm and moderate degree of nuclear pleomorphism intimately associated with plumped fibroblasts and thickened collagen bundles are evident. C, Note mitotic figures' activity (arrows) (D).

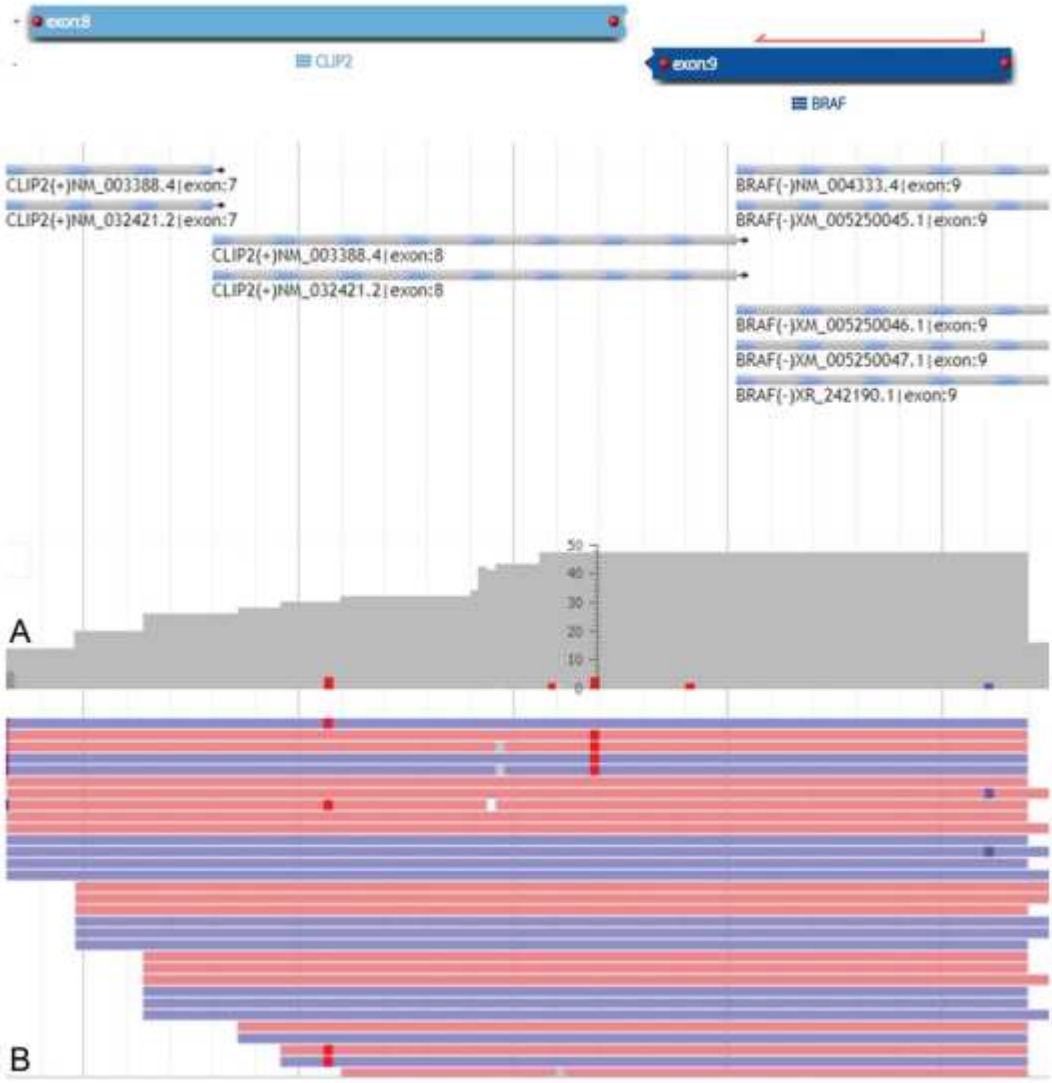

Fig.2 Schematic presentation of the CLIP2-BRAF fusion transcript as revealed by next-generation sequencing. The upper AU6 section: the scheme of joining of exon 8 of CLIP2 gene and exon 9 of BRAF gene. The lower section: the sequencing coverage of point of fusion in gray, several unique reads in red and blue, respectively.

Immunohistochemistry showed a diffuse positivity of the neoplastic cells for S-100 protein and tyrosinase, whereas Melan-A was only focally expressed in the upper part

of the lesion. Diffuse and strong nuclear and cytoplasmic positivity of p16 was observed in almost all the melanocytes.

FISH assay for chromosomal numeric aberrations revealed homozygous loss in locus 9p21 (CDKN2A), whereas no other alterations were detected, using probes targeting 6p25 (RREB1), 6q23 (MYB), 6p25 (RREB1), 11q13 (CCND1), and 8q24 (MYC), as described elsewhere.11 *TERT-promoter* (*TERT-p*) hotspot mutation analysis, performed with PCR and Sanger sequencing, was negative [56]. The Illumina TruSight Tumor 170 (TS170) panel was used for genomic rearrangement and somatic mutations detection as previously described {Skalova, 2018 #462.

The TruSight Tumor 170 Panel, both DNA and RNA parts, targets the following genes: *AKT1, AKT2, AKT3, ALK, APC, AR, ARID1A, ATM, ATR, BAP1, BARD1, BCL2, BCL6, BRAF, BRCA1, BRCA2, BRIP1, BTK, CARD11, CCND1, CCND2, CCND3, CCNE1, CD79A, CD79B, CDH1, CDK12, CDK4, CDK6, CDKN2A, CEBPA, CREBBP, CSF1R, CTNNB1, DDR2, DNMT3A, EGFR, EP300, ERBB2, ERBB3, ERBB4, ERCC1, ERCC2, ERG, ESR1, EZH2, FAM175A, FANCI, FANCL, FBXW7, FGF1, FGF10, FGF14, FGF19, FGF2, FGF23, FGF3, FGF4, FGF5, FGF6, FGF7, FGF8, FGF9, FGFR1, FGFR2, FGFR3, FGFR4, FLT1, FLT3, FOXL, GEN1, GNA11, GNAQ, GNAS, HNF1A, HRAS, CHEK1, CHEK2, IDH1, IDH2, INPP4B, JAK2, JAK3, KDR, KIT, KRAS, LAMP1, MAP2K1, MAP2K2, MCL1, MDM2, MDM4, MET, MLH1, MLL, MLLT3, MPL, MRE11A, MSH2, MSH3, MSH6, MTOR, MUTYH, MYC, MYCL1, MYCN, MYD88, NBN, NF1, NOTCH1, NOTCH2, NOTCH3, NPM1, NRAS, NRG1, PALB2, PDGFRA, PDGFRB, PIK3CA, PIK3CB, PIK3CD, PIK3CG, PIK3R1, PMS2, PPP2R2A, PTEN, PTCH1, PTPN11, RAD51, RAD51B, RAD51C, RAD51D, RAD54L, RAF1, RB1, RET, RICTOR, ROS1, RPS6KB1, SLX4, SMAD4, SMARCB1, SMO, SRC, STK11, TERT, TET2, TFRC, TP53, TSC1, TSC2, VHL, and XRCC2*. The quality of the extracted DNA was checked by qPCR using the Illumina FFPE QC kit, whereas the quality of RNA was tested using Agilent RNA 6000 Nano Kit on bioanalizer 4200 TapeStation. RNA sequencing identified a *CLIP2-BRAF* fusion. A complementary FISH study with a BRAF break-apart probe confirmed the presence of this gene rearrangement. DNA

sequencing for the detection of somatic mutations in 153 genes commonly involved in solid tumors was negative. Given the histological and molecular findings, a diagnosis of atypical Spitz tumor was made. No sentinel lymph node biopsy was performed. The patient is disease-free without recurrence after 5 years and 2 months of follow-up.

1.1.3 Discussion

The largest series on the histopathological features of *BRAF*-fused Spitzoid lesions reported to date was published by Amin et al who described *BRAF*-fused Spitz tumors and compared their molecular and morphological features with Spitz tumors harboring *ALK* and *NTRK1* fusion [57]. In comparison with the other 2 groups, BRAF-positive cases were predominantly composed of epithelioid melanocytes with moderate- to high-grade nuclear atypia with a sheet-like growth pattern in the dermis, with some cases showing single cells dispersed with a sclerotic stroma at the base. Moreover, the dysplastic Spitz architecture was also observed only in the *BRAF* fusion group. These lesions showed more likely copy number gains involving the kinase domain of the fusion protein and positive result with the melanoma FISH assay. Recently, 2 cases of unclassified sclerosing malignant melanoma harboring AKAP9-BRAF gene fusion have been reported [55]. The first case was a dermatofibroma-like lesion occurred in the lumbar region of a 47-year-old man that histologically mimicked a desmoplastic melanoma. The second case was a 42-year-old woman presenting with an exophytic genital lesion. A biopsy specimen exhibited a complex morphology, with junctional nests composed of large spindled cells and a dermal component of nevoid melanocytes surrounded by a dense fibrous/sclerotic background. Both the cases harbored numerous partial chromosomal gains and losses suggesting a diagnosis of melanoma. To our eye, the cytological details of the 2 cases may be regarded as those of Spitzoid lesions. Further studies reported the presence of *BRAF*-fusion in Spitzoid and non-Spitzoid melanocytic tumors including metastatic

and lethal cases [54 58], [59], [60], [61], [62]. The case we report further expands the molecular and morphological variations associated with BRAF-fused Spitz neoplasms. Histologically, the tumor presented as a large polypoid lesion with well-formed medium-sized vessels and a prominent fibrosclerotic stromal component, reminiscent of previously described polypoid Spitz nevus [63]. The prominent feature was the presence of fascicles of plumped fibroblasts alternating with nests and single cells of moderately pleomorphic epithelioid melanocytes with brisk mitotic activity. Because the lesion occurred in a 78-year-old male patient, it raised a concern of a malignant neoplasm and prompted us to perform further studies for risk stratification to establish whether the neoplasm harbors molecular alterations associated with an aggressive behavior, including homozygous deletion 9p21 and *TERT-p* mutations [64], [65], [66]. The FISH analysis revealed homozygous loss of 9p21, which was unexpected due to strong and diffuse nuclear staining for p16 on immunohistochemistry (previous studies reported a good correlation between "checkerboard nuclear pattern" and 9p21 preservation at FISH assay) [67], [68]. Although several studies described a strong association between homozygous deletion of 9p21 and an aggressive clinical course in Spitz tumors, its prognostic value has been questioned, and *TERT-p* hotspot mutations have been proposed as a more reliable predictive marker [69], [70]. In our neoplasm, we observed no *TERT-p* mutation. Moreover, DNA sequencing of 153 genes commonly involved in solid tumors failed to identify any somatic mutation. In a previous mutational landscape study, a low somatic mutation burden was reported in both Spitz and conventional nevi (34.41 ± 9.42), whereas both Spitzoid (747.22 ± 137.55) and conventional melanoma (758.03 ± 96.76) showed a high somatic mutation rate [71]. The low mutation burden in our case can be explained by the different methodologies used in our study and in that of Lazova et al who performed whole-exome sequencing but may still be used as an additional argument against the diagnosis of Spitzoid melanoma. Correlating these molecular data with the uneventful clinical course and taking into account atypical histological features that are not however sufficient to make the diagnosis of an overt malignancy, we consider the

lesion as atypical Spitz tumor. TS170 RNA sequencing for the detection of fusion transcripts in 55 genes yielded a *CLIP2-BRAF* fusion, extending the list of 50 fusion partner of the *BRAF* gene. To date, 33 different 50 fusion partner have been described for BRAF in melanocytic tumors, including *AGK, AGT7, AKAP9, AGAP3, ARMC10, BAIAP2L1, BGTF21, CCDC91, CDC27, CEP89, CUX1, DGKI, DYNC112, EML4, FCHSD1, KCTD7, KIAA1549, LSM14A, MAD1L1, MZT1, NFIC, NUDCD3, PAPSS1, PLIN3, RAD18, SLC12A7, SOX6, TAX1BP1, TNEM178, TRIM24, ZNF767, ZKSCAN1,* and *ZKSCAN5* [21, 57, 54, 56, 58, 59, 60, 61, 72, 62, 73]. To the best of our knowledge, the CLIP2-BRAF fusion has never been reported in melanocytic lesions but has been described in patients with histiocytic disorders and was implicated in constitutive MAPK pathway activation. A possible role of 50 fusion partner in the determination of the biological behavior has been hypothesized in other solid tumors [74]. Because the catalytic domain of the kinases is preserved in the rearrangements, the N-terminal fusion partner may determine the function of the gene product [75]. In conclusion, we have described a case of polypoid atypical Spitz tumor with fibrosclerotic stroma, homozygous loss of 9p21, p16 immunopositivity, and a CLIP2-BRAF fusion that has not been previously described in melanocytic lesions.

1.2 Primary Cutaneous Desmoplastic Melanoma With Collagen Rosettes and Pseudoglandular Features *

* *This article has been published in American Journal of Dermatopathology in 2021 (Am J Dermatopathol. 2021 Mar 1;43(3):221-224.).*

1.2.1 Introduction

Cutaneous desmoplastic melanoma (DM) is an uncommon variant of spindle cell melanoma accounting for less than 4% of primary melanomas of the skin. The most common clinical presentation is a firm nonpigmented nodule or plaque on severely sun-damaged skin of elderly male individuals [76]. Histologically, DM is a heterogeneous group of melanocytic tumors phenotypically ranging from a scar-like paucicellular proliferation of bland fusiform melanocytes separated by a dense collagenous stroma to high-grade sarcoma-like pleomorphic spindled cells with a variable degree of stromal desmoplasia [77], [78], [79], [80], [81], [82]. An atypical junctional melanocytic proliferation in the overlying epidermis and lymphocytic aggregates at the periphery of the tumor are often a feature, representing useful diagnostic clues, although the so-called DM arising "de novo" lacks a junctional melanocytic component [83]. Histopathological variations in DM include striking neurotropism with perineural and endoneurial invasion (neurotropic desmoplastic melanoma), prominent Schwannian and perineural features (neural transformation), marked myoid/myofibroblastic differentiation in the stroma, and others [84], [85], [86], [87]. Molecular analysis of DM reveals a high-mutation burden, ultraviolet (UV) signature, and frequent mutations in *NF1* (55%), *TP53* (48%), and *CDKN2A* (47%) [88], [89], [90], [85]. In this article, we present a very unusual case of neurotropic DM with collagen rosette formation, clear cell change, epithelioid cells, and pseudoglandular features.

1.2.2 Case Report

An 85-year-old man with a personal history of 2 melanomas diagnosed 10 and 11 years earlier (superficially spreading melanomas, Breslow thickness 0.6 and 1.5 mm; located on the ear and lower leg, respectively) presented with a 1.1-cm grayish nodule on the forehead clinically interpreted as basal cell carcinoma. A deep excisional biopsy revealed a dermal proliferation composed of highly pleomorphic cells embedded in a

prominent myxocollagenous stroma focally infiltrating the underlying adipocytic tissue. A majority of the neoplastic cells appeared as plumped spindled cells arranged in short intersecting fascicles. At foci, small roundish nodules of rather epithelioid cells with cytoplasmic clearing and pronounced vacuolization resulting in a pseudoglandular appearance were noted. Scattered multinucleated giant cells were also observed. A conspicuous finding was neoplastic cell aggregations or whorling of the tumor cells around central dense homogenized collagen resulting in peculiar rosette-like structures. Multiple areas of neurotropism and perivascular disposition of neoplastic cells were observed, as were lymphocytic aggregates at the periphery of the lesion. The mitotic rate was 4 mitoses/mm2, with atypical mitotic figures easily found. The assessed Breslow thickness was at least 4.7 mm; the lesion involved the deep margin of excision. Immunohistochemically, the neoplastic cells showed intense and diffuse positivity for S-100 protein, SOX-10, nestin, p75 (nerve growth factor receptor), WT1, and p53. Other melanocytic markers (tyrosinase, melan A, HMB-45, and melanocyte inducing transcription factor), cytokeratins (OSCAR, CK7, and K903), muscle markers (desmin, calponin, and smooth muscle actin), p63, 2F11, carcinoembryonic antigen, epithelial membrane antigen, H3K27Me3, TTF1, CDX2, podoplanin, p16, and CD31 were negative. Collagen IV staining highlighted collagen stromal deposits within rosette structures (Fig. 3). Alcian blue (pH 2.5) staining revealed mucin deposits in the stroma, with no mucin within pseudoglandular structures. Molecular analysis performed by TruSight Tumor 170 panel (Illumina, San Diego, CA) 2 yielded a clinically significant mutation in the *NF1* gene, namely c.4084C . T, p.(Arg1362Ter),
AF: 9%, COSM24443. Molecular analysis performed by FusionPlex Solid Tumor Kit (ArcherDX) containing 288 targets in 53 genes, and all steps were performed according to the Archer's FusionPlex protocol for Illumina (ArcherDX, Inc, Boulder, CO) detected two pathogenic mutations in *TP53* [c.742C . T, p.(Arg248Trp), AF:12%, COSM1640831 and c.528C . G, p.(Cys176Trp), AF:12%, COSM11114] and a mutation in *GNAS* [c.601C . T, p.(Arg201Cys), AF: 9%, COSM123397].

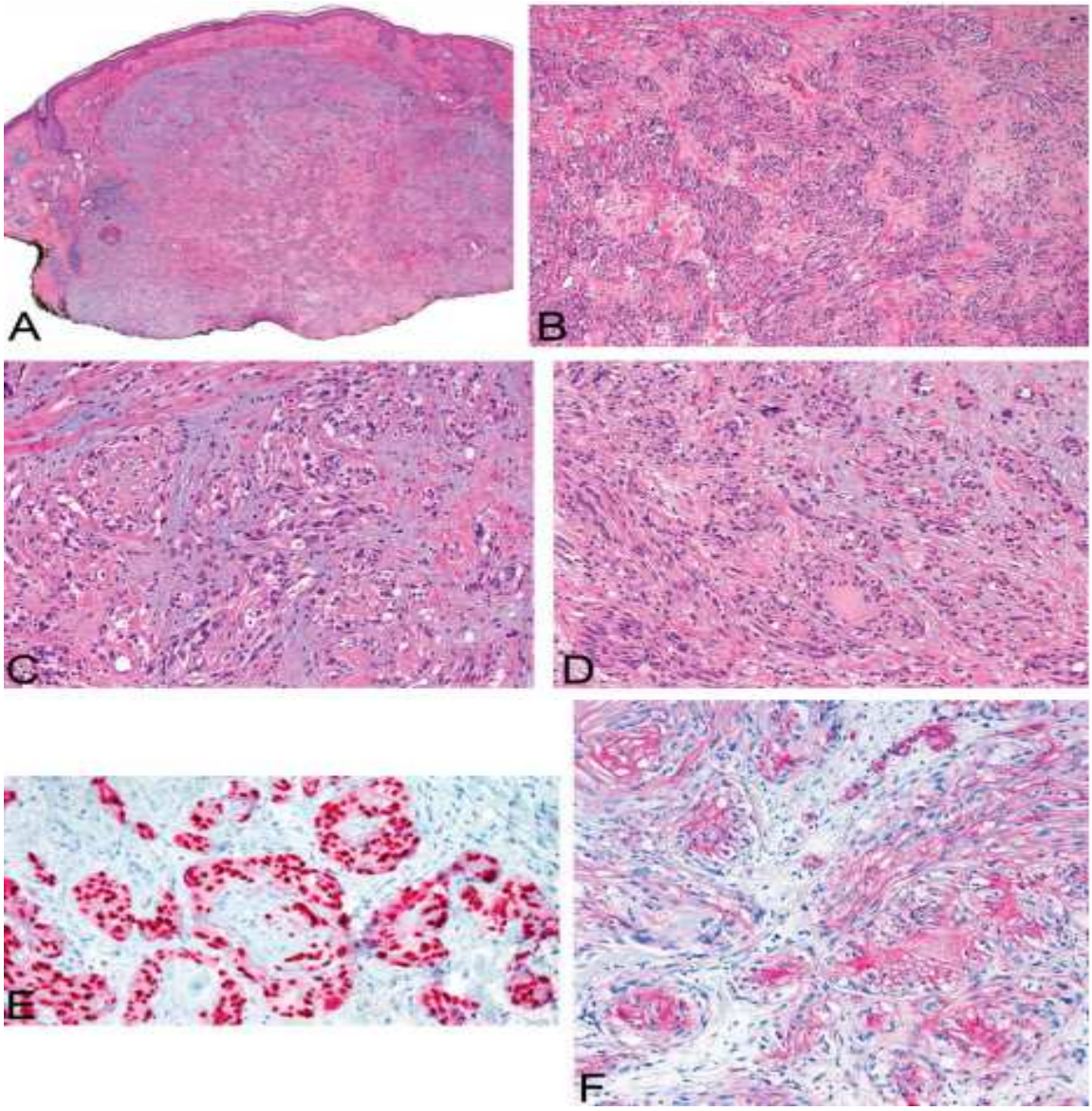

Fig.3 Scanning magnification shows a dermal nodule embedded in a prominent myxocollagenous stroma; the slightly hyperkeratotic epidermis is separated from the neoplastic proliferation by a grenz zone with moderate/severe solar elastosis and dilated capillary vessels. Lymphocytic aggregates are seen at the periphery of the lesion (A). The neoplastic population is composed of plumped spindled melanocytes arranged in short intersecting fascicles intermixed with small roundish nodules of epithelioid cells with cytoplasmic clearing (B). Neoplastic cells are disposed around central dense homogenized collagen forming peculiar rosette-like structures (C). A close-up view: highly pleomorphic melanocytes with prominent eosinophilic nucleoli, scattered multinucleated cells, and mitotic figures. Note the pronounced cytoplasmic vacuolization resulting in a pseudoglandular appearance (D). SOX-10 immunostaining shows a diffuse and intense nuclear staining in all neoplastic cells, including cells around rosette-like structures (E). Collagen IV staining highlights the rosette-like structures formed by dense homogenized collagen (F).

1.2.3 Discussion

The tumor we report on showed several unique and unusual features for a primary cutaneous DM, including a conspicuous epithelioid cell component, pseudoglandular structures, clear cell change, and collagen rosettes, requiring the differential diagnosis from several entities. First of all, given the history of 2 melanomas, a metastatic melanoma had to be excluded. As the previous melanocytic lesions were relatively thin superficial spreading melanomas and the current tumor was desmoplastic melanoma with characteristic mutations in the NF1 and TP53 genes, the probability of an isolated cutaneous metastasis was very low. Because of conspicuous epithelioid cytological features and the absence of a junctional melanocytic proliferation, the main differential diagnosis in our case was epithelioid malignant peripheral nerve sheath tumor (MPNST) that also shows immunoreaction for S-100 protein and SOX10. In contrast to conventional MPNST, epithelioid MPNST occurs mainly in the superficial soft tissue and is rarely associated with neurofibromatosis, type 1. In most cases, epithelioid MPNST shows loss of expression of INI1, a product of tumor suppressor gene SMARCB1/INI1 localized on chromosome 22q11 [91]. Albeit, epithelioid MPNST may occur at any age with a wide range of site distribution; it more frequently affects the lower extremities and trunk of the middle-aged patients. In contrast to DM, which is mainly located in the dermis with a characteristic infiltration of the underlying adipocytic tissue, epithelioid MPNST is more often located in the subcutaneous tissue, may extend upward to the overlying dermis, and shows weaker or focal expression for S-100 protein on immunohistochemistry. In our case, striking neurotropism, lymphocytic aggregates at the periphery of the neoplasm, strong immunoreactivity for S-100 protein and others markers considered to be specific for DM, including WT-1, nestin, and p75 (nerve growth factor receptor), intact INI1 nuclear staining, absence of any molecular alteration in *SMARCB1*, and pathogenic mutations in *NF1* and *TP53* gene strongly favored the diagnosis of primary cutaneous DM. Pseudoglandular structures are rarely seen in melanoma and seem to result in our case from prominent vacuolar degeneration of melanocytes [92], [93]. Pseudoglandular features have been recently reported in a primary intrafascial DM with aberrant expression of cytokeratins

[94]. Previously, the authors have encountered a case of conventional melanoma with a focal spindle cell component associated with highly fibrotic collagen bundles reminiscent of DM, displaying oncocytoid and signet-ring cells arranged in a pseudoglandular pattern [95]. In 1971, Conley et al introduced the term desmoplastic melanoma as a variant of spindle cell melanoma that "produces or elicits the production of abundant collagen" [83]. Apart from a collagenous stroma, we observed very peculiar and distinctive collagen rosettes that have never been reported in DM, to the best of our knowledge. Similar structures are typical of the so-called "hyalinizing spindle cell tumor with giant rosettes," a variant of low-grade fibromyxoid sarcoma (LGFMS) that have metastatic potential and is characterized by *FUS-CREB3L2, FUS-CREB3L1,* or *EWSR1-CREB3L1* gene fusion [96] [97]. Recently, a case of sclerosing perineurioma with conspicuous collagen rosette formation has also been reported [98]. Both these neoplasms may present with a myxocollagenous stroma and whorling arrangement of spindled cells, but they do not show striking atypical features such as severe nuclear pleomorphism, high mitotic rate, and atypical mitotic figures. Moreover, immunohistochemical analysis with diffuse positivity for S-100 protein and SOX10 excluded the diagnosis of both these entities that are characterized by positive immunoreaction for MUC4 (LGFMS) and epithelial membrane antigen, CD34, claudin, and glut-1 (perineurioma). The source of collagen production in DM is still unclear. The concept of "adaptive fibroplasia" that denotes melanocytic differentiation toward a fibroblastic phenotype at the base collagen production in DM has been widely accepted for a long time [99]. Later on, based on histological, immunohistochemical, and in vitro data, it has been proposed that fibroblasts present in DM represent the main source of collagen production under paracrine stimuli released by melanocytes [100]. However, an in vitro study reported melanocytes incorporating C14 into hydroxyproline containing peptide and directly produce collagen IV [101]. Noteworthy, in our case, all cells surrounding collagen rosette strongly express S-100 protein and SOX10 in the absence of CD34 expression, suggesting that melanocytes are directly involved in the deposition of collagen. Clear cell changes along with the expression of

S-100 and SOX10 by neoplastic cells lead us to consider in the differential diagnosis cutaneous clear cell sarcoma and a recently recognized cutaneous melanocytoma with *CRTC1-TRIM11* fusion. The former is rarely encountered on the skin especially in the head and neck area [102]. In these rare occasions, they occur in young adult patients, microscopically present with a nested architecture, fibrous septa, wreath-like multinucleated giant cells, lack of high mitotic rate, and highly pleomorpihic cells, almost always express HMB-45 and harbor *EWSR1-ATF1/CREB1* fusion in 90% of the cases.29 Cutaneous melanocytoma with *CRTC1-TRIM11* fusion is a low-risk melanocytic neoplasm that presents microscopically as an intradermal nodular unpigmented proliferation of spindled and epithelioid melanocytes arranged in coalescent nests and fascicles and may display cytological atypia, high mitotic rate, and tumoral necrosis. The neoplasm lacks desmoplastic stroma and perineural invasion.30 Histological appearances, lack of *EWSR1* fusions, and negative *CRTC1* break-apart probe in our case excluded these 2 entities. In conclusion, we have described a unique case of primary cutaneous DM with collagen rosettes, epithelioid cells, and pseudoglandular features extending the morphological spectrum of these challenging melanocytic neoplasms.

CHAPTER 2: RESEARCH PROJECT N°2

*2. MAP2K1-Mutated Melanocytic Neoplasms With a SPARK-Like Morphology **

* *This article has been published in American Journal of Dermatopathology in 20201 (Am J Dermatopathol. 2021 Jun 1;43(6):412-417).*

2.1 Introduction

Spitz tumors are a heterogeneous group of melanocytic lesions characterized by large epithelioid and/or spindled melanocytes arranged in fascicles or nests sometimes accompanied by characteristic epidermal and stromal changes. Recent novel molecular data have been integrated into the clinical and histologic classification of these neoplasms [10]. Several studies have shown that Spitz tumors are characterized by mutually exclusive genomic alterations such as a mutation of the *HRAS* gene or structural rearrangements involving various receptor tyrosine kinases, including *ALK, ROS1, NTRK1, NTRK3, MET,* and *RET* and the serine– threonine kinase *BRAF* [103], [22], [21], [104], [105], [25], [24], [26]. For some of these subgroups, a correlation of the histopathologic features with an underlying genetic alteration has been found [22], [105], [26], [106]. Most recently, alterations involving MAPK genes, mainly *MAP3K8* fusions and *MAP3K3* fusions, have been detected in a subgroup of spitzoid neoplasms apparently constituting a distinctive clinicopathologic group [107], [108], [42]. Compared with the other subgroup of Spitz tumors, MAPK-driven neoplasms have been found to mostly occur in younger patients (median age 18 years), microscopically showed primarily an epithelioid morphology, multinucleated giant cells, notable melanin pigment and tended to have high-grade nuclear atypia, qualifying a high proportion of the lesions as Spitz melanoma (malignant Spitz tumor) [42], [109]. Apart from lesions characterized by *MAP3K8* fusions, a single case with *MAP2K1* deletion was identified [109]. The authors have encountered 4 melanocytic lesions with a *MAP2K1* mutation that all had similar histopathologic features, resembling so-called SPARK nevus, that is a melanocytic lesion with a spitzoid cytology (SP for Spitz) having architectural feature of a dysplastic nevus (ARK for Clark) [110]. The question has arisen whether this can represent another new subtype of melanocytic lesion with a genetic correlate. Herein, we report on these cases and review the pertinent literature.

2.2 Materials and Methods

The 4 cases constituting the subject of this report were encountered in routine or referral practice of the authors and were identified among 346 melanocytic lesions studied by DNA and RNA next generation sequencing (NGS), using 2 panels (VariantPlex and FusionPlex Solid tumor; ArcherDX, Boulder, CO), as reported elsewhere [26]. The Archer VariantPlex Solid Tumor Kit (VST) includes hotspot regions of the following genes: *ABL1, AKT1, ALK, APC, ATM, AURKA, BRAF, CCND1, CCNE1, CDH1, CDK4, CDKN2A, CSF1R, CTNNB1, DDR2, EGFR, ERBB2, ERBB3, ERBB4, ESR1, EZH2, FBXW7, FGFR1, FGFR2, FGFR3, FLT3, FOXL2, GNA11, GNAQ, GNAS, H3F3A, HNF1A, HRAS, IDH1, IDH2, JAK2, JAK3, KDR, KIT, KRAS, MAP2K1, MDM2, MET, MYC, MYCN, MLH1, MPL, NOTCH1, NPM1, NRAS, PDGFRA, PIK3CA, PIK3R1, PTEN, PTPN11, RB1, RET, RHOA, ROS1, SMAD4, SMARCB1, SMO, SRC, STK11, TERT, TP53, VHL.* The assay does not contain the MAP3K8 gene.

Immunohistochemical staining was performed on 4-mm sections cut from formalin-fixed, paraffin-embedded tissue using Ventana Benchmark XT automated stainer (Ventana Medical System, Inc, Tucson, AZ), according to the manufacturer's protocol. The following antibodies were used: S-100, SOX-10, HMB-45, tyrosinase, ALK, ROS1, TRK, and p16. One case (case 1) was also studied by Fluorescence in situ hybridization (FISH), using a 4-probe assay targeting 6p25 (RREB1), 6q23 (MYB), 11q13, and Cep6 and a second 4-probe assay targeting 6p25 (RREB1), 9p21 (CNDK2A), 11q13 (CCND1), and 8q24 (MYC), as described elsewhere [111], [51]. Clinical follow-up was obtained from the patients, their physicians, or from referring pathologists.

2.3 Results

2.3.1 Clinical Features

There were 3 female and 1 male patients with ages ranging at diagnosis from 20 to 61 years (median age, 44.5 years, mean 42.5 years). Three lesions occurred on the lower leg and one on the back. The clinical presentation was a flat or slightly

elevated pigmented lesion with a diameter ranging from 0.5 to 1.1 cm. The clinical diagnoses included atypical nevus (cases 1 and 4), melanoma (case 2), and halo nevus (case 3). All lesions were surgically excised, with 3 lesions re-excised after the histologic diagnosis was rendered. The patient with melanoma underwent clinical investigation with a sentinel lymph node biopsy which was negative. The patients had no evidence of disease at 3, 12, and 14 months, respectively. Case 4 was too recent for a meaningful clinical follow-up.

2.3.2 Histopathologic and Immunohistochemical Findings

All 4 lesions showed a flat or slightly elevated configuration with a plaque-like or hinted wedge-shaped (case 2) silhouette and a median Breslow thickness of 0.8 mm (range from 0.5–1.1 mm). They were barely symmetrical to slightly asymmetrical compound melanocytic proliferations with a predominant junctional component of broad shoulders of nested and lentiginous melanocytes extending beyond a centrally located, superficial dermal component. In all cases, there was epidermal hyperplasia; in case 2 focal atrophy and consumption of the epidermis was additionally observed. The neoplastic population was composed of spindled and epithelioid melanocytes with moderate to severe (case 3) nuclear pleomorphism (Fig.4). In 2 cases (cases 1 and 3), melanocytes in the basal layer had a starburst appearance with hyperchromatic nuclei retracted from the cytoplasm, sometimes highlighting dendrites. Junctional melanocytes manifested both a lentiginous and nested growth pattern with confluent, horizontally arranged nests, bridging the adjacent rete ridges. Scattered pagetoid melanocytes were mainly confined to the central part of the lesions in all cases. Kamino bodies were encountered in 1 case (case 4). In the upper dermis, a minor component of conventional-appearing melanocytes was intermixed to the atypical spindled and epithelioid melanocytes, resulting in at least focal impaired maturation toward the base of the lesion. Whereas in 3 cases the lower border of the lesion was flat, in case 2 splaying of melanocytes between dermal collagen bundles resulted in an infiltrative reticular pattern. In 3 cases, granular intracytoplasmic melanin pigment

was observed in both junctional and dermal melanocytes that were surrounded by a moderate to heavy lymphocytic inflammatory infiltrate. In 2 cases, stromal melanin deposits and melanophages were associated with more prominent vascular and fibrotic stroma changes. Occasional multinucleated melanocytes and prominent nuclear pseudoinclusions were noted in 3 cases (cases 1, 3, and 4). In case 2, 2 dermal mitoses/mm2 including deep mitoses were noticed. In the other 3 cases, only junctional mitoses were found. Follicular involvement was observed in 2 cases (cases 1, and 2). In case 4, arrector pili muscle and eccrine ducts were involved. All 4 lesions showed diffuse and intense positivity for a melanocytic marker (S-100, SOX-10, tyrosinase and HMB45), whereas p16 staining showed a checkerboard nuclear pattern. Stains for ROS1, ALK and TRK studied in 3 cases (cases 1, 2 and 4) were negative. PrkaR1a performed in 2 cases (cases 1 and 2) maintained cytoplasmic staining. Two cases (case 2 and 4) were diagnosed as melanocytic nevi with dysplastic phenotype and spitzoid cytological features (SPARK). Case 3 was diagnosed as atypical Spitz tumor, whereas case 2 was diagnosed as melanoma.

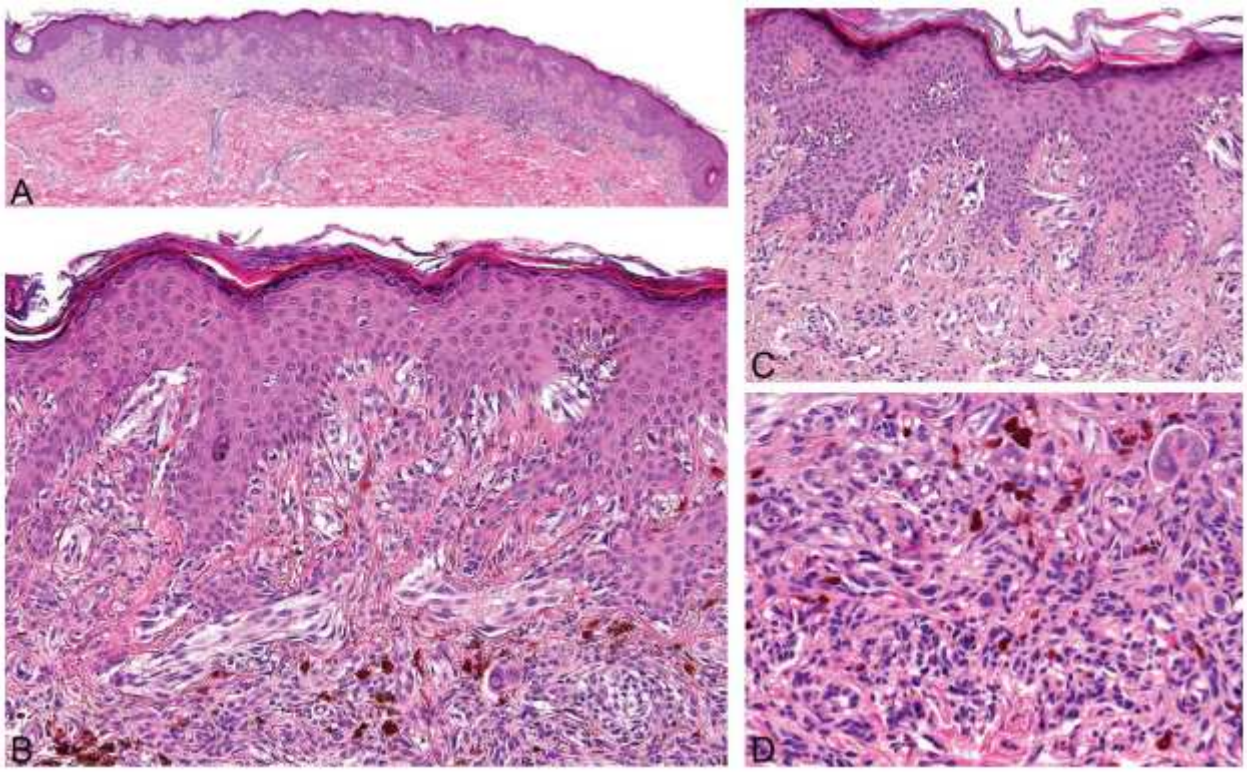

Fig.4 Low-power magnification shows a barely symmetrical compound melanocytic proliferation with a predominant junctional component of broad shoulders of melanocytes arranged in nests over a minor

dermal component (A). Junctional melanocytes show both a lentiginous and nested growth pattern with confluent, horizontally arranged nests and bridging of the adjacent rete ridges. Note predominantly spindled melanocytes within the nests (B). Melanocytes in the basal layer showing a starburst appearance with hyperchromatic nuclei retracted from the cytoplasm. Note occasional cells with dendrites (stellate cells) and lamellar fibrosis in the papillary dermis (C). A close-up of a dermal component in which atypical and conventional-appearing melanocytes associated with melanophages can be seen (D).

Table 1. Summary of clinical, histological and molecular data
NED –no evidence of disease, VAF variation allele frequency, SLNB- sentinel lymph node biopsy

Case	Sex/Age	Site	Clinical size/diagnosis	Histological diagnosis	Treatment and Follow-up (months)	*MAP2K1* mutation
1	F/20	Right shin	0.9 cm Halo nevus	Nevus (SPARK)	Excision and re-excision NED at 14 months	c.173_187del, p.(Gln58_Glu62del) VAF 6%, coverage 235x
2	F/61	Back	1.1 cm Melanoma	Melanoma pT2a	Excision and re-excision SLNB; negative NED at 3 months	c.173_187del, p.(Gln58_Glu62del) VAF 19%, coverage 175x
3	F/44	Ankle	0.5 Atypical nevus	Atypical Spitz tumor	Excision and re-excision NED at 12 months	c.167_182delinsC, p.(Gln56_Gly61delinsPro) VAF 3%, coverage 473x
4	M/45	Lower leg	Atypical nevus. Spitzoid lesion? Melanoma?	Nevus (SPARK)	Recent case	c.308T>A, p.(Ile103Asn), AF:8%, coverage 144x

2.3.3 Molecular Genetic Studies

NGS analysis identified a *MAP2K1* (NM_002755.3) mutation, namely c.173_187del, p.(Gln58_Glu62del) in cases 1 and 2, c.308T.A, p.(Ile103Asn) in case 4, whereas in case 3, c.167_182delinsC, p.(Gln56_Gly61delinsPro) were found. FISH analysis performed in case 1 was negative. No further molecular alterations were detected, including those involving genes related to tumor progression in melanocytic lesions such as *CDKN2A, CCDN1, MYC, PTEN,* and *TERT* (Table 1).

2.4 Discussion

The neoplasms herewith reported manifested cytological features corresponding to a spitzoid lesion, whereas the architectural features were those of a dysplastic nevus, matching the description of so-called SPARK nevus [110]. All 4 neoplasms were superficial compound type lesions composed of variably pleomorphic spindled and epithelioid melanocytes showing dysplastic-like features including confluent horizontally arranged nests bridging of the adjacent rete ridges and broad epidermal/junctional shoulders. Moreover, they displayed epidermal hyperplasia and fibrovascular stromal changes associated with stromal melanin deposits and melanophages. Because of marked cytological atypia, the diagnosis of atypical Spitz tumor was rendered in one lesion (case 3), whereas the lesion in case 2 manifested several atypical histologic features, including slight asymmetry, focal epidermal atrophy and consumption, a moderate to heavy lymphocytic inflammatory infiltrate, mitoses at the base of the lesion where the splaying of melanocytes among the dermal collagen bundles resulted in an infiltrative reticular pattern, and was classified as a melanoma. From a molecular viewpoint, all the tumors harbored a mutation in the *MAP2K1* gene, suggesting that they may represent a distinctive clinicopathologic variant of a melanocytic neoplasm. *MAP2K1* encodes MEK1, a dual specificity protein kinase (serine–threonine and tyrosine kinase) directly downstream of RAF, which acts as an essential component of the mitogenactivated protein kinase (MAPK) signal transduction pathway [112], [113]. Activating mutations of *MAP2K1* leading to a RAF-independent, constitutive activation of MAPK/ERK pathway have been reported in several solid tumors and hematological malignancies including melanoma, lung adenocarcinoma, colorectal cancer, follicular lymphoma, hairy cell leukemia, Langerhans and non-Langerhans cell histiocytosis [114], [115], [116], [117], [118], [119], [120]. Moreover, *MAP2K1* mutations are involved in secondary/acquired resistance to BRAF and MEK inhibitors [121], [122].. On the base of their mechanism of activation of ERK signaling, 3 distinct classes of *MAP2K1* mutations have been proposed, namely RAF-dependent (class I), RAF-regulated (class II), and RAF-independent (class III) [123]. In class I, various point mutations involving *MAP2K1* have been detected in association with a

co-mutation in *BRAF, NRAS,* or *NF1*; these alterations have been considered to amplify the ERK signaling rather than autonomously activate it (RAF dependent). Class II encompasses point mutations and deletions spanning codons 51–58 encoding the negative regulatory region of MEK1; these mutations are less frequently associated with other known driver mutations but can be further activated when phosphorylated by RAF (RAF-regulated). Class III encompasses deletions involving the 98–104 positions of MAP2K1 encoding the kinase domain; they are unassociated with coexistent mutations that activate RAF signaling (RAF-independent) and are insensitive to the ERK-dependent feedback inhibition of RAS and RAF. This classification has important clinical implications in that class II *MAP2K1* mutations account for resistance to RAF inhibitors, whereas neoplasms harboring class III mutations are insensitive to allosteric MEK inhibitors [123]. We reviewed the literature to identify melanocytic lesions with *MAP2K1* mutations reported so far to compare with our group of lesions. *MAP2K1* alterations have been reported among 0.5%–7% of primary and metastatic melanomas, consisting mostly of RAF-dependent and RAF-regulated alterations [114], [124], [125], [126], [127]. Recently, 37 primary and metastatic melanomas harboring *MAP2K1* in-frame deletions have been detected in a cohort of 7119 advanced melanomas. All these alterations involved the kinase domain locus of *MAP2K1* corresponding to class III *MAP2K1* mutations (RAF-independent) except for 6 cases characterized by c.173_187del, p.(Gln58_Glu62del). Given the absence of other detectable driver mutations, the authors proposed *MAP2K1* in-frame deletions as a mitogenic driver in melanoma development. The histologic features of 4 primary melanomas were also reported. These neoplasms presented with a variable morphology and comprised 2 nodular and 2 superficial spreading melanomas. All 4 tumors had a spitzoid cellular morphology, with 3 cases composed of epithelioid cells and one case by both epithelioid and spindled melanocytes. The neoplasms were asymmetric, exophytic neoplasms with an epidermal involvement, an irregular nested dermal growth pattern and were surrounded by a non-brisk lymphocytic infiltrate. Pagetoid spread and ulceration was observed in 3 and 2 cases, respectively; one neoplasm

manifested focal cytoplasmic pigmentation. Both superficial spreading melanomas presented an extension beyond the dermal component. Limitations of this study were the collection of the sample exclusively from patients with advanced melanoma and the lack of follow-up [124]. In-frame deletion involving the kinase domain of MEK1 was also identified in one atypical Spitz tumor in the series reported by Quan et al, occurring as an entirely intradermal melanocytic proliferation with a strong predominance of epithelioid morphology, notable melanin pigment and moderate nuclear atypia,14 in one lesion among 16 cases of pigmented epithelioma (PEM)-like melanocytic neoplasm which was described as a dermal proliferation with a plexiform growth pattern composed of high-grade epithelioid cells and in deep penetrating nevus (DPN) [34], [41]. In 2 cases of our series, we identified *MAP2K1* c.173_187del, p.(Gln58_Glu62del) in-frame deletion. This mutation involves the negative regulatory region of MEK1 and is frequently observed in a subset of Langerhans cell histiocytosis and in extracranial arteriovenous malformations, whereas in melanocytic neoplasms it has been detected in one PEM-like lesion and in one DPN [41], [128], [129], [130]. In case 3, we detected *MAP2K1* c.167_182delinsC, p.(Gln56_Gly61delinsPro) also involving the negative regulatory region of MEK1. This alteration was detected with a low allele frequency (3%). The neoplasm consisted of a mainly junctional melanocytic proliferation with only a minimal dermal component. Cohen et al reported 2 melanocytic tumors with a PEM-like “pure” morphology harboring the same *MAP2K1* c.167_182delinsC, p.(Gln56_Gly61delinsPro) and c.173_187del, p.(Gln58_Glu62del) as were identified in our study [130]. These neoplasms were a mainly dermal, heavily pigmented melanocytic proliferation with a wedge-shaped silhouette and an infiltrative appearance at the base and periphery of the lesion. There was associated irregular epidermal hyperplasia and melanocytes exhibiting accentuation around adnexal structures. Both lesions showed loss of expression of PrkaR1a cytoplasmic staining, without genetic aberration involving the *PRKAR1A* gene. One patient had sentinel lymph node subcapsular and parenchymal tumor deposits.44 In a series of 18 DPN characterized mainly by *CTNNB1* mutations, Yeh et al detected MAP2K1 mutations in

6 cases (33%), including small in-frame deletions and indel mutations as identified in our study [41]. All these mutations were located in the kinase domain except for one case harboring c.173_187del, p.(Gln58_Glu62del). Although the molecular analysis was performed with a limited pan-cancer panel, no other detectable mutations promoting the activation of the MAPK/ERK pathway were found in all these cases, including the main mitogenic drivers commonly seen in solid tumors and melanocytic neoplasms. Our findings and the review of the literature leads us to suggest that deletion involving the region spanning codons 56–62 should be also considered as to be able to activate the ERK signaling pathway in a RAF-independent manner. Although it is not stated that the c.173_187del, p.(Gln58_Glu62del) belongs to the class III in Gao et al, the authors declare the 58th codon as the farthest codon to be deleted in class II. The functional analysis of c.173_187del, p.(Gln58_Glu62del) showed similar RAF-independent activation as with another deletion belonging to the class III (c.306_311del, p.(Ile103Lys104del)). None of the 10 cases with c.173_187del, p.(Gln58_Glu62del) reported in melanocytic neoplasms so far has a MEK activating comutation, which is in line with the class III definition of RAF-independent activation [41], [130]. The neoplasm in case 4 harbored c.308T.A, p.(Ile103Asn), a point mutation hitherto unreported in melanocytic neoplasms, but it was identified by massively parallel sequencing in melanoma cell line resistant to MEK inhibitors.31 This mutation is considered likely pathogenic according to the ClinVar database and it is located along the C helix of MEK1, in the region corresponding to class III as defined by Gao et al [123]. From a morphologic viewpoint, although based on a small series and a literature review, MAP2K1 mutated melanocytic tumors may represent a distinctive variant of spitzoid melanocytic lesions encompassing a morphologic spectrum that ranges from a SPARK-like lesion (when mainly junctional) to PEM-like (when mainly or completely intradermal). A careful histopathologic evaluation associated with a mutational analysis including genes related to melanoma progression are needed to exclude an aggressive biological behavior. In our small series, the neoplasms showed predilection for female patients and lower legs. Presently, there are not enough data to

clump this entity together with *MAP3K8*-fused melanocytic neoplasms that seem to present an early onset of malignant transformation driven by a *CDKN2A* mutation (33% of cases) [42]. Further studies on similar lesion with a longer follow-up are warranted to better characterize their clinicopathologic features and to clarify their relationship with other well-defined variants of melanocytic tumors.

CHAPTER 3: RESEARCH PROJECT N°3

3.1 RAF1 Gene Fusions as a Possible Driver Mechanism in Rare BAP1-Inactivated Melanocytic Tumors: A Report of 2 Cases *

* *This article has been published in American Journal of Dermatopathology in 2021 (Am J Dermatopathol. 2020 Dec;42(12):961-966).*

3.1.1 Introduction

Cutaneous BRCA1-associated protein (*BAP1*)-inactivated melanocytic tumor (BIMT) (a.k.a *BAP1* inactivated melanocytic nevus/melanocytoma, Wiesner nevus, *BAP1* deficient tumor, melanocytic *BAP1* mutated atypical intradermal tumor etc.) is a group of epithelioid melanocytic neoplasms characterized by the loss of function of *BAP1*, a tumor suppressor gene located on chromosome 3p21 [36]. BAP1 protein is a nuclear-localized deubiquitinase involved in several cellular processes including cell cycle regulation, chromatin remodeling, DNA damage response, differentiation, and cell death [131], [132], [133]. Cutaneous BIMTs occur at any age with equal sex distribution and clinically present as a flesh-colored papule or nodule with a predilection for the head and neck region, followed by the trunk and upper extremities [37]. They occur sporadically or, less commonly, in the setting of an autosomal-dominant cancer susceptibility syndrome caused by a *BAP1* germline inactivating mutation that predisposes to the development of different malignancies including uveal and cutaneous melanoma, mesothelioma, renal cell carcinoma, lung cancer, and several other neoplasms [134], [135], [136], [137], [38]. Histologically, BIMTs mostly present as a polypoid or dome-shaped lesion composed of a mainly dermal proliferation of large epithelioid, usually moderately pleomorphic melanocytes with well-demarcated cytoplasmic borders and copious eosinophilic cytoplasm often surrounded/ permeated by a variably dense lymphocytic infiltrate [138], [139]. A BAP1-negative epithelioid cell component is associated with the residua of a BAP1-positive conventional melanocytic nevus in a majority of cases. From a molecular viewpoint, it has been postulated that *BAP1* inactivation occurs mostly in a preexisting *BRAF* mutated conventional nevus, the latter being consider to represent a driver mutation associated with the conventional melanocytic part of the lesions [140]. Apart from a *BRAF* mutation, an *NRAS* mutation has been reported in rare cases, whereas in some lesions no cooperating/mitogenic driver mutation has been detected [141], [142], [143], [144]. Here, we report 2 cases of BIMT harboring both *BAP1* mutations and *RAF1* fusions, suggesting that the latter can be a mitogenic driver genetic event.

3.1.2 Clinical Case Reports

The first patient (case 1) was a 12-year-old girl who underwent surgical excision of a 0.4-cm lesion on her upper trunk clinically interpreted as a wart. Her medical and available family history was unremarkable. The patient showed no evidence of disease at 26 months follow-up. The second patient (case 2) was a 25-year-old woman who presented with a 1-cm retroauricular nodule. She reported no personal or family history of *BAP1*-associated neoplasms. She was followed up for 15 months; several melanocytic lesions were removed, all of them were conventional nevi and retained BAP1 nuclear expression immunohistochemically.

3.1.3 Histopathological and Immunohistochemical Studies

The lesions in both cases appeared as a polypoid or dome-shaped combined melanocytic neoplasm with a predominant dermal population of closely packed, medium-sized to large epithelioid melanocytes and minor, mostly peripherally located residua of a conventional nevus represented by small type B melanocytes, with a Breslow thickness of 1.9 and 8.4 mm, respectively (Figs. 5A and 5A). The epithelioid melanocytes possessed moderately pleomorphic, sometimes eccentrically located nuclei and abundant eosinophilic cytoplasm with prominent cytoplasmic membranes (Fig. 5C). Binucleated epithelioid cells and single necrotic (pyknotic) melanocytes were observed. In both cases, there was cytoplasmic clearing, being more prominent and extensive in case 2. Some epithelioid cells showed large vacuoles that have dislodged the nucleus at the periphery of the cells, imparting them a signet-ring cell appearance. Occasional cells with cytoplasmic clearing resembled the so-called ball-in-mitt structures [145]. Whereas in case 1 only a single dermal mitosis was found after a search on serial sections, in case 2 the mitotic rate was 2 mitoses/mm2, including mitotic figures in the deeper part of the lesion. An inflammatory infiltrate was moderate-to-heavy in case 1 and scarce in case 2. In both lesions, there was bridging of the adjacent melanocytic nests at the dermo-epidermal junction, occasioning a resemblance to dysplastic features (Figs. 5B). Whereas in case 1 the junctional nests

were composed of intermixed small and large melanocytes, in case 2 only small conventional melanocytes were seen, but, in addition, concentric fibrosis around the junctional nests was present. In case 1, rare intraepidermal epithelioid melanocytes, arranged both as solitary units and small nests were noted, a feature not evident in case 2 (Fig. 5E). In addition, in case 2, the conventional melanocytes formed single cells stands or broader trabecules (congenital nevus features) merging gradually with large epithelioid cells that retained strand-like and trabecular arrangement at the transitional area. Immunohistochemically, in both cases, the whole neoplasms were negative for BRAF staining. Epithelioid melanocytes showed negative nuclear immunoreaction for BAP1, with unspecific granular cytoplasmic positivity in case 2. Conventional type B melanocytes mainly retained BAP1 nuclear staining, but some small cells were negative both in the junctional nests (including dysplastic-like areas) and in rare nests located in the superficial dermis (mixed nests) (Figs. 5D–F). In case 2, the proliferation index (MIB1) was ,2% with an isolated hotspot (about 10%) in the center of the dermal nodule. Melanocytes partially retained p16 nuclear expression.

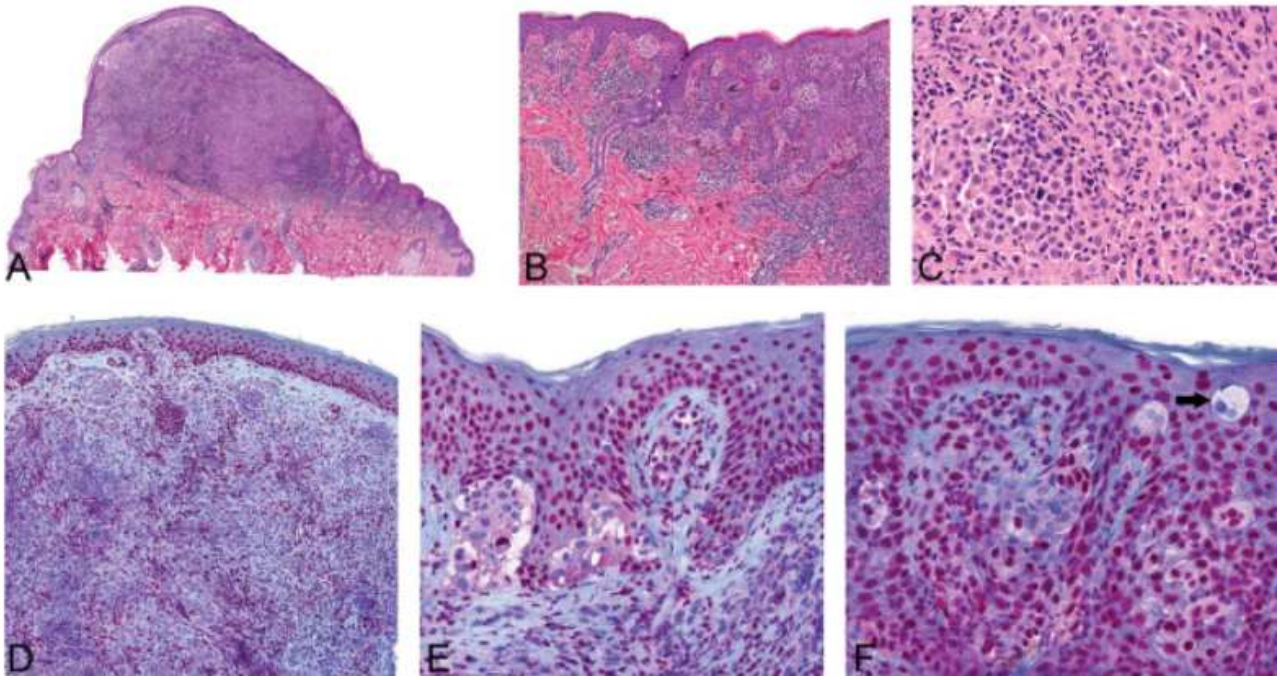

Fig.5 A dome-shaped combined melanocytic neoplasm with a predominant dermal population and a flat base (A). Dysplastic-like features at the junction with bridging of adjacent melanocytic nests (B). A close-up view of the dermal population shows medium-sized to large epithelioid melanocytes with moderately pleomorphic,

sometimes eccentrically located nuclei and abundant eosinophilic cytoplasm (C). BAP1 staining highlights nuclear loss in both junctional and dermal epithelioid melanocytic component (D). Dysplastic junctional nests composed of both BAP1-negative and positive melanocytes (E). Note a "mixed nest" composed of BAP1-positive and BAP1-negative melanocytes and an intraepidermal binucleated epithelioid melanocyte (arrow) (F).

3.1.4 Molecular Genetic Studies

Both cases were tested by Sanger sequencing for *BAP1* gene mutation, using polymerase chain reaction amplification of the whole coding sequence with in-house designed primers, with the annealing temperature of was 608C and by DNA and RNA next generation sequencing (NGS), using 2 panels (VariantPlex and FusionPlex Solid tumor, ArcherDX, Boulder, CO), as reported elsewhere [26]. In addition, case 1 was tested using the TruSight Tumor 170 panel (Illumina, San Diego, CA) described previously [146]. In case 1, the TruSight Tumor 170 panel identified a *BAP1* gene mutation (c.14 G.A, p. Trp5Ter) with an allele frequency of 6% (verified by repeating the NGS from independent DNA sample), whereas the RNA panel showed a *TRAK1-RAF1* fusion. Both *BRAF* and *NRAS* tested wild type. The lesion also yielded a mutation in the *PIK3CG* gene and copy number gain of *FGFR1* and *ERCC2*. In case 2, Sanger sequencing revealed a *BAP1* mutation (c.1832_1842del, p. Glu611GlyfsTer3) and the FusionPlex Solid Tumor panel identified a GIT2-RAF1 fusion (Fig. 6).

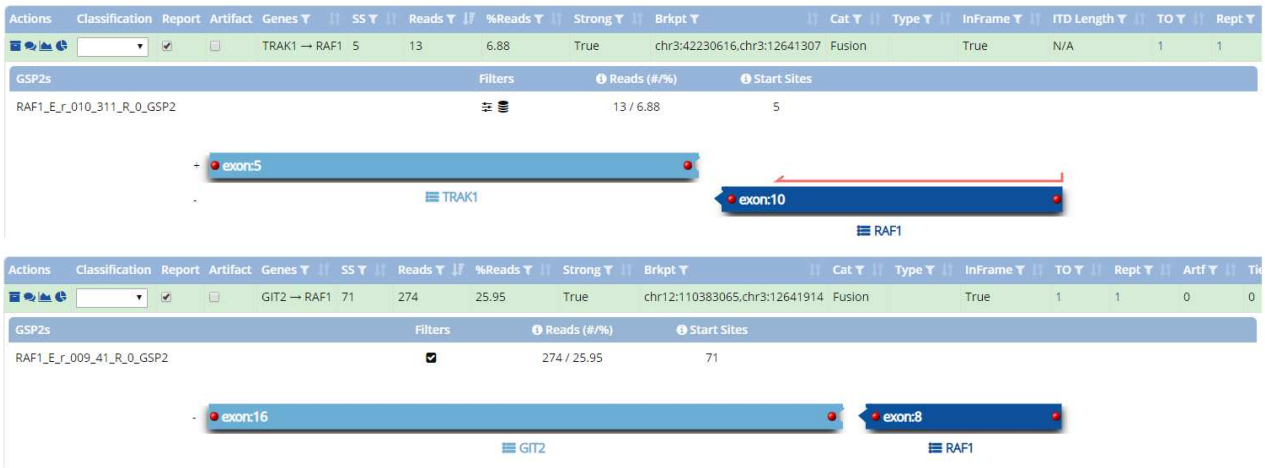

Fig.6 Screenshot from the Archer Analysis software, depicting the details of the detected (A) *TRAK1-RAF1* and (B) *GIT2-RAF1* fusions: SS—the number of unique start sites supporting the event. Reads—the number

of unique reads supporting the event. % Reads—the percent of reads supporting the event. Strong—true/false value indicating whether the fusion has passed all strong evidence filters. Brkpt—exact genomic coordinates of the detected RNA breakpoint. InFrame—true/false/unknown value indicating whether the event is predicted to be in-frame, and thus a functional transcript.

3.1.5 Discussion

Previous studies identified a *BRAF V600E* mutation as the mitogenic driver mutation in BIMTs [36] [147]. In addition, 2 cases of cutaneous BIMTs with an *NRAS* mutation have so far been reported. Both lesions manifested remnants of a conventional nevus and had typical cytological features. However, bean-shaped nuclei of epithelioid cells and intracytoplasmic melanin have been observed, leading the authors to suggest some histological deviation from BRAF-mutated cases [144], [148].Our review of the literature on BIMTs revealed that in 17 cases (18%) with available molecular genetic data, neither *BRAF* nor *NRAS* mutation was detected (Table 2), suggesting another initiating genetic mechanism for these lesions [36], [135], [138], [149], [140], [148], [144], [141], [150], [142], [143], [39].

Authors/ year	***BRAF* (positive/tested cases)**	***NRAS* (positive/tested cases)**	**Method**
Wiesner et al. 2011	37/42	NA	Sanger
Njauw et al. 2011	4/6 (1 nevoid melanoma)	NA	*BRAF* sequencing
Wiesner et al. 2012	8/9	NA	Sanger
Carbone et al 2012	9/9	NA	Multiplex PCR + automated fluorescent labeling
Busam et al. 2013	1/1	NA	Sanger
Blokx et al. 2014	0/1	1/1	NGS
Yeh et al. 2014	12/17	1/17	Sanger
Gerami et al. 2015	0/3 (2 melanomas)	NA	Cobas 4800 BRAF V600
Ardakani et al. 2015	1/1	0/1	NGS
Requena et al. 2015	0/1	0/1	Sanger
Soares de Sà et al. 2019	2/3	0/3	Targeted NGS
Aung et al. 2019	1/1 (BAP1-melanomas)	NA	*BRAF* sequencing
Total	75/94 (80%)	2/23 (8%)	

Table 2 Summary of previous molecular genetic studies on BIMTs

We present herein 2 *BAP1*-inactivated melanocytic lesions associated with a *RAF1* fusion, a hitherto undescribed event. As both neoplasms proved to be *BRAF* and *NRAS* wild type, we suggest that *RAF1* fusions can represent an underlying mitogenic driver genetic event in these cases. *RAF1* fusions have been reported in various types of tumors including melanoma [126]. Recently, *RAF1* fusion have been reported in 0.6% of melanomas (40 cases on a cohort of 7119) analyzed with comprehensive genomic profiling by a hybrid capture-based DNA sequencing platform. Recurrent partners identified included *MAP4, CTNNA1, LRCH3, GOLGA4, CTDSPL,* and *PRKAR2A*. All the detected fusions preserved the region encoding the RAF1 kinase domain [151]. With respect to the fusions detected in our study, *TRAK1-RAF1* fusion found in case 1, has been identified in one sample of the dataset of the TCGA Research Network (https://www. cancer.gov/tcga) of Skin Cutaneous Melanoma (1/476). In our case, we observed a breakpoint joining exons 5 and 10, whereas in the TCGA case, the breakpoints involved exons 9 and 7 of *TRAK1* (NM_014965.4) and *RAF1* (NM_002880.3), respectively. The *GIT2-RAF1* fusion detected in case 2 is joining exons 16 and 8 of *GIT2* (NM_057169.3) and *RAF1* (NM_002880.3), respectively. To the best of our knowledge, *GIT2* has so far not been described as a fusion partner of *RAF1*. Both fusions we detected preserve the tyrosine kinase domain. The fusions of RAF1 kinase domain to diverse 50 partners lead to MAPK pathway activation and are sensitive to multi-kinase inhibitors and partially responsive to MEK inhibitors. RAF proto-oncogene serine/threonineprotein kinase (CRAF) encoded by RAF1 functions as an alternative MAPK signaling mechanism as it forms dimers with wild type BRAF [152], [153], [154], [155]. In case 1, the allele frequency of the *BAP1* mutation is relatively low, suggesting it is a somatic mutation. In case 2 we have determined that the origin of detected *BAP1* mutation is somatic by analyzing a peripheral blood sample from the patient. Apart from *RAF1* fusions and *BAP1* mutation, a mutational analysis performed in both our lesions failed to detect copy number variation in 6p, 11q, and 9p21 (*CDKN2A*) or promoter hotspot mutations of *TERT* found frequently in melanoma. The analysis of case 1 showed additional mutation in *PIK3CG* and copy number variation

in *FGFR1* and *ERCC2*. The effects of these alterations in this setting are unknown and establishment of their significance is beyond the scope of this study. Few histopathological changes detected in our cases merit a short comment, as some of them have never been reported. For example, we have identified nests composed of both BAP1-positive and BAP1-negative melanocytes, both epithelioid and conventional ones (Figs. 5E-F). The presence of BAP1-inactivated melanocytes in several conventional nests located in different parts of the lesion, along with transitions of strands and trabecules of conventional type B-melanocytes to epithelioid melanocytes retaining the same arrangement supports the proposed progression model in which a BAP1-inactivated clone starts inside a *BRAF/NRAS* mutated (congenital) nevus replacing the original nevus population by BAP1-inactivated cells with epithelioid morphology. Mixed nests might have been overlooked in the previously published articles. Similar mixed nests can be recognized in the first series reported by Wiesner et al (Fig. 3D, same figures showed in the last edition of WHO classification of skin tumors) but were not specifically commented on [36]. Furthermore, both lesions we report herein manifested junctional changes resembling dysplastic phenotype (Figs. 5B). The association with a dysplastic nevus in BIMTs is rare and has been observed in only 4/94 combined cutaneous BIMTs [37]. Gerami et al described a patient with *BAP1* germline mutation who presented with multiple phenotypically dysplastic nevi. Six lesions showed an epithelioid morphology and intraepidermal changes typical of a superficial spreading melanoma, including extensive pagetoid spreading. In all these cases, melanocytes were both BAP1 and BRAF negative on immunohistochemistry, and no *BRAF* mutation was found by a molecular analysis performed in 2 cases [141]. In both lesions we describe, there was cytoplasmic vacuolization, being more conspicuous in case 2 in which mononucleated cells, binucleated cells with mirroring nuclei, multinucleated cells and scattered highly pleomorphic giant melanocytes displayed this alteration. In some melanocytes, the appearances were reminiscent of intracytoplasmic lumina and resembled signet-ring cells. Clear cell change has been previously observed in cutaneous BIMTs and has been considered to be the expression of alterations in

degeneration/senescence pathways affecting melanogenesis; we concur [143]. BAP1 protein implied in several cellular processes could play a role in degenerative clear cell changes. A thick granular cytoplasmic pattern of BAP1 staining representing cytoplasmic accumulation of the altered protein was a conspicuous finding in case 2. This displayed a nodular expansile growth pattern with a deep pushing border. In the upper part, the epithelioid cell nodule squeezed conventional melanocytes with intermixed trabecules, nests, and single BAP1-inactivated cells showing an infiltrative pattern. Two dermal mitoses/mm2 including a mitosis at the base of the lesion were seen. On immunohistochemistry, an isolated hotspot of 10% of MIB-1 positive cells in the center of the dermal nodule was found. We believe these atypical features do not qualify the neoplasm as melanoma. According to the Working Group of the WHO, this lesion can be classified as BAP1-inactivated melanocytoma [10]. In conclusion, we have reported 2 cases of cutaneous BIMT in which, along with a *BAP1* mutation, *RAF1* fusions have been identified. We suggest that *RAF1* fusions may represent a mitogenic driver genetic mechanism, but additional cases to support this presumption are needed to be identified.

3.2 Vulvar Pigmented Epithelioid Melanocytoma with a Novel HTT-PKN1 Fusion: A Case Report *

* *This article has been published in American Journal of Dermatopathology in 2020 (Am J Dermatopathol. 2020 Jul;42(7):544-546.).*

3.2.1 Introduction

Pigmented epithelioid melanocytoma (PEM) is a melanocytic neoplasm microscopically characterized by a mainly dermal proliferation of epithelioid and spindled melanocytes with copious intracytoplasmic melanin admixed with melanophages [30]. This term was introduced to encompass histologically similar or indistinguishable melanocytic lesions formerly named as “animal-type” or pigment-synthesizing melanoma and epithelioid blue nevus occurring in the

setting of Carney complex or sporadically [31] [32]. Clinically, PEM typically presents with a darkly pigmented nodule located on the face, trunk, extremities, or genitalia of young patients. Although PEM may present with alarming histological features such as rare deep mitotic figures and areas of necrosis, it is considered a low-grade melanocytic tumor with a high rate (44%–60%) of regional lymph nodes involvement but with an indolent clinical course [30] [156]. Specific genomic aberrations in the regulatory subunit alpha (PRKAR1A) mutations have been detected in both syndromic and sporadic forms of PEM, while protein kinase C alpha isoform (PRKCA) fusion has been frequently observed in the sporadic cases [33], [157], [34]. However, no molecular alterations have been found in some cases. We hereby report a PEM occurring on the vulva of a young woman in which RNA sequencing detected a novel fusion transcript *HTT-PKN1*, expanding the molecular spectrum of PEM. In addition, an ATM missense mutation was found.

3.2.2 Case Report

A 24-year-old woman with no personal or family history of melanoma or other Carney complex–associated neoplasms presented with a 1-cm darkly pigmented nodule on the vulva of unknown duration. The lesion was excised with wide margins, and histological examination revealed a polypoid skin with a symmetrical heavily pigmented dermal nodule separated from the normal overlying epidermis by a grenz zone. Breslow thickness was 2.3 mm. The neoplastic cells were arranged as small clusters of closely packed cells separated by thin strands of collagen bundles forming a nodular or sheet-like growth pattern. Scattered pigmented single cells infiltrating between the collagen bundles were observed at the periphery. Copious amounts of melanin pigment in the cytoplasm occasioned a resemblance to melanophages at first glance. The cytologic details were appreciated in the melanin-bleached sections that revealed monomorphic to slightly atypical epithelioid cells with round to oval nuclei, visible eosinophilic nucleolus, a thickened nuclear membrane, and abundant gray cytoplasm. No cellular maturation was observed toward the base of the lesion. Melanophages were rare and intermixed with the melanocytic population. Lymphocyte’s inflammatory infiltrate

was scarce. No mitotic figures were found. Intralesional necrosis was not observed. There was no evidence of a pre-existing melanocytic nevus (Fig. 7). F1 Immunohistochemical analysis revealed diffuse-positive stain for melanocytic markers tyrosinase, Melan-A, HMB-45, Sox10, and S-100. Expression of cyclic AMP-dependent protein kinase 1 R1a (PrkaR1a) was retained in all melanocytes. The FusionPlex Solid Tumor kit (ArcherDX) containing 288 targets in 53 genes was used, and all steps were performed after the Archer's FusionPlex protocol for Illumina (ArcherDX, Inc, Boulder, CO). RNA sequencing analysis identified a single fusion composed by the intact catalytic domain of the serine/threonine *PKN1* fused in frame with the N-terminal of *HTT*. VariantPlex Solid Tumor (ArcherDx) for the detection of single-nucleotide variants, copy number variations, insertions, and deletions in 67 genes associated with solid detected ATM c.1229T.C and p.(Val410Ala) missense mutation, COSM21825. No further mutations including a *TERT-promoter* hotspot mutation were detected. Based on the clinical, histological, and molecular findings, a diagnosis of PEM was made. Whole-body positron emission tomography–computed tomography revealed no extracutaneous spread. The patient is alive without recurrence at a 6-month follow-up.

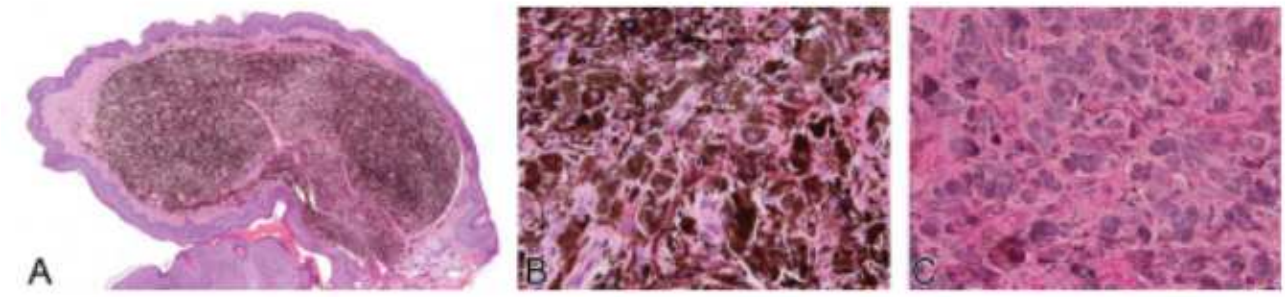

Fig.7 A symmetrical polypoid neoplasm showing a heavy pigmented dermal nodule separated from the normal overlying epidermis by a grenz zone (A). A close-up view of the lesion: small clusters of closely packed melanocytes separated by thin strands of collagen bundles with copious amount of melanin pigment in the cytoplasm (B). Melanin-bleached sections show monomorphic to slightly atypical epithelioid cells with round to oval nuclei AU4 and abundant gray cytoplasm (C). Note the visible eosinophilic nucleoli (arrow).

3.2.3 Discussion

Two molecular studies conducted on large series of PEM identified at least 2 subtypes with different clinical, histological, and molecular profiles. The first one, characterized by PRKCA fusions, is comprised of sporadic cases occurring in young patients and microscopically demonstrates a sheet-like pattern of monomorphic epithelioid cells with a high mitotic rate (,1 to 3/mm2), reveals epidermal hyperplasia, and lacks a conventional nevus component ("pure" PEM). The second variety occurs either sporadically or in the setting of Carney complex and apparently follows a two-hit model with biallelic inactivation of *PRKAR1A* gene in a *BRAF*-mutated melanocytic nevus ("combined" PEM). In the latter, melanocytes show loss of PRKAR1A expression in PEM component [34], [35]. However, in several PEMs, no genetic alterations have been found. The possible involvement of genes of the adenylate cyclase complex or additional kinase fusions has been hypothesized [35]. We hereby reported a case of sporadic PEM occurred on the vulva of a young patient in which RNA sequencing detected a novel *HTT-PKN1* fusion and a missense mutation in *ATM*. Protein kinase N1 (PKN1) is an atypical serine/ threonine protein kinase having a catalytic domain homologous to that of PKC [158]. PKN1 acts as a Rho effector in several contexts and can regulate AKT and mitogen-activated protein kinase pathways (MAPK) [159]. PKN1 fusions have been detected in different samples of solid tumors with four 50 fusion partners: *TECR, ANXA4, GIPC1,* and *LDLR* [160], [161]. It has been speculated that fusions resulting in a PKN1 deletion of the regulatory N-terminal domain may lead to constitutive activation by derepression of the kinase activity and the subsequent enhanced cell proliferation in the absence of any contribution from the nonkinase fusion partners [161]. Interestingly, *PKN1* has been implicated in the complex regulation of the Wnt/b-catenin pathway in melanoma [162]. However, the role of *PKN1* is not fully understood. We also detected a missense mutation in *ATM*. This molecular alteration has been observed with a high frequency (11%) as a concomitant mutation in *KIT*-mutated melanomas [163]. However, the role of this mutation is still unclear. Histologically, our lesion was entirely dermal with an uninvolved overlying epidermis and composed by highly pigmented sheet-like aggregates of monomorphic epithelioid

melanocytes resembling tumoral melanosis at first glance.20 In melanin-bleached sections, densely packed monomorphic to slightly atypical epithelioid melanocytes with eosinophilic nucleoli and thickened nuclear membrane were appreciated. No conventional nevus component was observed. Albeit pure PEM is considered a distinctive entity, a PEM-like morphology has been observed in several melanocytic lesions harboring genomic alteration characteristic of Spitz tumor or blue nevi, including *BRAF, MAP2K1, GNAQ, CYSLTR2* mutations, and *NTRK1, NTRK3*, and *ALK* fusions [34], [35] [44]. Lesions harboring genetic alterations in *GNAQ* and *CYSLTR2* have been classified as blue nevi. Potential diagnostic clues suggested by the authors included smaller melanocytes surrounded by a sclerotic stroma in *GNAQ*-mutated lesions and a fascicular arrangement of mediumto large-sized spindled melanocytes in tumors with *CYSLTR2* mutations [35], [44]. *NTRK1, NTRK3,* and *ALK* fusions detected in PEM-like neoplasms rather put them in the category of Spitz tumors. Interestingly, both *PRKAR1A* mutation and *MYO5A– NTRK3* fusion have also been reported in one PEM [34]. Of note, *MAP2K1* alterations have been identified in pure PEM suggesting that a subset of PEM develops from a *MAP2K1* alteration followed by a defect in the *PRKAR1A* gene. These data indicate that PEM may represent a genetically heterogeneous group of melanocytic tumors. In conclusion, this is the first case of PEM harboring a novel *HTT–PKN1* fusion. The lesion occurred as a sporadic lesion and presented with a pure PEM morphology that is in accordance with the recent observation that fusion-driven PEMs display a pure PEM morphology characterized by a relatively monomorphic population of epithelioid melanocytes.

CHAPTER 2: RESEARCH PROJECT N°4

4. Novel insights into the BAP1-inactivated melanocytic tumor *

* *This article has been published in Modern Pathology in 2021 (Mod Pathol. 2021 Dec 2).*

4.1 Introduction

BAP1-inactivated melanocytic tumor (BIMT) is a distinctive melanocytic neoplasm, nowadays listed in the WHO classification among combined nevi [10]. The rationale for such an interpretation is the identification of remnants of a conventional nevus with retained nuclear expression of BAP1 in many cases of BIMT that is otherwise mainly composed of BAP1-negative large epithelioid melanocytes with well-demarcated cytoplasmic borders and copious eosinophilic cytoplasm. From a molecular biological viewpoint, it is characterized by a *BRAF* mutation (or, rarely, *NRAS* mutation or *RAF1* fusion) considered to represent a mitogenic driver alteration and biallelic inactivation of the *BAP1* gene, leading to dysfunction of BAP1 protein [20], [148], [164], [138], [12]. BIMTs may occur at any age, with equal sex distribution and clinically present as a flesh-colored papule or nodule favoring the head and neck region, trunk, and upper extremities [37], [36]. They occur sporadically or, less commonly, in the setting of an autosomal dominant cancer susceptibility syndrome caused by a *BAP1* germline inactivating mutation that predisposes to uveal and cutaneous melanoma, mesothelioma, renal cell carcinoma, lung cancer, and several other neoplasms [134], [135], [136], [137], [36]. Most BIMTs seem to follow an indolent clinical course but cases of *BAP1*-inactivated melanomas have been

reported, suggesting a possible progression into an aggressive neoplasm. [36] [135], [150], [165], [141], [39]. For lesions with atypical features, the term "melanocytoma" has been proposed by the WHO classification; however, no clear-cut criteria are established [10]. Albeit most BIMTs microscopically manifest peripherally located residua of a conventional nevus, occasional neoplasms are exclusively composed of large epithelioid melanocytes [138]. Other reported microscopic variations include binucleation and multinucleation of epithelioid cells, conspicuous lymphocytic infiltrate, small epithelioid melanocytes, rhabdoid cells, clear cells, and neoplasms with a conventional nevus-like morphology, suggesting a wider spectrum of histological presentation [36], [37], [135] [149] [166], [167]. In fact, in our practice, we observed some hitherto underrecognized microscopic features, especially regarding several types of multinucleated/giant epithelioid melanocytes, nuclear characteristics (nuclear blebbing, nuclear budding, micronuclei, shadow nuclei), cell-in-cell structures (entosis), and other features that suggest more complex underlying pathophysiological events. We hereby report a clinical, morphological, and molecular analysis of 50 BIMTs, extending the morphological and mutational spectrum of the neoplasm.

4.2 Materials and Methods

4.2.1 Case Selection

All 50 BIMTs from 36 patients were identified prospectively and retrospectively from the institutional and referral databases of the authors from 2004 to 2020. The inclusion criteria were the typical microscopic features with the loss of BAP1 nuclear staining on epithelioid melanocytes detected immunohistochemically. Clinical follow-up was obtained from the patients, their physicians, or from referring pathologists. Four cases have been previously reported [164], [168].

4.2.2 Microscopic assessment

Histological features were individually assessed by two dermatopathologists (D.V.K. and M.D.). The assessment parameters included the silhouette of the lesion (polypoid,

verrucous, dome-shaped, or flat), symmetry, tumor thickness (Breslow index), type of lesion (combined one, that is having residua of a conventional nevus or “pure” one which is exclusively composed of BAP1- inactivated melanocytes), epidermal changes (irregular hyperplasia, atrophy/consumption, ulceration, or irritation), junctional component (presence and extension of BAP1-inactivated melanocytes), dermal growth pattern (nodular, sheet-like, nests, trabecular arrangement, areas with dyscohesive growth), cytological features, degree of nuclear pleomorphism, mitotic rate and mitoses distribution, cellular maturation, adnexal, vascular or perineural extension, lymphocytic infiltrate (scarce to absent versus moderate to heavy) and stromal changes (mucin deposits, melanin deposits, adipocytic metaplasia, presence of prominent fibrosis). While accessing cytological characteristics, we encountered and detected changes reported in the context of senescence, and cell-in cell structures (entosis).

4.2.3 Immunohistochemical studies

Immunohistochemical staining for BAP1 was mostly performed initially at the time of the diagnosis (in a few cases retrospectively) but were repeated for consistency using BAP1 (C-4, Santa Cruz) 4-µm sections cut from formalin-fixed, paraffin-embedded (FFPE) tissue using Ventana Benchmark XT automated stainer (Ventana Medical System, Inc, Tucson, AZ), according to the manufacturer’s protocol. Additionally, staining for tyrosinase, S100 (polyclonal, Ventana), and BRAF V600E (VE1, Ventana) were performed in all cases.

4.2.4 Molecular analysis

Sample preparation

The FFPE tissue from selected cases was evaluated by a pathologist and relevant blocks were selected for molecular genetic analyses. For next-generation sequencing (NGS) RNA-based analyses, the total nucleic acid was extracted using an FFPE DNA kit (with the modified protocol for total nucleic acid extraction, automated on Maxwell RSC 48 Instrument, Promega, Madison, Wisconsin, USA). For DNA-based methods, DNA was

isolated using a DNA mini kit (Qiagen, Hilden, Germany). Purified DNA and RNA were quantified, using the Qubit Broad Range DNA and RNA Assays, respectively (Thermo Fisher Scientific, Waltham, Massachusetts, USA).

Sanger sequencing of BAP1

PCR amplification of the whole coding sequence using in-house designed primers and Sanger Sequencing of *BAP1* were performed. The primers and PCR conditions were reported elsewhere [26]. From eight patients, either peripheral blood or saliva was tested for germline *BAP1* mutations after obtaining the patient's written consent.

BAP1 (3p21.1) copy number changes by fluorescence in situ hybridization (FISH)

For the detection of BAP1 loss, a ready-to-use BAP1/CCP3 FISH Probe kit (Cytotest Inc., Washington DC, Maryland, USA) was used. The FISH procedure was performed as described earlier [169]. One hundred randomly selected non-overlapping tumor nuclei were evaluated in all samples. *BAP1* gene loss was calculated as the number of cells with loss (only one specific signal) divided by the total number of nuclei counted. The test was considered positive when >45% of nuclei had gene loss (mean +3 standard deviation in normal non-neoplastic tissues).

BRAF hotspot mutations

Analysis of eight *BRAF* hotspot mutations using the BRAF 600/601 StripAssay (ViennaLab Diagnostics GmbH Vienna, Austria) with analytical sensitivity 1% of the mutated allele was performed according to the manufacturer's instructions.

Fusion detection

Fusion transcripts detection was performed using the FusionPlex Solid Tumor kit (ArcherDX Inc., Boulder, CO) and TruSight Tumor 170 (Illumina, San Diego, CA), both according to the manufacturer's instructions. The process of FusionPlex library preparation and sequencing was described previouslys and the data analysis was performed using the Archer Analysis software version 6.2.1 [146]. The details of fusion detection using the RNA part of TruSight Tumor 170 are described below.

Mutation analysis and copy number variations (CNVs) using NGS

Two gene panels of similar content (Comprehensive Cancer Panel, Qiagen; and TruSight Tumor 170, Illumina) were used for mutation detection. For both kits, the quality of DNA was assessed using the FFPE QC kit (Illumina), whereas the quality of RNA was tested using Agilent RNA ScreenTape Assay (Agilent, Santa Clara, CA). DNA samples with Cq < 5 and RNA samples with DV200 ≥ 20 were used for further analysis. The TruSight Tumor 170 kit DNA and RNA libraries were prepared according to the manufacturer's protocol, except for DNA enzymatic fragmentation using KAPA FragKit (KAPA Biosystems, Washington, MA). Sequencing was performed on the NextSeq 500 sequencer (Illumina) following the manufacturer´s recommendations. Data analysis was performed using the TruSight Tumor 170 application on BaseSpace Sequence Hub (Illumina). CNVs were reported from the TruSight Tumor 170 application and the internal cutoff for reporting was set at >1.5 or <0.5 fold change. DNA small variant filtering and annotation were performed using the cloud-based tool Variant Interpreter (Illumina). Custom variant filter was set up including only variants with coding consequences and The Genome Aggregation Database database (GnomAD) frequency value <0.01 [170]. Known benign variants according to the ClinVar database were excluded [171]. The remaining subset of variants was checked visually and suspected artefactual variants were excluded. Alternatively, a library of 271 cancer-related genes using Comprehensive

Cancer Panel was constructed using 250 ng of DNA. The library was sequenced on Nextseq 500, aiming at average coverage 350× after deduplication of molecular barcodes to detect 10% allele frequency with 95% sensitivity. Variants were called using Qiagen's proprietary pipeline. Subsequently, the variants were filtered using the calculated limit of detection for each sample. Variants more frequent than 0.01 in the GnomAD database were excluded as were known benign variants according to the ClinVar database. The remaining subset of variants was checked visually, and suspected artefactual variants were excluded. Two tumors from one patient with multiple lesions were tested using

NGS with MelArray, which comprises analysis of 57 genes, including BAP1, and BRAF, CNVs, tumor mutation burden (TMB), and HLA-typing [172].

FISH for copy number changes of RRB1, CCND1, MYB, MYC, and CDKN2A

FISH analysis and interpretation for a four-probe assay targeting 6p25 (RRB1), 11q13 (CCND1), 6p23 (MYB), and CEP6 (Vysis, Abbot Molecular) and for a three-probe assay targeting 9p21 (CDKN2A), 8q24 (MYC), and CEP9 were used as previously described by Gerami el al. [51]. The probes were hybridized on 4 μm-thick FFPE tissue sections, and the number and localization of the hybridization signals were assessed in a minimum of 100 randomly selected interphase nuclei with well-delineated contours.

4.3 Results

4.3.1 Clinical findings

The clinical results are summarized in Table 3. There were 25 female and 11 male patients, with a mean age of 30.4 years (range 7–81 yrs, median 25 yrs). Eight patients (22%) had more than one BIMT. Two patients were first-degree relatives. Locations included the head and neck area (n = 19), trunk (n = 24), upper extremities (n = 3), and genital area (n = 1); in three cases location was not specified. The clinical presentation was a flesh-colored exophytic lesion in all cases, with a median size of 0.6 cm (range 0.2–1.2 cm). In some lesions, a peripheral pigmented rim was evident, like a halo reaction. A melanocytic nevus was suspected by clinicians in 16 cases, in six of which the presence of focal pigmentation was also specified. Other clinical diagnoses included hemangioma, histiocytoma, pigmented basal cell carcinoma, and fibroma. In 21 patients, personal history of malignancy was known, and the diagnoses included uveal melanoma (n = 1), cutaneous melanoma (n = 5), mesothelioma (n = 1), renal (n = 3), lung (n = 3), breast (n = 1), thyroid cancer (n = 1) and schwannoma of the cerebellopontine angle (n = 1). In 15 cases, family or personal history of malignancy was unknown. All cutaneous tumors were completely excised. No lymph node

enlargement was clinically evident at the time of diagnosis. Clinical follow-up was available in 21 cases (34.3 months; range 6–106 months). All but two patients were alive and well without recurrence or metastasis). Two patients with the adverse clinical course included a 7-year-old girl with a family history of melanoma and a lesion on the lower neck developed a nodal metastasis in the ipsilateral triangular muscular space lymph node 6 years after the excision of the primary tumor; 8 years later after the onset of the disease, she underwent surgery for a second BIMT. Presently, she has no evidence of disease at the 8-year follow-up. The other patient also presented with multiple lesions and developed local recurrence in the scar (time after surgery remained unknown).

Table 3. Main clinicopathological data

Clinical data	**Frequency**
Gender distribution	
Male	11
Female	25
Age, yrs	
Range	7-81
Mean	30.4
Median	25
Size (mm)	
Range	0.2-1.2
Mean	0.6
Median	0.5
Location	
Head/Neck	19
Trunk	24

Upper extremities	3
Genital area	1
Unknown	3
Personal (p) or family (f) history of malignancies	
Multiple BIMTs (patients)	8
Uveal melanoma (p)	1
Cutaneous melanoma (p)	5
Mesothelioma (p)	1
Renal cell carcinoma (p&f)	3
Colorectal carcinoma (f)	3
Lung& bronchial cancer (p&f)	3
Prostata carcinoma (f)	2
Breast cancer (p)	1
Leukemia (f)	1
Schwannoma (p)	1
Thyroid cancer (p)	1
Renal cell carcinoma (f)	1
Gynecological malignancy, NS (f)	1
Unknown (f)	15
Follow-up (months)	
Range	6-106
Mean	34.3
Median	30

NS: not specified p personal history, f family history

4.3.2 Histopathological findings

The accessed histopathological features are summarized in Table 4. The most common microscopic presentation was a predominantly dermally based melanocytic neoplasm with a dome-shaped or polypoid silhouette and an uneven, flat, or wedge-shaped base. A bulb-like deep extension was observed in nine cases. The mean Breslow thickness was 3.1 mm (range from 0.4 to 11 mm). Most neoplasms (n = 45, 90%) were associated with the remnants of a conventional melanocytic nevus (combined BMITs), whereas five lesions (10%) were exclusively composed of BAP1-negative epithelioid melanocytes (pure BMITs). In most combined lesions, the remnants of conventional nevus were a minor component, usually situated at the periphery of neoplasm, as intact pre-existing nests or nests being surrounded and infiltrated by epithelioid melanocytes, resulting in mixed nests (Fig. 8). There were congenital (n = 26, 52%) features (splaying of melanocytes between collagen bundles, adnexotropism) and, rarely, dysplasticlike features (bridging of the adjacent junctional nests of conventional and/or epithelioid melanocytes with or without concentric/lamellar fibrosis) (n = 7, 14%). Dermal conventional melanocytes at the transitional area often appeared to be squeezed by growing epithelioid melanocytes (n = 17, 34%) that mainly formed large expansile nodules, often coalescing and producing sheet-like areas, merging with the residual conventional nevus. There were also well-defined nests composed of exclusively epithelioid melanocytes, sometimes infiltrated by lymphocytes “dissolving” them (Fig. 8C). Epithelioid melanocytes also often demonstrated a dyscohesive or trabecular growth and/ or single-cell arrangement toward the periphery of the lesion. The predominant cell population was comprised of round to oval epithelioid melanocytes with well-demarcated cytoplasmic borders. The nuclei of the epithelioid cells displayed extreme variability in size, ranging from small (size of lymphocyte or plasma cell) to large/giant (five times or more the size of lymphocyte/plasma cell), with an approximately equal mixture of small, medium-sized and large epithelioid cells in 20

cases (40%). Large epithelioid melanocytes clearly dominated in 14 cases (28%), whereas small epithelioid cells dominated in 16 (32%) cases. Akin to nuclei, the amount of the cytoplasm of the epithelioid cells was variable. In most cases (80%), the cytoplasm of epithelioid cells, irrespective of the size and shape (see below), contained micronuclei (1/3 or smaller compared to the main nucleus), sometimes detaching from the main nucleus.

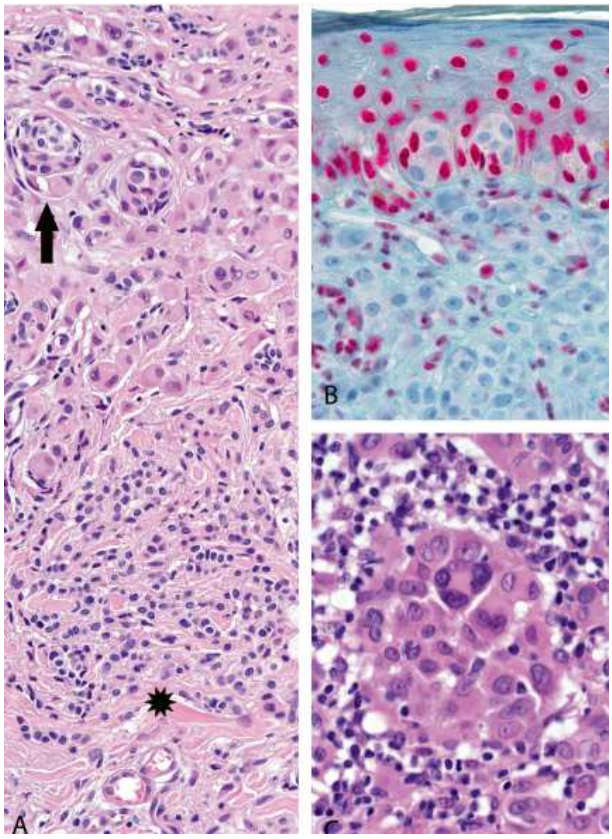

Fig.8 Mixed and "dissoved" nests in BIMT. Remnants of conventional nevus with congenital features showing the splaying of melanocytes between collagen bundles (asterisk). Note the BAP1-inactivated epithelioid cells merging with conventional melanocytes wrapping around the nests, resulting in mixed nests composed of both conventional melanocytes and epithelioid cells (arrow) (A). Mixed nests composed of both BAP1-inactivated and BAP1-positive conventional melanocytes at the junction (B). A nest composed of exclusively BAP1-inactivated epithelioid melanocytes infiltrated by lymphocytes resulting in a dyscohesive growth pattern ("dissolved" nest) (C).

Often, cells with cytoplasmic protrusions resembling proboscis were seen (ant-bear cells), with nuclei or micronuclei at the end of the protrusions (Fig. 9B).

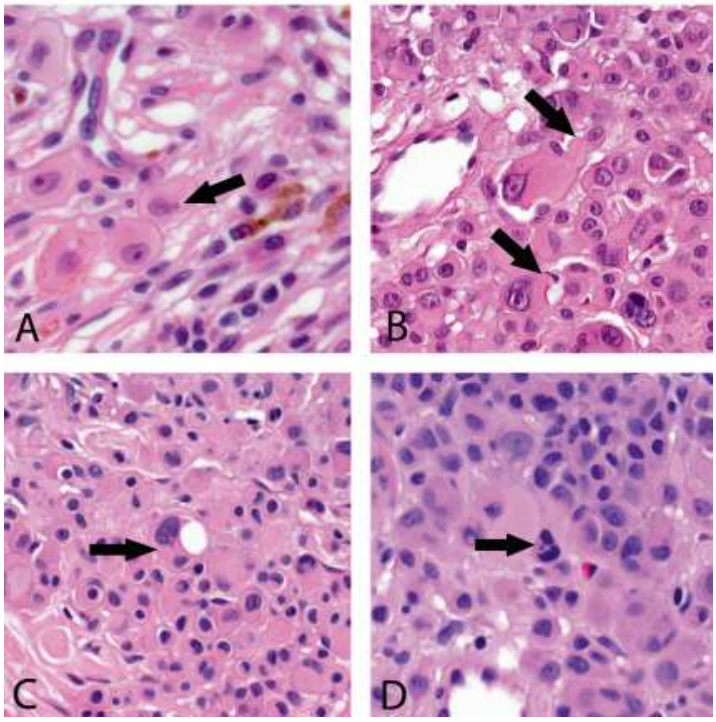

Fig.9 Micronuclei, ant-bear cells and nuclear budding in BIMT. Micronucleus in a BAP1-inactivated melanocyte. Micronuclei are defined as a small nucleus or nuclear buds being 1/3 or smaller compared to the main nucleus presented with a similar or slightly lighter non-refractile staining intensity (arrows). They are observed in the cytoplasm of epithelioid melanocytes, as well as lying in contact with their membrane. Compare their dimension with the nucleus of a lymphocyte or plasma cell (arrowheads) (A). Large epithelioid melanocytes with cytoplasmic protrusions resembling proboscis (ant-bear cells). Note the micronucleus and small nucleus at the end of the protrusions (arrows) (B). Nuclear budding in BAP1-inactivated melanocytes. The nuclei of the epithelioid cells display extreme variability in size, shape, and stain intensity. Note nuclear buds of variable dimension detaching from the main nucleus (C, D).

Apart from cell size variability, there were also variations in shapes and nuclear appearances within an individual lesion, accounting for certain pleomorphism. Rare cells with large irregular nuclei resembling blebbing were seen, as were large, mononuclear cells with clumped chromatin (Fig. 10A, B). There were cells exclusively composed of large eosinophilic cytoplasm with only a shadow/ vestige of a nucleus (Fig. 10C). Rare apoptotic epithelioid melanocytes with large, smudged nuclei and ample dense eosinophilic cytoplasm resembling mummified cells were also commonly encountered (n = 39; 78%). Clear and/or eosinophilic nuclear pseudoinclusions were observed in over half cases, with rare cells containing both types of nuclear pseudoinclusions (Fig. 10C).

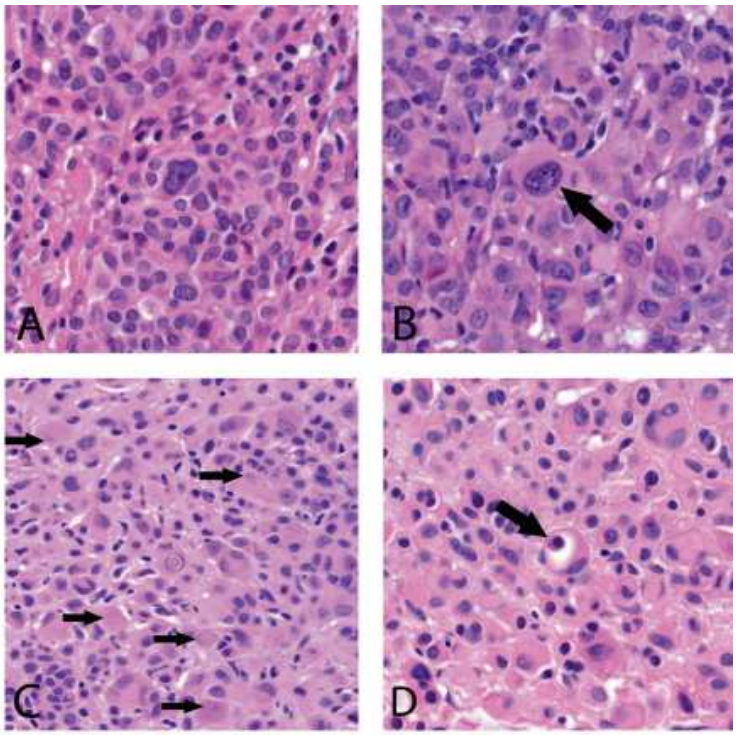

Fig.10 Other cytological features in BIMT. Cells with large irregular nuclei resembling blebbing. Note the mosaic-like disposition of the surrounding cells (A). Large epithelioid melanocytes with enlarged nuclei showing clumped chromatin (arrow) (B). Cells are exclusively composed of large eosinophilic cytoplasm with only a shadow/vestige of a nucleus (arrows). Epithelioid melanocyte with an eosinophilic nuclear pseudoinclusion can be seen in the center (C). Cells with a lumina-like empty intracytoplasmic inclusion encasing small to mediumsized melanocytes occasioning a resemblance to the so-called ball-in-mitt structures. This kind of cell-in-cell structure likely represents entosis in which a tumor cell (host) contains another cell (internalized cell) that displaces the nucleus of the host cells towards the cell periphery resulting in so-called "bird"s- eye cells' morphology (arrow) (D).

Multinucleated/giant epithelioid melanocytes were always evident in varying numbers. Most conspicuous were binucleated cells with mirroring nuclei occasioning a resemblance to ReedSternberg cells. Other multinucleated cells included wreath-like cells, popcorn cells, floret-like cells, and coin-on-a-plate cells. Akin to mononuclear epithelioid cells, the nuclei within multinucleated epithelioid cells and the amount of cytoplasm manifested marked variation in size (Fig. 11).

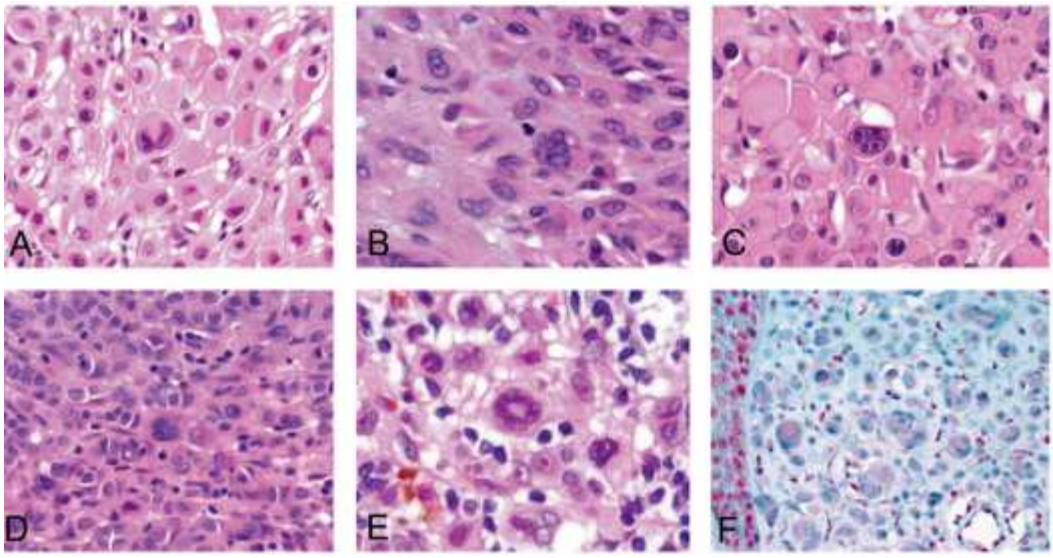

Fig.11 Multinucleated/giant epithelioid melanocytes in BIMT. Binucleated cells resembling Reed-Sternberg cells (A) and multinucleated/ giant cells with overlapping nuclei result in a popcorn, coin-on-a-plate, or wreath-like morphology (B–E). Note prominent eosinophilic nucleoli in the nuclei of some cells (A–D). Multinucleated/giant cell showing BAP1 nuclear loss (F).

Prominent cytoplasmic vacuolization of occasional epithelioid cells resulting in a clear cell appearance was common (n = 35; 70%). There were also cells with an eccentric nucleus dislodged to the periphery by a large clear vacuole or abundant eosinophilic cytoplasm resembling so-called signet-ring cells or rhabdoid cells (n = 29; 58%). Other peculiar morphological aspects frequently noticed were cells with a lumina-like empty intracytoplasmic inclusion often encasing small to medium-sized melanocytes occasioning a resemblance to the so-called ball-in-mitt structures (n = 38; 76%) and likely representing entosis (Fig. 9D)29,30. In the majority of the cases (n = 45; 90%), the dermal mitotic count was ≤2 mitoses/mm2 . In four tumors, there were 5 mitoses/ mm2, and in one neoplasm 3 mitoses/mm2 were seen. Mitotic figures near the base of the lesions were noted in 13 lesions (26%). Most lesions (96%) displayed at least focal impaired cellular maturation toward the base of the lesion were an admixture of small to medium-sized BAP1-inactivated cells, conferring a chaotic aspect or resulting in pseudomaturation. A moderate-to-heavy lymphocytic infiltrate was present in 35 cases (70%), usually with occasional lymphocytes lying in contact with the cell membrane of the BAP1-inactivated melanocytes. Plasma cells were noted in 11 cases (22%). The

epidermis showed focal atrophy and consumption in almost half the cases (n = 24; 48%), rarely in association with focal epidermal hyperplasia within the same lesion. In about a quarter of neoplasms, irritation was detected, while ulceration was never observed. Junctional BAP1-inactivated melanocytes were noted in 23 cases (46%) with extensive junctional involvement in 12 cases (24%). Lentiginous growth of epithelioid melanocytes within the basal cell layer of the epidermis was focally observed. Rare findings (<15%) included intracytoplasmic melanin in epithelioid melanocytes, spindling of epithelioid melanocytes, pigment incontinence, stromal adipocytic metaplasia, mucin deposit, prominent stromal fibrosis and vascularization, and perineural arrangement of cells (Table 4).

Table 4. Summary of the microscopic features in 50 BAP1-inactivated melanocytic tumors

Feature	**Frequency**
Thickness	
Range	0.4-11 mm
Mean	3.1 mm
Silhouette	
Polypoid with collarette	19 (38%)
Verrucous	3 (6%)
Dome-shaped	27 (54%)
Flat	1 (re-excision) (2%)
Base/Border	
Flat base	20 (40%)
Wedge shaped base	20 (40%)
Deep extension (bulb)	9 (18%)
Pushing border	4 (8%)
Epidermal changes	
Epidermal hyperplasia (irregular)	9 (18%)

Epidermal atrophy/consumption (focal)	24 (48%)
Ulceration	0
Irritation	12 (24%)
Junctional component	
Basal BAP1-inactivated melanocytes	23 (46%)
Extensive junctional component	12 (24%)
Architecture and growth patterns	
I. Pure	5 (10%)
II. Combined	45 (90%)
Associated nevus	
Dysplastic features	7 (14%)*
Congenital features	26 (52%)*
Minimal residual nevus	18 (36%)
Mixed nests (with BAP1+ and BAP1- cells)	
Junctional	18 (36%)
Dermal	27 (54%)
Arrangement of large epithelioid melanocytes	
Nodular/Sheet-like	43 (86%)
Nests	26 (52%)
Trabecules	43 (86%)
Discohesive (focal)	44 (88%)
Cytological features epithelioid melanocytes	
Large mainly (3 x type B melanocytes)	14 (28%)
Small mainly (1 x type B melanocytes)	16 (32%)
Equal	20 (40%)
Pleomorphism	
Mild	13 (26%)

Moderate	36 (72%)
Severe	0
Cellular morphology of epithelioid melanocytes	
Large Hodgkin-like	46 (92%)
Binucleated with mirroring nuclei (Reed-Sternberg-like)	47 (94%)
Clear lacunar-like cells/ cytoplasmic vacuolization	35 (70%)
Multinucleated Popcorn/Coin-on- a-plate/ Wreath-like	49 (98%)
Apoptotic (Mummified cells)	39 (78%)
Signet ring /Rhabdoid cells	29 (58%)
Ghost cells	45 (90%)
Ball-in-mitts (Entosis)	38 (76%)
Micronuclei	40 (80%)
Spindled epithelioid cells (focally)	3 (6%)
Pigmented epithelioid cells	6 (12%)
Clear nuclear pseudoinclusions	28 (56%)
Eosinophilic nuclear pseudoinclusions	26 (52%)
Mitotic rate in epithelioid melanocytes	
≤2 mitoses/mm^2	45 (90%)
>2 mitoses/ mm^2	5 (10%)
Mitoses near base	13 (26%)
Adnexal, vascular or perineural extension	
Adnexal involvement	13 (26%)
Perineural arrangement	6 (12%)
Intravascular invasion	0
Stromal changes	
Melanin deposits	35 (70%)
Mucin deposits	5 (10%)

Adipocytic metaplasia	6 (12%)
Prominent vascular and/or sclerotic stroma	5 (10%)
Inflammatory response	
Absent to scarce	15 (30%)
Moderate to heavy	35 (70%)
Plasma cells	11 (22%)
Other	
"Squeezed" conventional melanocytes	17 (34%)
"Kissing" lymphocytes	47 (94%)
Impaired maturation (focal)	46 (92%)

*3 cases manifested both dysplastic-like and congenital-like features.

4.3.3 Immunohistochemical features

All 50 lesions manifested nuclear loss of BAP1 staining in at least a subset of melanocytic population. Conventional melanocytes with retained BAP1 nuclear expression were observed in 45 cases (90%). In many combined type BIMTs, mixed nests composed of both BAP1-negative and BAP1-positive melanocytes were seen at the dermoepidermal junction (36%) or within the dermis (54%) (Fig. 8B). Nests composed exclusively of BAP1-inactivated mela- nocytes were seen in half the cases. Micronuclei were always negative for BAP1 to distinguish them from lymphocytes.

4.3.4 Molecular results (Table 5)

Table 5. Summary of the genetic data on BIMTs

Gene	**Frequency**
BRAF V600E	24/26
RAF1 fusion	2/14
BAP1 bi-allelic mutation	4/22
BAP1 single allele mutation	16/24

BAP1 germline mutation	5/9*
BAP1 heterozygous loss	11/22
FISH for RRB1, CCND1, MYB, MYC, CDKN2A	1/21**
TERT-p mutation	0/14
Copy number variations (NGS)	2/8***
Tetraploid mononuclear cells	5/21

* In 3 patients, a germline *BAP1* mutation was detected using blood or saliva, while in the

BAP1 mutation analysis and BAP1 (3p21.1) copy number changes

Of the 26 lesions analyzed for BAP1 mutations, 16 harbored a single BAP1 mutation, 4 neoplasms yielded 2 different mutations (biallelic mutation), 4 were negative and the remaining 2 lesions were not analyzable. Two cases initially tested negative by Sanger sequencing proved subsequently positive with NGS. Novel BAP1 mutations included NM_004656.3: c.14 G>A p.(Trp5Ter), c.25G> T p.(Glu9Ter), c.249_250delinsT p.(His84ThrfsTer3), c.390_412del p.(Ile131Glnf- sTer4), c.700G> C p.(Val234Leu), and c.856 A > T p.(Lys286Ter) (Fig. 12). Eight patients were tested for BAP1 germline mutations (saliva & peripheral blood) and four proved positive. An additional patient with multiple neoplasms, in whom two tumors were tested with the MelArray, revealed an identical BAP1 mutation (c.1717delG). Of the 27 cases tested for BAP1 CNVs by FISH, ten proved positive (heterozygous loss of BAP1), nine negative, whereas the remaining eight cases were not analyzable. Of the ten positive cases with BAP1 loss identified by FISH, seven also harbored a BAP1 mutation, whilst the remaining three lesions were not studied. Additionally, one of the two lesions tested for BAP1 copy number changes by the MelArray, revealed heterozygotous loss of BAP1, while another did not (identical BAP1 mutation were found in both lesions). In combined results for BAP1 mutations and BAP1 CNVs, there were five lesions negative for both BAP1 mutation and BAP1 CNVs. Another case negative for a BAP1 mutation was not analyzable for CNVs by FISH.

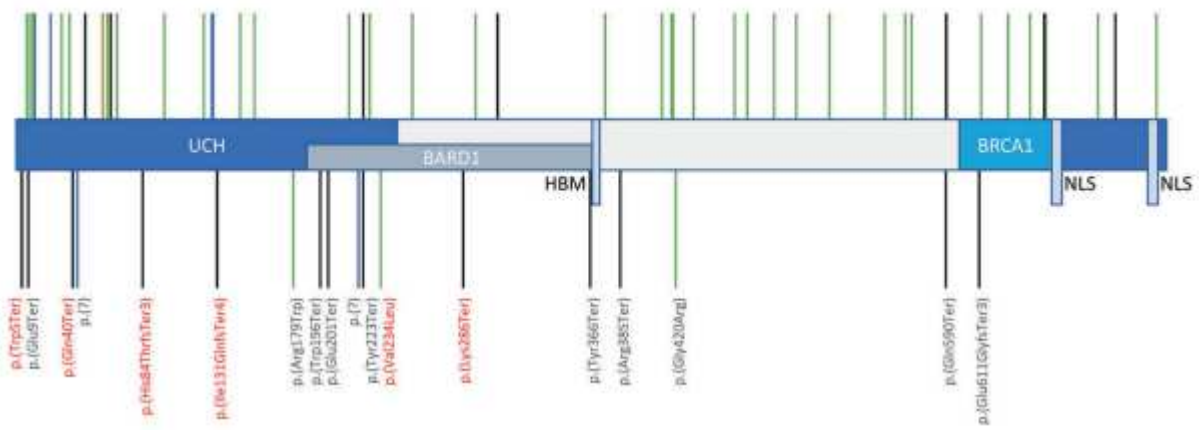

Fig.12 BAP1 mutations identified in our study. BAP1 diagram with protein domains. UCH Ubiquitin C-terminal hydrolase, HBM Host cell factor C1 binding motif, NLS Nuclear localization signal, BARD1 BRCA1-associated RING domain protein 1 gene binding domain, BRCA1 BR CA1 gene binding domain. A Published mutation in skin neoplasms in TCGA database–green lines = missense mutations, black lines = truncating mutations, brown line = small deletion. B Mutations found in this study–red text of mutation name = novel mutation, blue line = splicing mutation, black line = truncating mutation, green line = missense mutation.

BRAF mutation

Among the 26 neoplasms tested for *BRAF* mutation, 24 lesions harbored *BRAFV600E* mutation.

Fusions detection. Two cases with RAF1 fusion, namely *TRAK1-RAF1* and *IGIT2-RAF1* have been previously published [138].

Mutation analysis and studies of CNVs using NGS

In nine BIMTs, additional mutations were detected. In one case (Case 7 A, 15-year-old girl), CNVs by NGS showed an isolated gain of *MYC* and in another lesion (Case 16), *FGFR1* and *ERCC2* gain were detected.

FISH for copy number changes of RRB1, CCND1, MYB, MYC, and CDKN2A

Of the 27 cutaneous lesions analyzed using the melanoma-specific probes, 20 were negative, 6 non-analyzable, whereas one neoplasm (Case 8) showed a gain of MYC and RREB1. Tetraploid mononuclear cells were observed in five cases, while

occasional multinucleated cells resulting in overlapping nuclei were always present and showed multiple signals but were not assessed and therefore were not considered tetraploid in our series. The lymph node lesion (Case 31C) was tested negatively.

4.4 Discussion

Consistent with the prior studies, BIMTs in our series were predominately small (0.2–1.2 cm), dome-shaped or polypoid lesions occurring mainly in young patients (median age 30.4 years, for germline mutated cases 24 years) sparing the lower extremities [37], [36], [135] [149] [147], [173]. In contrast to the previous studies, we found a female predominance (female to male ratio is 2.3:1).

Microscopically, a vast majority of the lesions were of combined type and were associated with a conventional melanocytic nevus frequently showing congenital-like features. In several cases, only careful evaluation of BAP1 staining and mapping with HE-stained slides allowed detection of small, scattered nests of residual conventional melanocytes retaining BAP1 nuclear expression at the periphery of the lesions. The BAP1-inactivated population was mainly located in the dermis and presented an expansile nodular pattern of growth displacing conventional melanocytes toward periphery and squeezing them beneath the overlying epidermis. At the transitional zone between the residua of the conventional nevus and epithelioid cells, the latter often focally retained the architecture of the nevus, that is a nested pattern (nests exclusively composed of BAP1-inactivated melanocytes) or single-cell files splaying between collagen bundles corresponding to a congenital pattern. Mixed nests composed of both BAP1-negative and BAP1-positive melanocytes were observed in the dermis and/or at the dermoepidermal junction in many lesions. In a few cases, BAP1-inactivated epithelioid melanocytes showed a perineural, perivascular, or periadnexal distribution. Toward the base of the lesion, BAP1-inactivated epithelioid melanocytes featured an infiltrative pattern with more dyscohesive areas, especially when accompanied by lymphocytes, and showed in some cases a deep bulb-like extension. Taken together, all these morphological findings suggest an advantage of the growth of the BAP1-

inactivated population that replaces the original conventional melanocytic one. In this view, pure type BIMTs that we encountered only in five cases (10%) may represent the end stage of the process of a clonal substitution of the original nevus cells by BAP1-inactivated melanocytes. This model of progression of BIMT from a benign nevus was proposed in the original description8 and is also supported from a molecular viewpoint, inasmuch as both combined and pure cases in our series and in the previously reported ones harbored a BRAFV600E mutation in the presence of BAP1 inactivation [140], [138], [144]. Moreover, combined type BIMTs have also been reported in association with an NRAS mutation and RAF1 fusions both known to act as a mitogenic driver in melanocytic neoplasms [148], [164], [144], [126]. Fusions involving receptor tyrosine kinases and serine/threonine kinases are mostly associated with Spitz lesions, whereas mutations are typical for conventional melanocytic lesions. However, there are well-known exceptions such as *HRAS* mutation in desmoplastic Spitz nevus and *MAP2K1* mutations in Spitz lesions [103], [174], [175]. RAF proto-oncogene serine/threonineprotein kinase encoded by RAF1 functions as an alternative MAPK signaling mechanism as it forms dimers with wild-type BRAF [155]. Although large epithelioid melanocytes with ample eosinophilic cytoplasm, well-demarcated cytoplasmic border represent the histological hallmark of BIMTs, extreme variability in cellular size, shapes, and degree of nuclear pleomorphism results in a remarkable intratumoral heterogeneity, which has been previously noted [144], [139]. Apart from binucleated cells mentioned in the previously published material, we identified several types of multinucleated cells, resembling those seen in Hodgkin lymphoma, including Reed-Sternberg cells, popcorn cells, coin-on-aplate cells, and mummified cells. Additionally, multinucleated cells with other appearances (floret cells, wreath-like cells) were noted. The question arises as to how one can explain this remarkable cellular heterogeneity and pleomorphism. Taking into account the clonal expansion of epithelioid melanocytes characterized by the loss of a tumor suppressor gene *BAP1* (the second genetic event) in a pre-existing conventional melanocytic nevus driven by a constitutively active mitogenic mutation (i.e. *BRAF*, primary genetic event), it seems reasonable to consider BIMTs a clonal model of tumor

progression of melanoma from a pre-existing nevus. However, the indolent clinical behavior in most cases argues against this interpretation. In addition, lesions with loss of BAP1 nuclear expression and no biallelic inactivation of BAP1 on molecular analysis identified by others and us suggest, among others, epigenetic changes that may account for the inactivation of the BAP1 gene [138]. A recent study demonstrated global transcriptional reprogramming during the progression of BIMTs comparing the gene expression profiles of *BRAF*-driven/*BAP1*-inactivated epithelioid melanocytes with the adjacent conventional melanocytic population [176]. Part of the cellular features in BIMTs can be related to cellular senescence that supposedly occurs early in this progression. Among them is multinucleation that is commonly encountered in conventional melanocytic nevi and less frequently in borderline lesions and overt melanomas [177], [178], [179], [42]. Despite high cellularity and expansile growth, others and we noted a relatively low mitotic activity. Peculiar chromatin patterns ranged from open (shadow nuclei) to clumped. Multinucleated wreath-like/floret-like/coin-on-a-plate cells and micronuclei may result from nuclear budding (Fig. 9C, D). In addition, nuclear budding with the internal perinuclear membrane wrapping around singular nuclei facilitating peculiar nuclear pseudoinclusions observed by others and us [165], [180]. On the whole, the extreme variability in cellular size and morphology may represent the expression of maturation and differentiation of small epithelioid cells. Our FISH analysis revealed tetraploidy in 5 of the 21 cases studied. Generally, FISH analysis is based on a threshold of positive cells and usually tends to scotomize scattered polyploid nuclei. In 2011, before the recognition of BIMT as a distinct lesion, Pouryazdanparast et al. reported tetraploid cells as a common feature in a proportion of nevi with an "atypical spitzoid epithelioid component" [181]. The authors postulated that as a result of senescent mechanisms that are activated, these cells become trapped in the tetraploid cell and do not undergo further division, thus linking senescent or ancient features with tetraploidy. Of further note, they reported that polyploidy changes were noticed only in cases with a low mitotic count. The pictures shown by the authors present the typical morphological features of BIMTs (Fig. 1B, D in ref. [181]). It has been recently observed

that compared to conventional melanocytic nevi, BIMTs have decreased ciliation and increased centrosome amplification, further linking BAP1 dysfunction to mitotic abnormalities and chromosomal instability [182]. Amplification of centrosome number has been shown to occur through failure to arrest at a G1 tetraploidy checkpoint after failure to segregate the genome in mitosis [183]. To the best of our knowledge, the only documented case of BIMT with an aggressive clinical course was reported by Aung et al. and the neoplasm was composed of atypical but rather nevoid melanocytes with BAP1 loss [39]. Prior case series of BIMTs had a relatively short mean follow-up (17 months) [184], [185]. Of the 21 patients with available follow-up in our series, only one patient did develop a locoregional lymph node metastasis 6 years after the removal of the primary tumor. The patient was a 7-year-old girl with a lesion located on the neck, had a considerable lymphocytic infiltrate, and showed relatively bland cytological features; binucleated and multinucleated cells were absent. The neoplasm was diagnosed as a nevus. Six years later (at the age of 13), she developed an enlarged lymph node under her scapula 5 cm from the previously removed skin lesion, and its biopsy demonstrated a dense infiltrate of small to large epithelioid melanocytic cells substituting the original lymphoid tissue. No other melanocytic lesion was known to be excised in between. After having received a second skin biopsy 2 years later in which a classical combined BIMT with remnants of a nevus and epithelioid melanocytes were seen, the original skin lesion and the lymph node specimen were retrospectively stained for BAP1. Loss of BAP1 nuclear expression was found in both specimens, with diffuse nuclear negativity in the skin lesion. Of note, in the tumor reported by Wiesner et al. [38], melanoma arising in BIMT manifested larger nuclei compared with the rest of the neoplasm but featured no striking pleomorphism to our eye and both melanoma and nevus showed loss of BAP1 nuclear expression by immunohistochemistry. Recently, cases of BAP1-inactivated melanocytic tumors showing a conventional morphology in the absence of the classical epithelioid component have been reported [166], [167]. To explain this phenomenon the authors postulated a time gap between genotype alterations and phenotype manifestations

related to progressive intracellular accumulation of the BAP1-altered protein in the affected melanocytes. Moreover, *BAP1*-inactivated tumors with a conventional morphology were frequently observed in younger patients harboring *BAP1* germline mutation [167]. Apart from the above-mentioned patient with a lymph node metastasis, we observed this histological presentation in other two lesions, each from a different patient. Both had multiple lesions and either family or personal history of cutaneous melanoma. In one of these two patients, germline mutation could not be studied, whereas in the other patient an identical *BAP1* mutation was found in two different neoplasms, strongly suggesting a germline mutation. Of note, one lesion from this patient manifested features of a conventional nevus with conspicuous dysplastic-like changes. Our genetic study revealed several findings that merit comment. We identified six novel, previously unreported *BAP1* mutations. All of these represent frame-shift mutations located in, or shortly after, the ubiquitin C-terminal hydrolase domain, causing truncation of parts of the domain and the rest of the protein, resulting in the loss of the protein's function. There were 5 cases in which neither *BAP1* mutation nor heterozygous loss of the *BAP1* gene was found, and there was a further case negative for *BAP1* mutation but not analyzable for CNVs. Since biallelic inactivation of *BAP1* is generally accepted to be required for BAP1 protein loss, these missing aberrations could be attributed either to a *BAP1* aberration outside the studied region, or to other unknown mechanisms of *BAP1* loss. Noteworthy was an 11-year-old girl with multiple lesions located predominantly on the back and extremities. All five lesions manifested typical features of BIMT with nuclear loss of BAP1 expression in the epithelioid melanocytes on immunohistochemistry. Her peripheral blood tested negative for *BAP1* mutation, as did two BIMTs. In addition, neither of the studied cutaneous neoplasms showed CNVs of *BAP1*. Apart from *BAP1*, DNA and RNA sequencing detected several mutations in other genes; the effects of these alterations in this setting are unknown. However, in one case (Case 1 A, 11-year-old girl with multiple lesions and family history of similar lesions), one of the neoplasms yielded a relatively high number of mutations, including a *POLE* mutation, compared to the rest

of the analyzed cases. The detected *POLE* mutation has been linked to high TMB [186]. The panels used in our study are not large enough to be able to access TMB accurately, however, the presence of a *POLE* mutation and a high number of mutations are indicative of high TMB. Microscopically, the neoplasm displayed only minimal residual conventional melanocytes while prominent giant epithelioid melanocytes with clumped chromatin. The patient is disease free after 51 months of follow-up. A recent study revealed two cases of BIMTs with FISH for copy number variations in melanoma-related genes such as 6p25 (RRB1), 11q13 (CCND1), and 9p21 (CDKN2A) [39]. In our series, only 1 out of the 21 analyzable lesions (Case 8, a 67-year-old man) did disclose amplification of both RREB1 and MYC. This neoplasm showed a pure morphology and inverse maturation with predominant small epithelioid cells growing in an infiltrative fashion at the periphery of the lesion. The patient died of an unrelated cause after an otherwise unremarkable follow-up of 72 months. In another case (Case 7 A, 15-year-old girl), copy number variation by NGS showed an isolated gain of *MYC* gene. Also, in this case, we observed only a minimal residuum of conventional melanocytes. Unfortunately, the follow-up of the patient is not available. This is the first study that has investigated mutations in the promoter region of the *TERT* gene (*TERT-p*), using an NGS panel. *TERT-p* hot-spot mutations have been associated with an aggressive clinical course in melanocytic neoplasms, especially in cases with ambiguous morphological features/borderline or low-grade tumors [66], [35]. None of the 14 neoplasms successfully sequenced harbored an alteration in the *TERT-p* region. In conclusion, our study of a large series of BIMTs extends their morphological spectrum and report novel *BAP1* mutations. BIMTs appear to represent a progression from a conventional senescent melanocytic nevus but certain microscopic features, together with cases without detectable molecular alteration in BAP1 gene and frequent tetraploidy, suggest more complex underlying pathological events, which needs to be studied. Albeit BIMTs may present with several alarming cytological and architectural features, we confirm an indolent clinical course in most cases; however, followup was relatively short. The only metastatic case in our series was a child with a nevoid-like

lesion with a pure morphology showing relatively bland cytological features. This relatively bland morphology was similar to that seen in a few previously reported cases as melanoma with *BAP1* inactivation [38], [39]. The working group of the WHO classification suggests the term melanocytoma for "atypical combined tumors (that) may be potential precursor lesions of melanoma" but some atypia is seen in almost all cases of BIMTs that rarely, if ever progress to melanoma. From a genetic viewpoint, according to the WHO classification, the term melanocytoma appears to be restricted for atypical combined melanocytic lesions with two distinctive genetic alterations. Yet, Yeh applied the designation melanocytoma for atypical Spitz tumor which does not have two critical genetic events [187]. Further studies are needed to define and characterize melanocytoma and study BIMTs with relatively bland (nevoid-like) cytology and adverse clinical events.

IMPACT OF MY RESEARCH PROJECT AND FUTURE PERSPECTIVES

1) RESEARCH PROJECT N°1

During these years of PhD we carried out several research projects, some of them were not included in this work as it would result longer as it is.

We used a systematic molecular approach on morphologically selected melanocytic lesions. We demonstrated that molecular analysis is an excellent ancillary tools to assist the pathologist in the differential diagnosis of unusual variants of malignant melanoma and uncommon melanocytic neoplasms. For a long time, these lesions

have been regarded as one of the most difficult challenges in the filed of pathology. Desmoplastic melanoma and *BRAF*-fused atypical Spitz tumor with a desmoplastic stroma share similar morphological aspect but have a very different biological behavior. To get a specific diagnosis among these morphologically overlapping neoplasms leads to completely different approach in patient's management. As we stated in discussion, the differential diagnosis in our case of desmoplastic melanoma was very broad and the genomic analysis allowed us to exclude a metastatic disease given the patient's personal history of two primary melanomas. Without the genetic data this it would be impossible to make it.

Although, the first two studies are carried out on extraordinary case report as in the case of our first research project, this should not be considered an absolute limitation given the goal of a tailored approach to the patient. As in the case of *BRAF* fusion in a polypoid melanocytic neoplasm we observed an uneventful 5-year follow-up in an elderly patient with a 2.3 Breslow thickness melanoma. However, the patient harbors a *CDKN2A* homozygous deletion that have been considered a risk factor of progression in Spitz tumor subgroup. Nevertheless, emerging evidence suggested that copy number variation in more than one melanoma-related genes (MYB, MYC, RREB1 and CDKN2A) is needed or other key factor should be altered such as *TERT-p* to confer an aggressive biological behavior to this morphologically ambiguous melanocytic neoplasm.

2) RESEARCH PROJECT N°2

In the second research project we focused on molecular-morphological correlation. With this approach we reported a series of morphologically similar melanocytic uncommon melanocytic neoplasms characterized by a spitzoid cytological morphology and a dysplastic architectural phenotype. This entity was previously described with the crasis SPARK (SP for spitzoid cytology and ARK for Clark, the eponym used for dysplastic nevus. An *MAP2K1* indel mutations identified in our study, together with other studies reported by other authors, suggest that this genetic

driver should be listed in the subgroup of Spitz tumor in the next WHO classification of skin tumors.

Moreover, in those cases with an aggressive biological behavior, the use of MEK-inhibitors could represent a therapeutic option in melanocytic neoplasm harboring MAP2K1 indel mutation.

3) RESEARCH PROJECT N°3

The NGS panels used in our study analyzed both DNA and RNA from tumor samples. Thanks to this analysis we detected novel genomic driver in melanocytic tumors. *PKN1* fusion and *RAF1* fusion were hitherto unreported mitogenic driver in uncommon melanocytic neoplasm. Also in these cases, a specific morphology was linked to these alterations. Both PEMs and BIMTs can unveil a syndromic disease. PEM harboring a genomic profile characterized by *BRAF* mutation and a germline mutation of *PARK1A* are the hallmark of Carney complex syndrome. Our work together with several other evidence suggested that a pure morphology, composed of heavy pigmented epithelioid melanocytes only, can be predictive of a non-syndromic disease. This can be possible thanks to the genetic analysis.

In a similar fashion, BIMTs could be unveil a germline *BAP1* mutation that predispose to development of several internal malignancy. None of our patients with a *RAF1*-fused BIMT had a *BAP1* germline mutation. Although, it has been proposed that familial cases presented a molecular profile characterized by *BRAF* mutation and *BAP1* inactivation, in our opinion this is merely statistic coincidence given the rarity of these neoplasms. To collect these new data represent the base of a molecular-morphological classification of these enigmatic entities.

4) RSEARCH PROJECT N°4

In research project n. 4 we explored a large series of BIMTs. This is the largest series hitherto reported with an extensive molecular study. In this study we perform a germline and somatic analysis on tumoral and normal tissue samples (blood or

saliva). In five patient (10%) we detected a germline mutation and suggested a screening for BAP1-related tumor for patients' first-degree relatives.

In two cases we detected alterations by FISH for copy number variation in melanoma related genes but none of them presented an aggressive behavior. Of note, none of the tumors presented in our series harbored a *TERT-p* hot spot mutation confirming the importance of this gene in predicting the biological behavior in ambiguous melanocytic neoplasms. Only one case give rise to a nodal deposit. The patient was a 7-year-old girl with a family history of melanoma and a *BAP1* germline mutation. She developed a locoregional nodal metastasis and 8 years later after the onset of the disease, she underwent surgery for a second BIMT. Presently, she has no evidence of disease at the 8-year follow-up. One of the reviewers of our paper ask us if we can exclude the possibility of primary nodal melanocytoma. Although, the DNA and RNA of the primary tumor was not analyzable, we performed the molecular analysis in the nodal deposit. We do not detect any alteration in melanoma progression genes, and we could not exclude the hypothesis of a nodal melanocytoma. If this hypothesis will be confirmed in the future, we will obtain an unexpected answer to unsolved questions.

Our molecular and morphological correlation support a clonal evolution to BIMT from a conventional nevus. On the other hand, other findings seem to suggest a more complex underlying pathophysiological events that deserve a mention as it could offer a novel point of view on some neglected histological aspects.

In our series of rare, peculiar neoplasms characterized by two specific genomic alterations we noticed a remarkable cytological intratumoral heterogeneity resulting in extreme variability in cellular size, shapes, and degree of nuclear pleomorphism with several unusual and/or neglected cytological features such as multinucleated cells. Two models have been proposed to explain tumor cells heterogeneity: 1) the stochastic model, in which a distinct population of biologically equivalent tumor cells progressively acquires the appropriate set of somatic mutations necessary to confer metastatic capability with phenotypic heterogeneity arising as a result of

random exposure to a variety of intrinsic and extrinsic factors and 2) the hierarchical model, also known as the cancer stem cell (CSC) model, which postulates that at the top rank in the hierarchy there are rare cancer cells, endowed of self-renewal and differentiation capability, that generate heterogeneous, differentiated cancer cells with lower or limited proliferative potentials, making up the bulk of the tumor [188], [189]. Part of the cellular features observed in our series including multinucleation can be related to cellular senescence. Cellular senescence has long been considered an irreversible cellular cycle arrest, emerging evidence suggests its role in cancer development and progression [190], [191]. Both in vitro and in vivo cancer model studies conducted on different tumor types reported multinucleated cancer cells as a source of stemness, tumor heterogeneity and resistance to conventional chemotherapy, targeted therapy, and radiation therapy [192], [193], [194]. To detect biomarkers selectively expressed by the polyploid/multinucleated cells could represent the rationale to develop synergic treatment to used together or during of response period to conventional drugs in order to prevent tumor recurrence.

PUBLICATIONS AND PAPERS DERIVED FROM THIS WORK

- ***Donati M,*** *Kastnerova L, Ptakova N, Michal M, Kazakov DV. Polypoid Atypical Spitz Tumor with a Fibrosclerotic Stroma, CLIP2-BRAF Fusion, and Homozygous Loss of 9p21 Am J Dermatopathol. 2020 Mar;42(3):204-207.*

- ***Donati M,*** *Kastnerova L, Cempírková D, Vanaecek T, Michal M. Kazakov D. Vulvar pigmented epithelioid melanocytoma with a novel HTT-PKN1 fusion: a case report Am J Dermatopath. 2020 Jul;42(7):544-546.*
- ***Donati M,*** *Martinek P, Kastnerova L, Persichetti P, Michal M and Kazakov DV. RAF1 Gene Fusions as a Possible Driver Mechanism in Rare BAP1-Inactivated Melanocytic Tumors: A Report of 2 Cases. Am J Dermatopath. 2020 Dec;42(12):961-966.*
- ***Donati M*****,** Nožička J, Hajkova V, *Kastnerova L, Persichetti P, Michal M and Kazakov DV.* Primary cutaneous desmoplastic melanoma with collagen rosettes and pseudoglandular features. *Am J Dermatopath 2021 Mar 1;43(3):221-224.*
- ***Donati M*****,** Nosek D, Waldenbäck P, *Martinek P,* Jonsson BA, Galgonkova P, Hawawrehova M, Berouskova P, *Kastnerova L, Persichetti P,* Crescenzi A, *Michal M and Kazakov DV* MAP2K1 mutated melanocytic neoplasms with a SPARK-like morphology. *Am J Dermatopath. 2021 Jun 1;43(6):412-417.*
- ***Donati M,*** *Martinek P, Steiner P, Grossman P, Vanecek T, Kolm I, Baneckova M, Donati P, Kletskaya I, Feit J, Blasch P, Szilagyi D, Kastnerova L, Persichetti P, Michal M and Kazakov DV.* Novel insights into the BAP1-inactivated melanocytic tumor. *Mod. Pathol. 2021 Dec 2.*

OTHER PEER-REVIEWED PAPERS PUBLISHED DURING MY PhD

- ***Donati M****, Kastnerova L, Martinek P, Grossmann P, Sticová E, Hadravský L, Torday T, Kyclova Jl Michal M. Kazakov D. Spitz tumors with ROS1 fusions, Am J of Dermatopathol. 2020 Feb;42(2):92-102.*
- ***Donati M,*** *Zelano G, Coppola R, Cinelli E, Verri M, Persichetti P, Perrella E, Devirgiliis V, Calvieri S, Crescenzi A, Panasiti V. Germline and somatic analysis of multiple SPMs developed under selective BRAF inhibition, It J Dermatol; 2021 Oct;156(5):593-598.*

- ***Donati M,*** *Vollono L, Ferrari A, Vulcano A, Persichetti P, Donati P.* Perineural Granulomas without neurological manifestations: the great mimicker strikes again*. J Cutan Pathol. 2020 May 3.*
- *Mazzilli S, Vollono L, Cosio T,* ***Donati M,*** *Piccolo A, DI Raimondo C, Campione E, Bianchi L. Reflectance Confocal Microscopy Applied to Linear (en Coup de Sabre) Morphea. Ski. Appendage Disord. 1–4 (2020).*
- *Tramutola A, Falcucci S, Brocco U, Triani F, Lanzillotta C,* ***Donati M,*** *Panetta C, Luzi F, Iavarone F, Vincenzoni F, Castagnola M, Perluigi M, Di Domenico F, De Marco F. Protein Oxidative Damage in UV-Related Skin Cancer and Dysplastic Lesions Contributes to Neoplastic Promotion and Progression. Cancers 2020 Jen 1*
- *Zanniello R,* ***Donati M,*** *Ferrari A, Vollono L, Cameli N. Vesicular-bullous prurigo pigmentosa in a young Italian man. G Ital Dermatol Venereol. 2020 Jun 15.*
- *Coppola R, Barone M, Zanframundo S, Devirgiliis V, Roberti V, Perrella E,* ***Donati M****, Palese E, Tenna S, Persichetti P, Panasiti V. Basal cell carcinoma thickness evaluated by high frequency ultrasounds and correlation with dermoscopic features. G Ital Dermatol Venereol. 2020 Sep 17.*
- *Paolino G, Muscardin L, Didona D, Panetta C,* ***Donati M,*** *Mercuri SR, Donati P.Pigmented porokeratosis with dermal deposits of amyloid: the different chromatic features. G Ital Dermatol Venereol. 2020 Apr;155(2):240-241.*
- *Vollono L, Paolino G, Buonocore A,* ***Donati M****. Assessing beauticians' knowledge of cutaneous melanoma and willingness to contribute to melanoma surveillance practices on the general population. An Bras Dermatol. Nov-Dec 2020;95(6):764-765*
- *Fania L, Didona D, Di Pietro FR, Verkhovskaia S, Morese R, Paolino G,* ***Donati M,*** *Ricci F, Coco V, Ricci F, Candi E, Abeni D, Dellambra E. Cutaneous Squamous Cell Carcinoma: From Pathophysiology to Novel Therapeutic Approaches. Biomedicines. 2021 Feb 9;9(2):171.*

1 Saginala, K., Barsouk, A., Aluru, J. S., Rawla, P. & Barsouk, A. Epidemiology of Melanoma. *Med Sci (Basel)* **9** (2021).
2 Toussi, A., Mans, N., Welborn, J. & Kiuru, M. Germline mutations predisposing to melanoma. *J Cutan Pathol* **47**, 606-616 (2020).
3 McGovern, V. J. The classification of melanoma.fusion in dogs. *Minn Med* **54**, 426-428 (1971).
4 Clark, W. H. J. A classification of malignant melanoma in man correlated with histogenesis and biologic behavior. *In: Montagna W, Hu F, eds. Advances in the Biology of the Skin Volume VIII. New York: Pergamon Press*
621–647. (1967).
5 Gershenwald, J. E. *et al.* Melanoma staging: Evidence-based changes in the American Joint Committee on Cancer eighth edition cancer staging manual. *CA Cancer J Clin* **67**, 472-492 (2017).
6 McGovern, V. J. The classification of melanoma and its relationship with prognosis. *Pathology* **2**, 85-98 (1970).
7 Clark, W. H., Jr., From, L., Bernardino, E. A. & Mihm, M. C. The histogenesis and biologic behavior of primary human malignant melanomas of the skin. *Cancer Res* **29**, 705-727 (1969).
8 Ackerman, A. B. Malignant melanoma: a unifying concept. *Hum Pathol* **11**, 591-595 (1980).
9 Bastian, B. C. The molecular pathology of melanoma: an integrated taxonomy of melanocytic neoplasia. *Annu Rev Pathol* **9**, 239-271 (2014).
10 Elder, D. E., Massi, D., Scolyer, R. A., Willemze, R. & eds. *WHO Classification of Skin Tumours. 4th ed. Lyon, France: International Agency for Research on Cancer (IARC).* (2018).
11 Bennett, D. C. Genetics of melanoma progression: the rise and fall of cell senescence. *Pigment Cell Melanoma Res* **29**, 122-140 (2016).
12 Shain, A. H. *et al.* The Genetic Evolution of Melanoma from Precursor Lesions. *N Engl J Med* **373**, 1926-1936 (2015).
13 Ackerman, A. B. Discordance among expert pathologists in diagnosis of melanocytic neoplasms. *Hum Pathol* **27**, 1115-1116 (1996).
14 Barnhill, R. L. *et al.* Atypical Spitz nevi/tumors: lack of consensus for diagnosis, discrimination from melanoma, and prediction of outcome. *Hum Pathol* **30**, 513-520 (1999).
15 Cerroni, L. *et al.* Melanocytic tumors of uncertain malignant potential: results of a tutorial held at the XXIX Symposium of the International Society of Dermatopathology in Graz, October 2008. *Am J Surg Pathol* **34**, 314-326 (2010).
16 Wechsler, J. *et al.* Reliability of the histopathologic diagnosis of malignant melanoma in childhood. *Arch Dermatol* **138**, 625-628 (2002).
17 Chapman, P. B. *et al.* Improved survival with vemurafenib in melanoma with BRAF V600E mutation. *N Engl J Med* **364**, 2507-2516 (2011).
18 Beaver, J. A. *et al.* FDA Approval of Nivolumab for the First-Line Treatment of Patients with BRAF(V600) Wild-Type Unresectable or Metastatic Melanoma. *Clin Cancer Res* **23**, 3479-3483 (2017).
19 Zedek, D. C. & McCalmont, T. H. Spitz nevi, atypical spitzoid neoplasms, and spitzoid melanoma. *Clin Lab Med* **31**, 311-320 (2011).

20 Busam, K. J. *et al.* Atypical spitzoid melanocytic tumors with positive sentinel lymph nodes in children and teenagers, and comparison with histologically unambiguous and lethal melanomas. *Am J Surg Pathol* **33**, 1386-1395 (2009).

21 Wiesner, T. *et al.* Kinase fusions are frequent in Spitz tumours and spitzoid melanomas. *Nat Commun* **5**, 3116 (2014).

22 Busam, K. J., Kutzner, H., Cerroni, L. & Wiesner, T. Clinical and pathologic findings of Spitz nevi and atypical Spitz tumors with ALK fusions. *Am J Surg Pathol* **38**, 925-933 (2014).

23 Yeh, I. *et al.* Filigree-like Rete Ridges, Lobulated Nests, Rosette-like Structures, and Exaggerated Maturation Characterize Spitz Tumors With NTRK1 Fusion. *Am J Surg Pathol* **43**, 737-746 (2019).

24 VandenBoom, T. *et al.* Genomic Fusions in Pigmented Spindle Cell Nevus of Reed. *Am J Surg Pathol* **42**, 1042-1051 (2018).

25 Yeh, I. *et al.* NTRK3 kinase fusions in Spitz tumours. *J Pathol* **240**, 282-290 (2016).

26 Donati, M. *et al.* Spitz Tumors With ROS1 Fusions: A Clinicopathological Study of 6 Cases, Including FISH for Chromosomal Copy Number Alterations and Mutation Analysis Using Next-Generation Sequencing. *Am J Dermatopathol* **42**, 92-102 (2020).

27 Kim, D. *et al.* BRAF fusion Spitz neoplasms; clinical morphological, and genomic findings in six cases. *J Cutan Pathol* **47**, 1132-1142 (2020).

28 Kim, D. *et al.* A Series of RET Fusion Spitz Neoplasms With Plaque-Like Silhouette and Dyscohesive Nesting of Epithelioid Melanocytes. *Am J Dermatopathol* **43**, 243-251 (2021).

29 Quan, V. L. *et al.* Integrating Next-Generation Sequencing with Morphology Improves Prognostic and Biologic Classification of Spitz Neoplasms. *J Invest Dermatol* **140**, 1599-1608 (2020).

30 Zembowicz, A., Carney, J. A. & Mihm, M. C. Pigmented epithelioid melanocytoma: a low-grade melanocytic tumor with metastatic potential indistinguishable from animal-type melanoma and epithelioid blue nevus. *Am J Surg Pathol* **28**, 31-40 (2004).

31 Kazakov, D. V., Rütten, A., Kempf, W. & Michal, M. Melanoma with prominent pigment synthesis (animal-type melanoma): a case report with ultrastructural studies. *Am J Dermatopathol* **26**, 290-297 (2004).

32 Carney, J. A. & Ferreiro, J. A. The epithelioid blue nevus. A multicentric familial tumor with important associations, including cardiac myxoma and psammomatous melanotic schwannoma. *Am J Surg Pathol* **20**, 259-272 (1996).

33 Zembowicz, A. *et al.* Loss of expression of protein kinase a regulatory subunit 1alpha in pigmented epithelioid melanocytoma but not in melanoma or other melanocytic lesions. *Am J Surg Pathol* **31**, 1764-1775 (2007).

34 Isales, M. C. *et al.* Distinct Genomic Patterns in Pigmented Epithelioid Melanocytoma: A Molecular and Histologic Analysis of 16 Cases. *Am J Surg Pathol* **43**, 480-488 (2019).

35 Cohen, J. N., Yeh, I., Mully, T. W., LeBoit, P. E. & McCalmont, T. H. Genomic and Clinicopathologic Characteristics of PRKAR1A-inactivated Melanomas: Toward Genetic Distinctions of Animal-type Melanoma/Pigment Synthesizing Melanoma. *Am J Surg Pathol* **44**, 805-816 (2020).

36 Wiesner, T. *et al.* Germline mutations in BAP1 predispose to melanocytic tumors. *Nat Genet* **43**, 1018-1021 (2011).

37 Garfield, E. M. *et al.* Histomorphologic spectrum of germline-related and sporadic BAP1-inactivated melanocytic tumors. *J Am Acad Dermatol* **79**, 525-534 (2018).

38 Wiesner, T. *et al.* Toward an improved definition of the tumor spectrum associated with BAP1 germline mutations. *J Clin Oncol* **30**, e337-340 (2012).

39 Aung, P. P. *et al.* Melanoma With Loss of BAP1 Expression in Patients With No Family History of BAP1-Associated Cancer Susceptibility Syndrome: A Case Series. *Am J Dermatopathol* **41**, 167-179 (2019).

40 Seab, J. A., Jr., Graham, J. H. & Helwig, E. B. Deep penetrating nevus. *Am J Surg Pathol* **13**, 39-44 (1989).

41 Yeh, I. *et al.* Combined activation of MAP kinase pathway and β-catenin signaling cause deep penetrating nevi. *Nat Commun* **8**, 644 (2017).

42 Houlier, A. *et al.* Melanocytic tumors with MAP3K8 fusions: report of 33 cases with morphological-genetic correlations. *Mod Pathol* **33**, 846-857 (2020).

43 Macagno, N. *et al.* Cutaneous Melanocytic Tumors With Concomitant NRASQ61R and IDH1R132C Mutations: A Report of 6 Cases. *Am J Surg Pathol* **44**, 1398-1405 (2020).

44 Goto, K., Pissaloux, D., Paindavoine, S., Tirode, F. & de la Fouchardière, A. CYSLTR2-mutant Cutaneous Melanocytic Neoplasms Frequently Simulate "Pigmented Epithelioid Melanocytoma," Expanding the Morphologic Spectrum of Blue Tumors: A Clinicopathologic Study of 7 Cases. *Am J Surg Pathol* **43**, 1368-1376 (2019).

45 Cellier, L. *et al.* Cutaneous Melanocytoma With CRTC1-TRIM11 Fusion: Report of 5 Cases Resembling Clear Cell Sarcoma. *Am J Surg Pathol* **42**, 382-391 (2018).

46 Kapur, P. *et al.* Spitz nevi and atypical Spitz nevi/tumors: a histologic and immunohistochemical analysis. *Mod Pathol* **18**, 197-204 (2005).

47 Vollmer, R. T. Use of Bayes rule and MIB-1 proliferation index to discriminate Spitz nevus from malignant melanoma. *Am J Clin Pathol* **122**, 499-505 (2004).

48 Koh, S. S. & Cassarino, D. S. Immunohistochemical Expression of p16 in Melanocytic Lesions: An Updated Review and Meta-analysis. *Arch Pathol Lab Med* **142**, 815-828 (2018).

49 Healy, E., Rehman, I., Angus, B. & Rees, J. L. Loss of heterozygosity in sporadic primary cutaneous melanoma. *Genes Chromosomes Cancer* **12**, 152-156 (1995).

50 Bauer, J. & Bastian, B. C. Distinguishing melanocytic nevi from melanoma by DNA copy number changes: comparative genomic hybridization as a research and diagnostic tool. *Dermatol Ther* **19**, 40-49 (2006).

51 Gerami, P. *et al.* A highly specific and discriminatory FISH assay for distinguishing between benign and malignant melanocytic neoplasms. *Am J Surg Pathol* **36**, 808-817 (2012).

52 de Klein, A., Koopmans, A. E. & Kilic, E. Multicolor FISH with improved sensitivity and specificity in the diagnosis of malignant melanoma. *Expert Rev Mol Diagn* **12**, 683-685 (2012).

53 Gammon, B., Beilfuss, B., Guitart, J. & Gerami, P. Enhanced detection of spitzoid melanomas using fluorescence in situ hybridization with 9p21 as an adjunctive probe. *Am J Surg Pathol* **36**, 81-88 (2012).

54 Botton, T. *et al.* Recurrent BRAF kinase fusions in melanocytic tumors offer an opportunity for targeted therapy. *Pigment Cell Melanoma Res* **26**, 845-851 (2013).

55 Perron, E. *et al.* Unclassified sclerosing malignant melanomas with AKAP9-BRAF gene fusion: a report of two cases and review of BRAF fusions in melanocytic tumors. *Virchows Arch* **472**, 469-476 (2018).

56 Thomas, N. E. *et al.* Utility of TERT Promoter Mutations for Cutaneous Primary Melanoma Diagnosis. *Am J Dermatopathol* **41**, 264-272 (2019).

57 Amin, S. M. *et al.* A Comparison of Morphologic and Molecular Features of BRAF, ALK, and NTRK1 Fusion Spitzoid Neoplasms. *Am J Surg Pathol* **41**, 491-498 (2017).

58 Dessars, B. *et al.* Chromosomal translocations as a mechanism of BRAF activation in two cases of large congenital melanocytic nevi. *J Invest Dermatol* **127**, 1468-1470 (2007).

59 Kim, H. S. *et al.* Oncogenic BRAF fusions in mucosal melanomas activate the MAPK pathway and are sensitive to MEK/PI3K inhibition or MEK/CDK4/6 inhibition. *Oncogene* **36**, 3334-3345 (2017).

60 Turner, J. *et al.* Kinase gene fusions in defined subsets of melanoma. *Pigment Cell Melanoma Res* **30**, 53-62 (2017).

61 Ross, J. S. *et al.* The distribution of BRAF gene fusions in solid tumors and response to targeted therapy. *Int J Cancer* **138**, 881-890 (2016).

62 Hutchinson, K. E. *et al.* BRAF fusions define a distinct molecular subset of melanomas with potential sensitivity to MEK inhibition. *Clin Cancer Res* **19**, 6696-6702 (2013).

63 Massi G, L. P. Spitz nevus variants, polypid spitz nevus. In: Massi G, LeBoit PE, eds. Histological Diagnosis of Nevi and Melanoma. New York, PA: Springer. 188 (2014).

64 Ludgate, M. W. *et al.* The atypical Spitz tumor of uncertain biologic potential: a series of 67 patients from a single institution. *Cancer* **115**, 631-641 (2009).

65 Gerami, P. *et al.* Risk assessment for atypical spitzoid melanocytic neoplasms using FISH to identify chromosomal copy number aberrations. *Am J Surg Pathol* **37**, 676-684 (2013).

66 Lee, S. *et al.* TERT Promoter Mutations Are Predictive of Aggressive Clinical Behavior in Patients with Spitzoid Melanocytic Neoplasms. *Sci Rep* **5**, 11200 (2015).

67 Yazdan, P. *et al.* Comparative analysis of atypical spitz tumors with heterozygous versus homozygous 9p21 deletions for clinical outcomes, histomorphology, BRAF mutation, and p16 expression. *Am J Surg Pathol* **38**, 638-645 (2014).

68 Harms, P. W. *et al.* Loss of p16 expression and copy number changes of CDKN2A in a spectrum of spitzoid melanocytic lesions. *Hum Pathol* **58**, 152-160 (2016).

69 Gerami, P. *et al.* Outcomes of atypical spitz tumors with chromosomal copy number aberrations and conventional melanomas in children. *Am J Surg Pathol* **37**, 1387-1394 (2013).

70 Lee, C. Y. *et al.* Atypical Spitzoid Neoplasms in Childhood: A Molecular and Outcome Study. *Am J Dermatopathol* **39**, 181-186 (2017).

71 Lazova, R. *et al.* Spitz nevi and Spitzoid melanomas: exome sequencing and comparison with conventional melanocytic nevi and melanomas. *Mod Pathol* **30**, 640-649 (2017).

72 Menzies, A. M. *et al.* Clinical activity of the MEK inhibitor trametinib in metastatic melanoma containing BRAF kinase fusion. *Pigment Cell Melanoma Res* **28**, 607-610 (2015).

73 Wu, G. *et al.* The landscape of fusion transcripts in spitzoid melanoma and biologically indeterminate spitzoid tumors by RNA sequencing. *Mod Pathol* **29**, 359-369 (2016).

74 Jun, H. J. *et al.* The oncogenic lung cancer fusion kinase CD74-ROS activates a novel invasiveness pathway through E-Syt1 phosphorylation. *Cancer Res* **72**, 3764-3774 (2012).

75 Hallberg, B. & Palmer, R. H. The role of the ALK receptor in cancer biology. *Ann Oncol* **27 Suppl 3**, iii4-iii15 (2016).

76 Chen, L. L., Jaimes, N., Barker, C. A., Busam, K. J. & Marghoob, A. A. Desmoplastic melanoma: a review. *J Am Acad Dermatol* **68**, 825-833 (2013).

77 Walsh, N. M., Roberts, J. T., Orr, W. & Simon, G. T. Desmoplastic malignant melanoma. A clinicopathologic study of 14 cases. *Arch Pathol Lab Med* **112**, 922-927 (1988).

78 Egbert, B., Kempson, R. & Sagebiel, R. Desmoplastic malignant melanoma. A clinicohistopathologic study of 25 cases. *Cancer* **62**, 2033-2041 (1988).

79 Anstey, A. *et al.* Desmoplastic malignant melanoma. An immunocytochemical study of 25 cases. *Am J Dermatopathol* **16**, 14-22 (1994).

80 Carlson, J. A., Dickersin, G. R., Sober, A. J. & Barnhill, R. L. Desmoplastic neurotropic melanoma. A clinicopathologic analysis of 28 cases. *Cancer* **75**, 478-494 (1995).

81 Longacre, T. A., Egbert, B. M. & Rouse, R. V. Desmoplastic and spindle-cell malignant melanoma. An immunohistochemical study. *Am J Surg Pathol* **20**, 1489-1500 (1996).

82 de Almeida, L. S. *et al.* Desmoplastic malignant melanoma: a clinicopathologic analysis of 113 cases. *Am J Dermatopathol* **30**, 207-215 (2008).

83 Conley, J., Lattes, R. & Orr, W. Desmoplastic malignant melanoma (a rare variant of spindle cell melanoma). *Cancer* **28**, 914-936 (1971).

84 Reed, R. J. & Leonard, D. D. Neurotropic melanoma. A variant of desmoplastic melanoma. *Am J Surg Pathol* **3**, 301-311 (1979).

85 Jain, S. & Allen, P. W. Desmoplastic malignant melanoma and its variants. A study of 45 cases. *Am J Surg Pathol* **13**, 358-373 (1989).

86 Riccioni, L., Di Tommaso, L. & Collina, G. Actin-rich desmoplastic malignant melanoma: report of three cases. *Am J Dermatopathol* **21**, 537-541 (1999).

87 Busam, K. J. Cutaneous desmoplastic melanoma. *Adv Anat Pathol* **12**, 92-102 (2005).

88 Shain, A. H. *et al.* Exome sequencing of desmoplastic melanoma identifies recurrent NFKBIE promoter mutations and diverse activating mutations in the MAPK pathway. *Nat Genet* **47**, 1194-1199 (2015).

89 Vogelstein, B. *et al.* Cancer genome landscapes. *Science* **339**, 1546-1558 (2013).

90 Wiesner, T. *et al.* NF1 Mutations Are Common in Desmoplastic Melanoma. *Am J Surg Pathol* **39**, 1357-1362 (2015).

91 Jo, V. Y. & Fletcher, C. D. M. SMARCB1/INI1 Loss in Epithelioid Schwannoma: A Clinicopathologic and Immunohistochemical Study of 65 Cases. *Am J Surg Pathol* **41**, 1013-1022 (2017).

92 Plaza, J. A. *et al.* Desmoplastic melanoma: an updated immunohistochemical analysis of 40 cases with a proposal for an additional panel of stains for diagnosis. *J Cutan Pathol* **43**, 313-323 (2016).

93 Tarlow, M. M., Nemlick, A. S., Rothenberg, J. & Schwartz, R. A. Pseudoglandular-type melanoma: a rare melanoma variant. *J Cutan Pathol* **35**, 588-590 (2008).

94 Saggini, A., Cerroni, L., Casini, B., Baciorri, F. & Cota, C. Primary intrafascial desmoplastic melanoma with pseudoglandular differentiation and aberrant cytokeratins expression: An exceptional presentation. *Pathol Res Pract* **215**, 152668 (2019).

95 Kacerovska, D., Sokol, L., Michal, M. & Kazakov, D. V. Primary cutaneous signet-ring cell melanoma with pseudoglandular features, spindle cells and oncocytoid changes. *Am J Dermatopathol* **31**, 81-83 (2009).

96 Folpe, A. L., Lane, K. L., Paull, G. & Weiss, S. W. Low-grade fibromyxoid sarcoma and hyalinizing spindle cell tumor with giant rosettes: a clinicopathologic study of 73 cases supporting their identity and assessing the impact of high-grade areas. *Am J Surg Pathol* **24**, 1353-1360 (2000).

97 Billings, S. D., Giblen, G. & Fanburg-Smith, J. C. Superficial low-grade fibromyxoid sarcoma (Evans tumor): a clinicopathologic analysis of 19 cases with a unique observation in the pediatric population. *Am J Surg Pathol* **29**, 204-210 (2005).

98 Creytens, D., Ferdinande, L. & Van Dorpe, J. A Sclerosing Perineurioma With Collagen Rosette Formation: Benign Mimic of Low-Grade Fibromyxoid Sarcoma. *Int J Surg Pathol* **26**, 145-147 (2018).

99 From, L. *et al.* Origin of the desmoplasia in desmoplastic malignant melanoma. *Hum Pathol* **14**, 1072-1080 (1983).

100 Tajima, S., Ura-Ishiko, A. & Hayashi, A. Melanogenesis, biosynthetic phenotype of fibronectin and collagen, and migrating activity in cloned B16 mouse melanoma cells. *J Dermatol Sci* **12**, 24-30 (1996).

101 Daniels, K. J. *et al.* Expression of type VI collagen in uveal melanoma: its role in pattern formation and tumor progression. *Lab Invest* **75**, 55-66 (1996).

102 Hantschke, M. *et al.* Cutaneous clear cell sarcoma: a clinicopathologic, immunohistochemical, and molecular analysis of 12 cases emphasizing its distinction from dermal melanoma. *Am J Surg Pathol* **34**, 216-222 (2010).

103 Bastian, B. C., LeBoit, P. E. & Pinkel, D. Mutations and copy number increase of HRAS in Spitz nevi with distinctive histopathological features. *Am J Pathol* **157**, 967-972 (2000).

104 Yeh, I. *et al.* Activating MET kinase rearrangements in melanoma and Spitz tumours. *Nat Commun* **6**, 7174 (2015).

105 Yeh, I. *et al.* Clinical, histopathologic, and genomic features of Spitz tumors with ALK fusions. *Am J Surg Pathol* **39**, 581-591 (2015).

106 Kastnerova, L. *et al.* A Clinicopathological Study of 29 Spitzoid Melanocytic Lesions With ALK Fusions, Including Novel Fusion Variants, Accompanied by Fluorescence In Situ Hybridization Analysis for Chromosomal Copy Number Changes, and Both TERT Promoter and Next-Generation Sequencing Mutation Analysis. *Am J Dermatopathol* 10.1097/dad.0000000000001632 (2020).

107 Newman, S. *et al.* Clinical genome sequencing uncovers potentially targetable truncations and fusions of MAP3K8 in spitzoid and other melanomas. *Nat Med* **25**, 597-602 (2019).

108 Quan, V. L. *et al.* Activating Structural Alterations in MAPK Genes Are Distinct Genetic Drivers in a Unique Subgroup Of Spitzoid Neoplasms. *Am J Surg Pathol* **43**, 538-548 (2019).

109 Quan, V. L. *et al.* The role of gene fusions in melanocytic neoplasms. *J Cutan Pathol* **46**, 878-887 (2019).

110 Ko, C. J., McNiff, J. M. & Glusac, E. J. Melanocytic nevi with features of Spitz nevi and Clark's/dysplastic nevi ("Spark's" nevi). *J Cutan Pathol* **36**, 1063-1068 (2009).

111 Gerami, P. *et al.* Fluorescence in situ hybridization (FISH) as an ancillary diagnostic tool in the diagnosis of melanoma. *Am J Surg Pathol* **33**, 1146-1156 (2009).

112 Roskoski, R., Jr. MEK1/2 dual-specificity protein kinases: structure and regulation. *Biochem Biophys Res Commun* **417**, 5-10 (2012).

113 Yuan, J. *et al.* Activating mutations in MEK1 enhance homodimerization and promote tumorigenesis. *Sci Signal* **11** (2018).

114 Nikolaev, S. I. *et al.* Exome sequencing identifies recurrent somatic MAP2K1 and MAP2K2 mutations in melanoma. *Nat Genet* **44**, 133-139 (2011).

115 Arcila, M. E. *et al.* MAP2K1 (MEK1) Mutations Define a Distinct Subset of Lung Adenocarcinoma Associated with Smoking. *Clin Cancer Res* **21**, 1935-1943 (2015).

116 Gounder, M. M., Solit, D. B. & Tap, W. D. Trametinib in Histiocytic Sarcoma with an Activating MAP2K1 (MEK1) Mutation. *N Engl J Med* **378**, 1945-1947 (2018).

117 Hechtman, J. F. *et al.* Identification of Targetable Kinase Alterations in Patients with Colorectal Carcinoma That are Preferentially Associated with Wild-Type RAS/RAF. *Mol Cancer Res* **14**, 296-301 (2016).

118 Schmidt, J. *et al.* Mutations of MAP2K1 are frequent in pediatric-type follicular lymphoma and result in ERK pathway activation. *Blood* **130**, 323-327 (2017).

119 Ozkaya, N. *et al.* The histopathology of Erdheim-Chester disease: a comprehensive review of a molecularly characterized cohort. *Mod Pathol* **31**, 581-597 (2018).

120 Waterfall, J. J. *et al.* High prevalence of MAP2K1 mutations in variant and IGHV4-34-expressing hairy-cell leukemias. *Nat Genet* **46**, 8-10 (2014).

121 Emery, C. M. *et al.* MEK1 mutations confer resistance to MEK and B-RAF inhibition. *Proc Natl Acad Sci U S A* **106**, 20411-20416 (2009).

122 Moriceau, G. *et al.* Tunable-combinatorial mechanisms of acquired resistance limit the efficacy of BRAF/MEK cotargeting but result in melanoma drug addiction. *Cancer Cell* **27**, 240-256 (2015).

123 Gao, Y. *et al.* Allele-Specific Mechanisms of Activation of MEK1 Mutants Determine Their Properties. *Cancer Discov* **8**, 648-661 (2018).

124 Williams, E. A. *et al.* Melanoma with in-frame deletion of MAP2K1: a distinct molecular subtype of cutaneous melanoma mutually exclusive from BRAF, NRAS, and NF1 mutations. *Mod Pathol* 10.1038/s41379-020-0581-5 (2020).

125 Hodis, E. *et al.* A landscape of driver mutations in melanoma. *Cell* **150**, 251-263 (2012).

126 Hayward, N. K. *et al.* Whole-genome landscapes of major melanoma subtypes. *Nature* **545**, 175-180 (2017).

127 Emelyanova, M. *et al.* Detection of BRAF, NRAS, KIT, GNAQ, GNA11 and MAP2K1/2 mutations in Russian melanoma patients using LNA PCR clamp and biochip analysis. *Oncotarget* **8**, 52304-52320 (2017).

128 Chakraborty, R. *et al.* Mutually exclusive recurrent somatic mutations in MAP2K1 and BRAF support a central role for ERK activation in LCH pathogenesis. *Blood* **124**, 3007-3015 (2014).

129 Couto, J. A. *et al.* Somatic MAP2K1 Mutations Are Associated with Extracranial Arteriovenous Malformation. *Am J Hum Genet* **100**, 546-554 (2017).

130 Cohen, J. N. *et al.* Genomic Analysis of Pigmented Epithelioid Melanocytomas Reveals Recurrent Alterations in PRKAR1A, and PRKCA Genes. *Am J Surg Pathol* **41**, 1333-1346 (2017).

131 Carbone, M. *et al.* BAP1 and cancer. *Nat Rev Cancer* **13**, 153-159 (2013).

132 Sowa, M. E., Bennett, E. J., Gygi, S. P. & Harper, J. W. Defining the human deubiquitinating enzyme interaction landscape. *Cell* **138**, 389-403 (2009).

133 Ventii, K. H. *et al.* BRCA1-associated protein-1 is a tumor suppressor that requires deubiquitinating activity and nuclear localization. *Cancer Res* **68**, 6953-6962 (2008).

134 Abdel-Rahman, M. H. *et al.* Germline BAP1 mutation predisposes to uveal melanoma, lung adenocarcinoma, meningioma, and other cancers. *J Med Genet* **48**, 856-859 (2011).

135 Njauw, C. N. *et al.* Germline BAP1 inactivation is preferentially associated with metastatic ocular melanoma and cutaneous-ocular melanoma families. *PLoS One* **7**, e35295 (2012).

136 Popova, T. *et al.* Germline BAP1 mutations predispose to renal cell carcinomas. *Am J Hum Genet* **92**, 974-980 (2013).

137 Testa, J. R. *et al.* Germline BAP1 mutations predispose to malignant mesothelioma. *Nat Genet* **43**, 1022-1025 (2011).

138 Wiesner, T. *et al.* A distinct subset of atypical Spitz tumors is characterized by BRAF mutation and loss of BAP1 expression. *Am J Surg Pathol* **36**, 818-830 (2012).

139 Llamas-Velasco, M., Pérez-Gónzalez, Y. C., Requena, L. & Kutzner, H. Histopathologic clues for the diagnosis of Wiesner nevus. *J Am Acad Dermatol* **70**, 549-554 (2014).

140 Busam, K. J., Sung, J., Wiesner, T., von Deimling, A. & Jungbluth, A. Combined BRAF(V600E)-positive melanocytic lesions with large epithelioid cells lacking BAP1 expression and conventional nevomelanocytes. *Am J Surg Pathol* **37**, 193-199 (2013).

141 Gerami, P. *et al.* Multiple Cutaneous Melanomas and Clinically Atypical Moles in a Patient With a Novel Germline BAP1 Mutation. *JAMA Dermatol* **151**, 1235-1239 (2015).

142 Requena, C. *et al.* BAP1-deficient and VE1-negative atypical Spitz tumor. *J Cutan Pathol* **42**, 564-567 (2015).

143 Soares de Sá, B. C. *et al.* BAP1 tumor predisposition syndrome case report: pathological and clinical aspects of BAP1-inactivated melanocytic tumors (BIMTs), including dermoscopy and confocal microscopy. *BMC Cancer* **19**, 1077 (2019).

144 Yeh, I. *et al.* Ambiguous melanocytic tumors with loss of 3p21. *Am J Surg Pathol* **38**, 1088-1095 (2014).

145 Kazakov, D. V. & Michal, M. Melanocytic "ball-in-mitts" and "microalveolar structures" and their role in the development of cellular blue nevi. *Ann Diagn Pathol* **11**, 160-175 (2007).

146 Švajdler, M. *et al.* Fibro-osseous pseudotumor of digits and myositis ossificans show consistent COL1A1-USP6 rearrangement: a clinicopathological and genetic study of 27 cases. *Hum Pathol* **88**, 39-47 (2019).

147 Piris, A., Mihm, M. C., Jr. & Hoang, M. P. BAP1 and BRAFV600E expression in benign and malignant melanocytic proliferations. *Hum Pathol* **46**, 239-245 (2015).

148 Blokx, W. A. *et al.* NRAS-mutated melanocytic BAP1-associated intradermal tumor (MBAIT): a case report. *Virchows Arch* **466**, 117-121 (2015).

149 Carbone, M. *et al.* BAP1 cancer syndrome: malignant mesothelioma, uveal and cutaneous melanoma, and MBAITs. *J Transl Med* **10**, 179 (2012).

150 Ardakani, N. M., Palmer, D. L. & Wood, B. A. BAP1 deficient malignant melanoma arising from the intradermal component of a congenital melanocytic naevus. *Pathology* **47**, 707-710 (2015).

151 Williams, E. A. *et al.* Melanomas with activating RAF1 fusions: clinical, histopathologic, and molecular profiles. *Mod Pathol* **33**, 1466-1474 (2020).

152 Jain, P. *et al.* CRAF gene fusions in pediatric low-grade gliomas define a distinct drug response based on dimerization profiles. *Oncogene* **36**, 6348-6358 (2017).

153 McEvoy, C. R. *et al.* Profound MEK inhibitor response in a cutaneous melanoma harboring a GOLGA4-RAF1 fusion. *J Clin Invest* **129**, 1940-1945 (2019).

154 Palanisamy, N. *et al.* Rearrangements of the RAF kinase pathway in prostate cancer, gastric cancer and melanoma. *Nat Med* **16**, 793-798 (2010).

155 Lavoie, H. & Therrien, M. Regulation of RAF protein kinases in ERK signalling. *Nat Rev Mol Cell Biol* **16**, 281-298 (2015).

156 Bax, M. J., Brown, M. D., Rothberg, P. G., Laughlin, T. S. & Scott, G. A. Pigmented epithelioid melanocytoma (animal-type melanoma): An institutional experience. *J Am Acad Dermatol* **77**, 328-332 (2017).

157 Bahrami, A. *et al.* Pigment-Synthesizing Melanocytic Neoplasm With Protein Kinase C Alpha (PRKCA) Fusion. *JAMA Dermatol* **152**, 318-322 (2016).

158 Mukai, H. The structure and function of PKN, a protein kinase having a catalytic domain homologous to that of PKC. *J Biochem* **133**, 17-27 (2003).

159 Yasui, T. *et al.* Protein kinase N1, a cell inhibitor of Akt kinase, has a central role in quality control of germinal center formation. *Proc Natl Acad Sci U S A* **109**, 21022-21027 (2012).

160 Yoshihara, K. *et al.* The landscape and therapeutic relevance of cancer-associated transcript fusions. *Oncogene* **34**, 4845-4854 (2015).

161 Stransky, N., Cerami, E., Schalm, S., Kim, J. L. & Lengauer, C. The landscape of kinase fusions in cancer. *Nat Commun* **5**, 4846 (2014).

162 James, R. G. *et al.* Protein kinase PKN1 represses Wnt/β-catenin signaling in human melanoma cells. *J Biol Chem* **288**, 34658-34670 (2013).

163 Siroy, A. E. *et al.* Beyond BRAF(V600): clinical mutation panel testing by next-generation sequencing in advanced melanoma. *J Invest Dermatol* **135**, 508-515 (2015).

164 Donati, M. *et al.* RAF1 Gene Fusions as a Possible Driver Mechanism in Rare BAP1-Inactivated Melanocytic Tumors: A Report of 2 Cases. *Am J Dermatopathol* **42**, 961-966 (2020).

165 Marušić, Z., Buljan, M. & Busam, K. J. Histomorphologic spectrum of BAP1 negative melanocytic neoplasms in a family with BAP1-associated cancer susceptibility syndrome. *J Cutan Pathol* **42**, 406-412 (2015).

166 Wysozan, T. R., Khelifa, S., Turchan, K. & Alomari, A. K. The morphologic spectrum of germline-mutated BAP1-inactivated melanocytic tumors includes lesions with conventional nevic melanocytes: A case report and review of literature. *J Cutan Pathol* **46**, 852-857 (2019).

167 Louw, A. *et al.* Histologically Diverse BAP1-Deficient Melanocytic Tumors in a Patient With BAP1 Tumor Predisposition Syndrome. *Am J Dermatopathol* 10.1097/dad.0000000000001719 (2020).

168 Foretová, L. *et al.* BAP1 Syndrome - Predisposition to Malignant Mesothelioma, Skin and Uveal Melanoma, Renal and Other Cancers. *Klin Onkol* **32**, 118-122 (2019).

169 Šteiner, P., Pavelka, J., Vaneček, T., Miesbauerová, M. & Skálová, A. Molecular methods for detection of prognostic and predictive markers in diagnosis of adenoid cystic carcinoma of the salivary gland origin. *Cesk Patol* **54**, 132-136 (2018).

170 Lek, M. *et al.* Analysis of protein-coding genetic variation in 60,706 humans. *Nature* **536**, 285-291 (2016).

171 Landrum, M. J. *et al.* ClinVar: improving access to variant interpretations and supporting evidence. *Nucleic Acids Res* **46**, D1062-d1067 (2018).

172 Hilbers, M. L. *et al.* Standardized diagnostic algorithm for spitzoid lesions aids clinical decision-making and management: a case series from a Swiss reference center. *Oncotarget* **12**, 125-130 (2021).

173 Haugh, A. M. *et al.* Genotypic and Phenotypic Features of BAP1 Cancer Syndrome: A Report of 8 New Families and Review of Cases in the Literature. *JAMA Dermatol* **153**, 999-1006 (2017).

174 Sunshine, J. C. *et al.* Melanocytic Neoplasms With MAP2K1 in Frame Deletions and Spitz Morphology. *Am J Dermatopathol* **42**, 923-931 (2020).

175 Donati, M. *et al.* MAP2K1-Mutated Melanocytic Neoplasms With a SPARK-Like Morphology. *Am J Dermatopathol* **43**, 412-417 (2021).

176 Webster, J. D. *et al.* The tumor suppressor BAP1 cooperates with BRAFV600E to promote tumor formation in cutaneous melanoma. *Pigment Cell Melanoma Res* **32**, 269-279 (2019).

177 Gray-Schopfer, V. C. *et al.* Cellular senescence in naevi and immortalisation in melanoma: a role for p16? *Br J Cancer* **95**, 496-505 (2006).

178 Michaloglou, C. *et al.* BRAFE600-associated senescence-like cell cycle arrest of human naevi. *Nature* **436**, 720-724 (2005).

179 Saggini, A. *et al.* Uncommon Histopathological Variants of Malignant Melanoma. Part 2. *Am J Dermatopathol* **41**, 321-342 (2019).

180 O'Shea, S. J. *et al.* Histopathology of melanocytic lesions in a family with an inherited BAP1 mutation. *J Cutan Pathol* **43**, 287-289 (2016).

181 Pouryazdanparast, P., Haghighat, Z., Beilfuss, B. A., Guitart, J. & Gerami, P. Melanocytic nevi with an atypical epithelioid cell component: clinical, histopathologic, and fluorescence in situ hybridization findings. *Am J Surg Pathol* **35**, 1405-1412 (2011).

182 Ye, J., Sheahon, K. M., LeBoit, P. E., McCalmont, T. H. & Lang, U. E. BAP1-inactivated melanocytic tumors demonstrate prominent centrosome amplification and associated loss of primary cilia. *J Cutan Pathol* 10.1111/cup.14073 (2021).

183 Borel, F., Lohez, O. D., Lacroix, F. B. & Margolis, R. L. Multiple centrosomes arise from tetraploidy checkpoint failure and mitotic centrosome clusters in p53 and RB pocket protein-compromised cells. *Proc Natl Acad Sci U S A* **99**, 9819-9824 (2002).

184 Fischer, A. S. & High, W. A. The difficulty in interpreting gene expression profiling in BAP-negative melanocytic tumors. *J Cutan Pathol* 10.1111/cup.13277 (2018).

185 Gammon, B., Traczyk, T. N. & Gerami, P. Clumped perinuclear BAP1 expression is a frequent finding in sporadic epithelioid Spitz tumors. *J Cutan Pathol* **40**, 538-542 (2013).

186 Hühns, M. *et al.* High mutational burden in colorectal carcinomas with monoallelic POLE mutations: absence of allelic loss and gene promoter methylation. *Mod Pathol* 10.1038/s41379-019-0430-6 (2019).

187 Yeh, I. New and evolving concepts of melanocytic nevi and melanocytomas. *Mod Pathol* **33**, 1-14 (2020).

188 McGranahan, N. & Swanton, C. Clonal Heterogeneity and Tumor Evolution: Past, Present, and the Future. *Cell* **168**, 613-628 (2017).

189 Reya, T., Morrison, S. J., Clarke, M. F. & Weissman, I. L. Stem cells, cancer, and cancer stem cells. *Nature* **414**, 105-111 (2001).

190 Zheng, L. *et al.* Polyploid cells rewire DNA damage response networks to overcome replication stress-induced barriers for tumour progression. *Nat Commun* **3**, 815 (2012).

191 Erenpreisa, J. & Cragg, M. S. Three steps to the immortality of cancer cells: senescence, polyploidy and self-renewal. *Cancer Cell Int* **13**, 92 (2013).

192 Puig, P. E. *et al.* Tumor cells can escape DNA-damaging cisplatin through DNA endoreduplication and reversible polyploidy. *Cell Biol Int* **32**, 1031-1043 (2008).

193 Sharma, S. *et al.* Small-molecule inhibitor BMS-777607 induces breast cancer cell polyploidy with increased resistance to cytotoxic chemotherapy agents. *Mol Cancer Ther* **12**, 725-736 (2013).

194 Jia, L. *et al.* Paclitaxel inhibits ovarian tumor growth by inducing epithelial cancer cells to benign fibroblast-like cells. *Cancer Lett* **326**, 176-182 (2012).